HIGH-TEMPERATURE CRITICAL INDICES FOR THE CLASSICAL ANISOTROPIC HEISENBERG...

David Jasnow

1969

Published on demand by
UNIVERSITY MICROFILMS
University Microfilms Limited, High Wycomb, England
A Xerox Company, Ann Arbor, Michigan, U.S.A.

FACILITY FORM 602

N71-38774
(ACCESSION NUMBER)

140
(PAGES)

CR-123148
(NASA CR OR TMX OR AD NUMBER)

(THRU)
00

(CODE)
33

(CATEGORY)

* * *

This is an authorized facsimile and was produced by microfilm-xerography in 1970 by University Microfilms, A Xerox Company, Ann Arbor, Michigan, U.S.A.

* * *

This dissertation has been
microfilmed exactly as received

69-15,325

JASNOW, David Michael, 1943-
HIGH-TEMPERATURE CRITICAL INDICES
FOR THE CLASSICAL ANISOTROPIC
HEISENBERG MODEL.

University of Illinois, Ph.D., 1969
Physics, solid state

University Microfilms, Inc., Ann Arbor, Michigan

6.60

HIGH-TEMPERATURE CRITICAL INDICES FOR THE CLASSICAL ANISOTROPIC HEISENBERG MODEL

BY

DAVID MICHAEL JASNOW
A.B., Cornell University, 1964
M.S., University of Illinois, 1965

THESIS

Submitted in partial fulfillment of the requirements
for the degree of Doctor of Philosophy in Physics
in the Graduate College of the
University of Illinois, 1969

Urbana, Illinois

72803-8

UNIVERSITY OF ILLINOIS

THE GRADUATE COLLEGE

FEBRUARY, 1969

I HEREBY RECOMMEND THAT THE THESIS PREPARED UNDER MY SUPERVISION BY DAVID MICHAEL JASNOW

ENTITLED HIGH-TEMPERATURE CRITICAL INDICES FOR THE CLASSICAL ANISOTROPIC HEISENBERG MODEL

BE ACCEPTED IN PARTIAL FULFILLMENT OF THE REQUIREMENTS FOR THE DEGREE OF DOCTOR OF PHILOSOPHY IN PHYSICS

Michael Wortis (signature below)
In Charge of Thesis

Head of Department

Recommendation concurred in†

Peter Cord
Gordon Baym
Frederick C. Brown
Michael Wortis

Committee on Final Examination†

† Required for doctor's degree but not for master's.

D517

ACKNOWLEDGMENT

The author wishes to express his appreciation to his thesis adviser, Professor Michael Wortis, for his advice, patience, and encouragement throughout the course of this work. He is grateful to him for many stimulating discussions concerning this work and related topics.

The author wishes to thank Professor L. P. Kadanoff for his continued interest and many helpful discussions and Professor M. E. Fisher for several helpful suggestions.

Special thanks go to Dr. M. A. Moore for some independent numerical checks and for frequent valuable conversations concerning various aspects of the analysis.

The author would like to thank his many colleagues, in particular Jack Swift and Will Saam, for many interesting discussions. He thanks Charles Bridges for answering his many questions concerning computer programming.

He is grateful to the National Aeronautics and Space Administration and Eastman Kodak Company for fellowship support. He acknowledges the hospitality of the Department of Physics of Brookhaven National Laboratory, where much of this manuscript was written.

The author thanks his wife, Carol, for her encouragement and her help in the preparation of this manuscript.

TABLE OF CONTENTS

		page
I.	INTRODUCTION	1
	A. Survey of Recent Developments	1
	B. The Present Work	7
II.	DERIVATION OF THE HIGH TEMPERATURE EXPANSIONS	15
	A. The Lattice	15
	B. Finding the Series Coefficients for the Classical Anisotropic Heisenberg Model	17
	C. Symmetry Properties	27
III.	EMBEDDING CONSTANTS	32
IV.	ANALYSIS OF SERIES	61
	A. The Neville Table	63
	B. Finding the Critical Point	64
	C. Evaluating the Critical Index	66
	D. Specific Methods for the Second-Moment Series	69
	E. The "n-shift" Method.	70
	F. Method of Padé Approximants	72
	G. Modification for Loose-Packed Lattices	72
	H. Comments	76
V.	RESULTS	79
	A. Critical Point	80
	B. Indices γ and ν_1	82
	C. The Specific Heat	91
	D. Comment on the S = ∞ Ising Model	92
	E. Summary and Comments on the Scaling Laws	93
	F. A Recent Experiment	95
VI.	THE PLANAR HEISENBERG MODEL	96
VII.	THE SPINEL	103
APPENDIX A.	SKETCH OF THE DERIVATION OF THE UNRENORMALIZED EXPANSION	108
APPENDIX B.	THE RENORMALIZATION	116
APPENDIX C.	SELECTED ZERO-FIELD SUSCEPTIBILITY, SECOND MOMENT AND SPECIFIC HEAT COEFFICIENTS	120
APPENDIX D.	DETERMINATION OF THE GROUND STATE	125
LIST OF REFERENCES		127
VITA		131

LIST OF FIGURES

Figure		page
1.	A reducible graph and its skeleton. (a) A graph contributing to $\mathcal{M}_{\alpha\beta}(12)$ in the unrenormalized theory. (b) The skeleton graph contributing to $\mathcal{M}_{\alpha\beta}(12)$ (and also $G_2(1;\gamma_1\gamma_2)$) in the renormalized theory.	22
2.	Removal of multiple lines in a graph in calculating $C[1,2;G]$. Graphs in (a) and (b) have the same skeleton (c).	33
3.	A ladder graph and its constituent parts G_1 and G_2.	34
4.	A ladder of paths connecting 3 and 4, one path a direct bond.	34
5.	The embedding constant for a graph with a node. . .	35
6.	The anomalous graphs for which the embedding constants cannot be calculated simply, using (i)-(v)..	40
7.	Forming a G_4 graph from a correlation graph. (a) Graph contributing to $\mathcal{M}_{\alpha\beta}(12)$. (b) G_4 graph from (a) by putting external vertices together. (c) Second correlation graph yielding G_4 graph, (b). .	57
8.	The critical temperature $t_c = kT_c/J$ vs. anisotropy λ for the f.c.c. lattice in the case of (a) prolate anisotropy and (b) oblate anisotropy. See Eq. (2.3d,e).	81
9.	The sequences $\{g_n\}$, defined by Eq. (3.9) applied to χ_z, vs. 1/n for various values of λ in the case of prolate anisotropy. From (3.5), $\{g_n\} \to (\gamma-1)$. .	86
10.	The sequence $\{\rho_n\}$ vs. 1/n for $\chi_z(1,1,1)$ on the B-site spinel.	106
11.	Graphical representation of the terms contributing to W_3.	113
12.	A contribution to M_2. A self-energy part G_3^0 attached to a vertex M_2^0 gives a M_5^0 contribution to M_2.	117

LIST OF TABLES

Table		page
1.	Critical indices.	2
2.	Square lattice n-chain embedding constants for the n-chain connecting the origin to $\underset{\sim}{R}$.	36
3.	The embedding constants $C[\underset{\sim}{R};n,t]$ for the anomalous graphs.	39
4.	Symmetry factors and embedding constants for correlation graphs, (n,t).	41
5.	Complete non-vanishing embedding constants $C[\underset{\sim}{R};n,t]$ for the f.c.c. lattice. 6-,7-, and 8-chain constants given separately.	47
6.	Set of correlation graphs (n,t) which yield the G_ℓ graphs. g' is the symmetry factor of the corresponding G_ℓ graph.	59
7.	Neville Table for $\{\rho_n\}$ from $\chi_z(0,0,1)$. Entries are estimates of t_c.	65
8.	The Neville Table for the sequence $\{t_n\}$ defined in (4.7) for $\chi_z(0,0,1)$ using g' = 0.25.	67
9.	Neville Table for $\{g_n = (\gamma-1)_n\}$ from $\chi_z(0,0,1)$ using Eq. (4.8) with $t'_c = 3.509$.	68
10.	n-shift estimates for t_c using (4.10) on $\chi_z(0,0,1)$.	71
11.	n-shift estimates for $(\gamma-1)$ using (4.11) on $\chi_z(0,0,1)$ with $t'_c = 3.509$.	73
12.	Estimates of t_c and γ from Padé Approximants to $\frac{d}{dv} \log \chi_z(0,0,1)$.	74
13.	Estimates of γ-1, calculated from (4.11) and (4.15) for $\chi_z(0,0,1)$ on the b.c.c. lattice. $t'_c = 2.299$..	77
14.	Indices γ and $2\nu_1$ for prolate and oblate anisotropy.	83

List of Tables (continued)

Table		page
15.	Indices γ and $2\nu_1$ for various typical combinations of the anisotropy parameters.	84
16.	Critical indices and ground state behavior as functions of the anisotropy parameters	88
17.	Critical indices and ground state behavior for the anisotropic planar Heisenberg model on the f.c.c. lattice as a function of anisotropy parameters. . .	101
18.	Selected zero-field susceptibility, second moment and specific heat coefficients for the planar Heisenberg model on the f.c.c. lattice.	102
19.	Zero-field susceptibility and second moment coefficients for the three limiting cases on the B-site spinel lattice.	105

I. INTRODUCTION

A. Survey of Recent Developments

The determination of the asymptotic behavior of the correlation and thermodynamic functions describing a many-body system as it approaches its critical point is a fundamental theoretical and experimental problem in the study of phase transitions. Apparently quite different phase transitions have striking similarities when viewed in terms of this limiting behavior.

In the vicinity of the critical point, the above functions behave in a fairly simple manner. The critical indices (exponents) have been introduced[1] to describe the various phase transitions and compare their critical behaviors. These indices measure the type and strength of the singular behavior of the associated physical quantities at the thermodynamic critical point. In Table 1 the exponents are defined in the terminology of magnetism. The similarity of phase transitions with qualitatively differing order parameters[2] appears in the equality or near equality of the analogous critical exponents.

Much of the recent study of critical phenomena, both theoretical[3] and experimental,[4,5] has centered on the determination of the critical indices* and the relations among them.**

---

*For complete details concerning the critical indices there are several good articles[1] and reviews.[3,4]

**The review by M. E. Fisher[3] contains extensive references concerning the theoretical situation. The experimental situation and techniques are discussed in the review by P. Heller,[5] and in the review by L. P. Kadanoff et al.,[4] the theory is discussed in combination with a detailed analysis of the experiments.

Table 1. Critical indices.

Physical Quantity	Range of Variables*		Asymptotic Behavior	Index Defined
	ϵ	H		
Spontaneous Magnetization	< 0	0	$M_o \sim (-\epsilon)^{\beta}$	β
Critical Isotherm	0	$\neq 0$	$M \sim \pm \lvert H \rvert^{1/\delta}$	δ
Zero-Field Susceptibility	> 0 < 0	0 0	$\chi \sim (\epsilon)^{-\gamma}$ $\chi \sim (-\epsilon)^{-\gamma'}$	γ γ'
Specific Heat at Constant Field	> 0 < 0	0 0	$C_H \sim (\epsilon)^{-\alpha}$ $C_H \sim (-\epsilon)^{-\alpha'}$	α α'
Correlation Length	> 0 < 0	0 0	$\xi \sim (\epsilon)^{-\nu}$ $\xi \sim (-\epsilon)^{-\nu'}$	ν ν'
Spin-Spin Correlation Function	0	0	$\mathcal{M}_{\alpha\beta}(12) \sim \dfrac{1}{\lvert \underset{\sim}{r}_1 - \underset{\sim}{r}_2 \rvert^{d-2+\eta}}$ (d is dimensionality of the system)	η

*$\epsilon = (T-T_c)/T_c$ measures the distance from the critical point; H is the magnetic field.

A recent area of theoretical progress has been in the suggestion that the critical indices are not independent, but rather that a set of relations exist connecting them. Several exponent inequalities can be rigorously proven,[6] and some plausibility arguments[7,8] have been set forth which lead to a combination of equations relating the indices. These scaling laws indicate that perhaps all the critical indices can be expressed in terms of just two. There is current interest in finding arguments that might indicate which (if any) of the indices are fundamental. These arguments, if they exist, will probably involve detailed investigations of equations for the pair correlation functions of the system.

In its simplest form there are still several levels of "scaling theory." A particularly intuitive "derivation" of the scaling laws is due to Kadanoff.[4,7] It is assumed that the correlations near the critical point do not depend on the details of the interactions and that the range of correlations is characterized by a single coherence length, which must diverge as the transition is approached. The requirement that near the transition the thermodynamic functions have the same form as the scale of length is changed.* yields a homogeneous form for, say, the free energy. Such a form had been proposed independently by Widom.[8] This result yields exponent relations among the indices γ, β, δ, and α, with the additional symmetry $\alpha = \alpha'$ and $\gamma = \gamma'$. These (with the possible

---

*Provided that the length scale is much smaller than the coherence length.

exception of the symmetry relations) are the least suspect of the whole class of relations.[3] If the logic is applied to the pair correlation function, a specific form is obtained which reflects explicitly the assumption of a single diverging coherence length. The integral of the pair correlation function over all space relates, by a fluctuation theorem, to the susceptibility (in magnetic language), yielding a relation connecting the indices γ, ν, η. The function also yields relations involving the dimensionality d of the system. These are the most questionable[3] of the scaling law relations.*

It is important that the scaling relations be derived in several alternative ways to see what modifications in the original assumptions can be made while preserving the relations which are believed correct. In their strongest form the assumptions going into scaling would lead one to the conclusion that there is one phase transition (that is, one set of indices) for a given dimensionality and type of order parameter.**

A theory of phase transitions must necessarily produce a set of indices for the system in question. The older theories of the critical point[2,4,9] had as their basis the assumption (explicit or implicit) that the free energy of the system could be expanded in a

---

*Table 14 in the review by M. E. Fisher[3] summarizes the exponent relations and the agreement with numerical data.

**By "type of order parameter" we mean the distinction between vector and scalar, for example.

Taylor series in appropriate variables at the critical point. These theories always yield the "classical" indices: $\gamma=\gamma'=1$, $\beta=\frac{1}{2}$, $\delta=3$, $\alpha=\alpha'=0$ (finite discontinuity). An essentially equivalent theory of the pair correlation function is due to Ornstein and Zernike.[10] The basic assumption there is that the "direct" correlation function remains short-ranged even at the critical point. This assumption implies a particularly simple form for that function in the long-wavelength limit, giving $\eta = 0$,* and $\nu=\nu'=\frac{1}{2}$.

The point to be made is that until rather recently there was no reason to doubt the classical theories. Critical phenomena experiments are terribly difficult to perform, and there was no real evidence on which to question the theories. The first real clue to the inadequacy of the older theories was Onsager's[11] evaluation of the zero-field partition function for the two-dimensional Ising model of a magnetic system. From his work and its extensions, it became evident that the older theories** of phase transitions did not correctly predict the Ising model behavior.*** More recently some convincing experiments[4,5] have been done showing further discrepancies between actual results and the predictions of the classical theories.

---

*This possibility, $\eta = 0$, is not yet ruled out in three dimensions if one allows for the non-classical values of γ.

**In the review by L. P. Kadanoff *et al.*[4] the older theories are discussed and the predictions are compared to the Ising model results.

***For discussions of the theory of the Ising model see, for example, the reviews by G. F. Newell and E. W. Montroll,[12] and C. Domb.[13]

Onsager's contribution was the beginning of modern work in the theory of critical phenomena. One of the most rewarding theoretical approaches has been the study of various model systems. Three-dimensional systems must be considered to make sensible comparisons with experiments. For such systems there are no general solutions, and in only a few cases can the existence of a transition be shown rigorously.[14] The models are frequently defined in the language of magnetism, where they take the form of interacting spin systems.* They are usually described by giving the Hamiltonian and the lattice, the sites of which the spins occupy. The common feature of most of these models is that the Hamiltonian is a bounded operator.

This fact has led to one of the most fruitful methods for gaining information about the critical behavior of various models. The physical quantities (including correlation functions) can be expanded in power series about infinite temperature or, in some cases, about $T = 0$. Remarkably enough, fairly precise estimates of the critical behavior of the model can be extracted from such a power series even though only a finite number of terms are known exactly.** Analysis of the series coefficients allows successive estimates of the parameters characterizing the phase transition to be made, and these estimates can be quite reliable if their "convergence" is reasonably rapid and regular.

---

*For a discussion of analogies with other types of physical systems see the review by M. E. Fisher.[3]

**This approach was originated by Domb, and the reader is referred to his comprehensive review.[13] More recent references are provided in the review by M. E. Fisher.[3]

The validity and the general performance of the numerical methods based on power series expansions may be judged in a case in which they can be checked – the two-dimensional Ising model. For example, determining the critical temperature for the triangle lattice from the expansion of the zero-field susceptibility in powers of T^{-1} gives, as a reasonable estimate, one within 3 parts in 10^4 of the exact result.[3] In addition, the value $\gamma = 7/4$ for the susceptibility index was conjectured by Domb and Sykes[15] before more recent derivations of correlation functions[16] confirmed that value. Also, on the basis of the first nine non-zero terms in the series for the spontaneous magnetization near $T = 0$, Domb[17] suggested $\beta \cong 0.12\text{-}0.13$ prior to Yang's famous result[18] that $\beta = 1/8$.

The overall record is impressive, and it should be borne in mind that the series for the three-dimensional lattices are usually better behaved than for equivalent models on two-dimensional ones.[15] However, the extrapolations based on series certainly are not rigorous. If realistic error estimates for the results are made, the method takes on the appearance of a "numerical experiment." Such terminology might be misleading – the important fact is that the error limits are frequently in the same range as those for present day critical point experiments.

B. The Present Work

As has been mentioned, when phase transitions are viewed in terms of their critical indices, the most striking observation

is the relative insensitivity of these indices (for fixed dimensionality) to the details of both kinematics and dynamics.* The scaling hypotheses in their strongest forms give an idea of what critical indices to expect given the dimensionality of the thermodynamic system and the nature of the order parameter.

It is now appreciated, however, that, within this context of broad similarity, there are small but nonetheless important differences in critical indices between systems with differing dynamics and/or kinematics. Note, as an example, the variation of the high-temperature susceptibility index, γ, in three-dimensions between the spin-1/2 Ising model[15,20] ($\gamma \cong 1.250$), the dynamically different spin-1/2 Heisenberg model[21] ($\gamma \cong 1.43$), and in turn, the kinematically different spin-infinity Heisenberg model[22,23] ($\gamma \cong 1.38$). One is led by these observations to the following questions:

(a) How many different types of critical behavior are there, as classified by the critical exponents?

---

*More precisely, some of these differences are actually not so small, for example, a change in sign of the interaction (dynamics) of the two-dimensional spin-1/2 Ising model on the triangular lattice converts a ferromagnet to a paramagnet having no phase transition. See, for example, the paper by G. Wannier.[19] However, we are emphasizing here the strong parallels between the critical behavior of, for example, the liquid-gas system and the ferromagnet (experimental) or the somewhat weaker similarity (theoretical) of the three-dimensional Ising and Heisenberg models.

(b) Which features of the dynamics and kinematics of a given system serve to determine its critical exponents and which are irrelevant?

(c) How, physically and mathematically, do the features which are relevant exert their influence on the critical indices?

Concerning (c), we have nothing to say other than to point out that the question remains almost entirely open, with the exception of a few exactly soluble models[3] and the crude but appealing "droplet theory."[24] It is the purpose of this work to explore questions (a) and (b) within the context of the classical (spin-infinity) anisotropic nearest-neighbor Heisenberg model by means of high-temperature series expansions.

The choice of this model is dictated by the following considerations: (i) variation of the anisotropy parameters allows one to interpolate continuously between a number of dynamically quite different situations. For example,* by varying the degree of longitudinal anisotropy, one progresses from the Ising model (longitudinal coupling only) through the isotropic Heisenberg model to the so-called x-y model[25] (totally transverse coupling). In addition, (ii) $S = \infty$ is suggested by convenience. First, as workers on the isotropic Heisenberg model have noted,[23,26,27] the computation of series expansion coefficients becomes simpler in the classical limit, when non-commutation may be neglected.** Second, the series once

*See Chapter II for details.

**As noted in the paper by G. Baker et al.,[21] there are also simplifications for S = 1/2. These, however, depend on isotropy in an essential way.

obtained are empirically observed to be smoother (and, thus, more reliably extrapolated) for $S = \infty$ than for finite spin.[28] Finally, (iii) the Ising and Heisenberg limits have been extensively studied previously and constitute a useful check.*

The anisotropic Heisenberg model has recently been investigated by Dalton and Wood[31] through a correlation function decoupling (random phase approximation) and via high-temperature series for spin-1/2 (through order T^{-5}). These authors interpolate with a purely longitudinal anisotropy between the Ising and isotropic Heisenberg limits and conclude that the critical exponents change discontinuously in the isotropic limit — a result previously conjectured by Fisher[32] and which the present work corroborates on the basis of longer and more regular series in the $S = \infty$ case. Obokata, Ono, and Oguchi[33] have independently obtained seven terms in the high temperature susceptibility series for S = 1/2 with longitudinal anisotropy only. On the basis of a Padé analysis, they are unable to draw strong conclusions.

---

*In the paper by C. Domb and M. F. Sykes,[28] six terms in the Ising susceptibility series and seven in the specific heat series for general spin are given. The best present susceptibility data for the classical Heisenberg model consist of eight terms (close-packed lattices) and nine terms (loose-packed lattices). See the papers by H. E. Stanley[23] and G. S. Joyce and R. G. Bowers.[22] In addition the coefficients of the specific heat series for the three cubic lattices are given in the paper of G. S. Joyce and R. G. Bowers.[22] Six terms for the second moment series of the spin-S isotropic Heisenberg model are given in an article by M. E. Fisher[1] and the thesis of R. J. Burford.[29] Second moment series for the S = 1/2 Ising model have been derived in the paper by M. E. Fisher and R. J. Burford.[30] For further references, see the reviews by M. E. Fisher[3] and C. Domb.[13]

To place the classical anisotropic Heisenberg model in the context of real magnetic materials, several comments can be made. There exist several insulating ferromagnets and antiferromagnets which have been studied experimentally.[4,5] The experimental difficulties are such that few substances have been studied completely. Typically the experiments are done over a range of $\epsilon = (T-T_c)/T_c$ of 3×10^{-1} - 10^{-2}, and the results usually indicate departures from the three-dimensional Ising model values.* The effective value of the localized spin is frequently relatively high, an example being S = 7/2 for the "Heisenberg model" EuS. Most magnetic materials have some degree of exchange anisotropy.[3,9] the qualitative effect of which we have determined in this work. In general our model should approximate magnetic insulators with high effective spin, short range interactions, and small single-ion anisotropy effects.

An example of an experimental "Heisenberg antiferromagnet" is $RbMnF_3$.[5] The manganese ions in that substance form a simple cubic lattice of S = 5/2 spins with nearest-neighbor antiferromagnetic exchange interactions. There is also a vanishingly small single-ion anisotropy.[5] The relatively high spin of the ions indicates that $RbMnF_3$ might be reasonably approximated by our model.**

The outline of the present work is as follows. Chapter II discusses the Hamiltonian of the model and outlines the graphical

---

*For example, experimentally[4,5] the value of γ is consistently near 4/3, whereas the Ising model value[15,20] is approximately 5/4.

**The author is indebted to Dr. M. Blume for a discussion concerning magnetic materials.

expansion used in the derivation of high-temperature series in powers of T^{-1} (inverse temperature) for the zero-field susceptibility (χ), second-moment of spatial correlations[30] (μ_2), and specific heat ($C_{H=M=0}$). These quantities are expected to have singular behavior[1,3,4] as $T \to T_c^+$:

$$\text{(a)} \quad \chi \sim (T-T_c)^{-\gamma}$$

$$\text{(b)} \quad \mu_2 \sim (T-T_c)^{-(2\nu_1+\gamma)}$$

$$\text{(c)} \quad C_{H=M=0} \sim (T-T_c)^{-\alpha} . \qquad (1.1)$$

Also discussed are some useful antiferromagnetic symmetries of the model when it is applied to loose-packed lattices. In Chapter III we present a method for calculating graph "embedding constants." A knowledge of these constants is necessary for the application of the graphical expansion method sketched in Chapter II. Constants for calculating χ, μ_2 and $T \cdot C_{H=M=0}$ through order $T^{-\delta}$ (close-packed lattices) and T^{-9} (loose-packed lattices) are given. Chapter IV describes the methods of extrapolation used to extract the critical indices* γ, ν_1, and α from the high-temperature series.

Chapter V is the central chapter of this work. We present our results for various lattices and anisotropies, and we discuss

---

*Following the work described in the paper by M. E. Fisher and R. J. Burford[30] we distinguish between the true and effective correlation ranges, whose divergences as $T \to T_c^+$ are characterized by the critical indices ν and ν_1 respectively. Scaling implies $\nu = \nu_1$, a result which for the $S = 1/2$ Ising model is exact in two-dimensions and confirmed numerically in three.

briefly the relation to the scaling laws that can be checked. In view of the considerable number of lattices, anisotropies, and different values of the critical exponents which will be considered, it will perhaps prove useful to summarize here our conclusions as they relate to the questions (a) and (b) posed at the outset. For the classical three-dimensional anisotropic Heisenberg model, we find that our results are consistent with the following hypothesis: The high temperature critical indices are correlated in a one-to-one manner with the symmetry group of the order parameter in the ground state manifold* ($T = 0$, zero field). For example, at $T = 0$ the magnetization of the isotropic Heisenberg ferromagnet is free to point in any direction, while the magnetization of the Ising or x-y models have, respectively, an up-down or planar-rotation degree of freedom only. We therefore expect and, in fact, find different critical indices for these three cases.

No exact results are available for our model concerning the thermodynamic properties of the low-temperature phase; however, it is plausible to assume that the symmetry of the order parameter in the low-temperature phase ($T < T_c$, zero field) is the same as its symmetry at $T = 0$. If this is so, then the hypothesis stated above correlates the critical indices with the symmetry of the ordered phase.

---

*Notice that since our model is classical, elementary arguments suffice to determine the ground state for a variety of anisotropies and lattices. See Chapter V and Appendix D.

Chapter VI presents the results of series analysis on the so-called classical anisotropic planar Heisenberg model. In that model the classical spins are confined to a plane. In view of recent interest in spinel structures and to present a graphic example of the dangers which lie in attempts to extrapolate too-short series, we give in Chapter VII some results for the three-dimensional spin model applied to that lattice. There are several appendices which give details of some of the derivations and the series coefficients for representative examples.

II. DERIVATION OF THE HIGH TEMPERATURE EXPANSIONS

In this chapter, the classical anisotropic Heisenberg model of a magnetic system is defined, and the method used to derive series expansions for the model is presented. The chapter is divided into three sections. In the first, the notation pertaining to the lattice is given, and the concept of a simple sublattice structure is introduced. In the second part, the method used to derive the expansions for the spin-spin correlation functions (and from them, the thermodynamic quantities) is indicated. In the third section, various symmetries of the model are discussed.

A. The Lattice

The sites of a d-dimensional lattice are numbered $i = 1,2,\cdots,N$, and the spatial position of the i^{th} site is $\underset{\sim}{R}_i$ (frequently, where no confusion will occur, i will be taken to mean the space point $\underset{\sim}{R}_i$). The lattice is taken to be cyclically connected, (that is, periodic boundary conditions are applied) so that there are no free edges, and there is complete translational invariance.*

The coordination number of the lattice is z, and the z lattice vectors are represented by $\{\underset{\sim}{\delta}\}$. Hence, the z vectors, $\underset{\sim}{\delta}$ connect a site to its nearest-neighbors. On the three cubic lattices

---

*The methods used to derive the expansions are completely general and can be applied to finite lattices, or lattices with artificial boundaries. The modifications which make the problem move difficult are the resulting changes in the "embedding constants" discussed in Chapter III.

and the square, the position vector of a site is given with reference to the Cartesian axes which define the edges of the cubic (square) unit cell. On the triangle lattice, we take the oblique set of primitive vectors to be $\underset{\sim}{a}_1 = (1,0)$ and $\underset{\sim}{a}_2 = (1/2, \sqrt{3}/2)$, defined in terms of square Cartesian axes. For the spinel* lattice, the primitive vectors (for the lattice of magnetic sites only) are taken to be $\underset{\sim}{a}_1 = (1,0,0)$, $\underset{\sim}{a}_2 = (1/2, \sqrt{3}/2, 0)$ and $\underset{\sim}{a}_3 = (1/2, \sqrt{3}/6, \sqrt{6}/3)$, in terms of cubic Cartesian axes. The magnetic sites occupy $\underset{\sim}{R} = n_1\underset{\sim}{a}_1 + n_2\underset{\sim}{a}_2 + n_3\underset{\sim}{a}_3$, where the three integers n_1, n_2, and n_3 must be

(a) all even; or

(b) 2-even; 1-odd.

The parameters for the above lattices are:

square (s.q.)	d=2	z=4
triangle	d=2	z=6
simple cubic (s.c.)	d=3	z=6
body centered cubic (b.c.c.)	d=3	z=8
face centered cubic (f.c.c.)	d=3	z=12
spinel	d=3	z=6 .

The concept of a lattice with a simple sublattice structure will be important in the discussion of results and symmetries (see below). For our purposes a lattice has a simple sublattice structure**

*We are considering a normal cubic spinel with non-magnetic A-sites.

**The word "simple" will frequently be dropped, however, and unless otherwise stated, we will mean the structure defined.

if the sites can be divided into two equivalent subsets, A and B, such that the nearest-neighbors of an element of A are in B and vice versa. The so-called loose-packed lattices, square, simple cubic, body centered cubic, are of this type.

B. Finding the Series Coefficients for the Classical Anisotropic Heisenberg Model

The various energies of the problem are expressed in terms of the inverse energy unit $\beta = 1/kT$, where k is Boltzmann's constant, and T is the absolute temperature. The Hamiltonian of the spin-infinity (classical) anisotropic Heisenberg model is

$$-\beta H = \sum_{1,\alpha} b_\alpha(1)\, S_\alpha(1) + \frac{1}{2} \sum_{1,2,\alpha} \eta_\alpha\, v(12)\, S_\alpha(1)\, S_\alpha(2) , \qquad (2.1)$$

where numerical arguments stand for lattice sites and are summed over the entire lattice, while the Greek index α stands for the Cartesian components x, y, z. The classical spin vector $\underset{\sim}{S}(1) = (S_x(1), S_y(1), S_z(1))$ has unit magnitude. $\underset{\sim}{b}(1)$ is the dimensionless magnetic field* at site 1. The dimensionless exchange interaction $v(12) = \beta J(12)$ measures the coupling strength between sites 1 and 2. The pure numbers η_α are anisotropy parameters. In computation we will always specialize to the case of zero field and nearest-neighbor interactions,

---

*$\underset{\sim}{b}(1) = m\underset{\sim}{H}(1)/kT$ where $\underset{\sim}{H}(1)$ is the magnetic field at the site 1 and m is the magnetic moment assigned to each site.

$$v(12) = \begin{cases} v, 1 \text{ and } 2 \text{ nearest neighbors} \\ 0, \text{ otherwise} \end{cases}$$

$$\underset{\sim}{b}(1) = 0, \text{ all sites } 1. \tag{2.2}$$

Familiar limiting forms of the Hamiltonian (2.1) are

(a) $\eta_x=\eta_y=\eta_z=1$, classical isotropic Heisenberg model[22,23,26,27]

(b) $\eta_x=\eta_y=0$, $\eta_z=1$, spin-infinity Ising model[28]

(c) $\eta_x=\eta_y=1$, $\eta_z=0$, classical x-y model

We will study in detail the interpolating forms

(d) $0 \leq \lambda=\eta_x=\eta_y \leq \eta_z=1$, prolate anisotropy, interpolates between (a) and (b)

(e) $1=\eta_x=\eta_y \geq \eta_z=\lambda \geq 0$, oblate anisotropy, interpolates between (a) and (c) . (2.3)

The thermodynamic behavior of the system follows from the partition function,

$$Z[\{v\},\{b\}] = \mathrm{Tr} e^{-\beta H} = \int \prod_1 d\Omega_1 e^{-\beta H}, \tag{2.4a}$$

which yields directly the dimensionless* free energy

$$W[\{v\},\{b\}] = \ell n\, Z. \tag{2.4b}$$

In (2.4) the trace for the classical system reduces to a simple integral over solid angle for each unit spin vector. Thermodynamic

---

*$W=-\beta F$ where F is the (Helmholtz) free energy with the properties (i) $(\partial F/\partial H)_{N,T}=-M$, the magnetization, and (ii) $(\partial F/\partial T)_{N,H}=-S$, the entropy.

averages are calculated as

$$\langle X \rangle \equiv \frac{1}{Z} \mathrm{Tr} e^{-\beta H} X. \tag{2.5}$$

In the absence of interaction

$$Z[\{v=0\},\{b\}] \equiv Z_o[\{b\}] = \prod_1 (4\pi) \frac{\sinh|\underset{\sim}{b}(1)|}{|\underset{\sim}{b}(1)|} , \tag{2.6}$$

and all correlation functions involving two or more distinct sites factor.

A particularly important quantity in our formulation is the spin-spin correlation function,

$$\mathcal{M}_{\alpha\beta}(12) \equiv \langle S_\alpha(1) S_\beta(2)\rangle - \langle S_\alpha(1)\rangle\langle S_\beta(2)\rangle = \frac{\delta^2}{\delta b_\alpha(1)\delta b_\beta(2)} \ln Z, \tag{2.7}$$

which becomes diagonal in α and β for $T \geq T_c$ (the critical temperature) and $\underset{\sim}{b} = 0$. Under the condition (2.2) we calculate (2.7) as a power series in v, the coefficients of which are, of course, functions of the anisotropy parameters η_α. Once the spin-spin correlation function is known, we can immediately form power series for the physical quantities to be studied[26,34]:

$$\chi_\alpha = \sum_2 \mathcal{M}_{\alpha\alpha}(12) = \chi_\alpha(\eta_x,\eta_y,\eta_z) \tag{2.8a}$$

$$\mu_2^\alpha = \sum_2 |\underset{\sim}{R}_1 - \underset{\sim}{R}_2|^2 \mathcal{M}_{\alpha\alpha}(12) \tag{2.8b}$$

$$C_\alpha = \frac{zv^2}{2} \eta_\alpha \frac{d}{dv} \mathcal{M}_{\alpha\alpha}(1,1+\underset{\sim}{\delta}) , \tag{2.8c}$$

where z is the number of nearest neighbors and $\underset{\sim}{\delta}$ is a nearest-neighbor lattice vector.* The zero-field dimensionless

*In writing (2.8) we have made use of the simplifications which occur for $T > T_c$ and under conditions (2.2).

susceptibility, χ_α, measures the linear response of the α-component of the magnetization per site to a homogeneous magnetic field in the α-direction. μ_2^α is the second moment of $\mathcal{m}_{\alpha\alpha}(12)$ and is a measure of the range of correlations.[30] C_α is the α contribution to the dimensionless specific heat per site at zero field, $C_{M=H=0} = \sum_\alpha C_\alpha$.

To calculate the spin-spin correlation function $\mathcal{m}_{\alpha\beta}(12)$, we have used a diagrammatic expansion developed by Englert and others[35,36] in the context of the Ising model. We present here without proofs an outline of our procedure for computing $\mathcal{m}_{\alpha\beta}(12)$. The interested reader is referred to the literature for further discussion.* There are two forms of the expansion, bare and renormalized. We have used the renormalized expansion; however, for pedagogical reasons, we give both here.

Define "bare semi-invariants" by

$$M_\ell^o(1;\alpha_1\cdots\alpha_\ell) = \frac{\delta^\ell}{\delta b_{\alpha_1}(1)\cdots\delta b_{\alpha_\ell}(1)} \ln Z_o[\{b\}] . \qquad (2.9)$$

Consider a particular connected graph, G, of n lines and p vertices. Take two of the vertices to be fixed (external), and label them by the lattice points 1 and 2. Label the remaining p-2 (internal) vertices $3,4,\cdots,p$ in some arbitrary manner. Label each line in the graph by a Cartesian index γ. Let ℓ_i denote the number of lines terminating in the vertex i. Assign to each such graph a contribution

---

*See also a paper to be published by M. Wortis, M. A. Moore and D. Jasnow.

to $\mathcal{M}_{\alpha\beta}(12)$ according to the following rules:

Rule A:

(i) for each line write a factor $\eta_\gamma v(ij)$, where i, j are the endpoints of the line and γ is its Cartesian label.

(ii) for each internal vertex (e.g. 3) assign a factor $M^o_{\ell_3}(3;\gamma_1\cdots\gamma_{\ell_3})$, where γ_i, $i = 1,\cdots,\ell_3$ are the Cartesian labels of the lines terminating in 3.

(iii) Assign to the two external vertices factors of $M^o_{\ell_1+1}(1;\alpha\ \gamma_1\cdots\gamma_{\ell_1})$ and $M^o_{\ell_2+1}(2;\beta\ \gamma_1\cdots\gamma_{\ell_2})$.

(iv) Sum freely the Cartesian label of each line over all directions and the lattice label of each internal vertex over all lattice sites.

(v) To find $\mathcal{M}_{\alpha\beta}(12)$, sum the contributions according to the above rule of all topologically distinct graphs with the two fixed vertices 1 and 2.*

The deviation of these rules is sketched in Appendix A. An example of a graph contributing to $\mathcal{M}_{\alpha\beta}(12)$ is shown in Fig. 1(a). Its contribution is

$$\frac{1}{2}\sum_{\gamma_1\cdots\gamma_7}\sum_{3,4,5,6}\Big(\prod_{i=1}^{7}\eta_{\gamma_i}\Big)\,v(12)v(13)v(23)v(34)^2v(25)v(56)$$
$$\times M^o_3(1;\alpha\gamma_1\gamma_2)M^o_4(2;\beta\gamma_1\gamma_3\bar{\gamma}_6)M^o_4(3;\gamma_2\gamma_3\gamma_4\gamma_5)$$
$$\times M^o_2(4;\gamma_4\gamma_5)M^o_2(5;\gamma_6\gamma_7)M^o_1(6;\gamma_7)\ .$$

---

*When the lattice points 1 and 2 are the same, there is an additional contribution $M_2(1;\alpha\beta)$ (see Eq. (2.11) below).

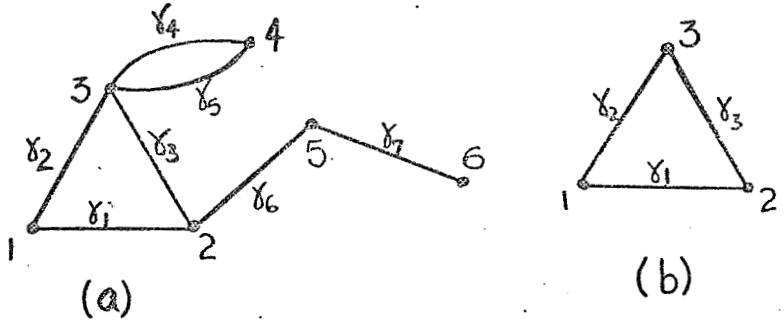

Figure 1. A reducible graph and its skeleton. (a) A graph contributing to $\mathcal{M}_{\alpha\beta}(12)$ in the unrenormalized theory. (b) The skeleton graph contributing to $\mathcal{M}_{\alpha\beta}(12)$ (and also $G_2(1;\gamma_1\gamma_2)$) in the renormalized theory.

In a uniform magnetic field the semi-invariants are independent of lattice site (although, of course, they still depend on the Cartesian indices). Thus, on specializing to the nearest-neighbor, zero-field situation (2.2), each graph G contributes a term of the form

$$\frac{v^n}{g}\, C[1,2;G] \sum_{\{\gamma\}} \Big(\prod_{\text{vertices}} M^0 \Big) \Big(\prod_{\text{lines}} \eta_\gamma \Big) , \qquad (2.10)$$

where $C[1,2;G]$ is the number of non-zero terms in the lattice sum A(iv) for fixed Cartesian labels γ. $C[1,2;G]$ is just the "embedding constant"[13,37] of the graph G with fixed points 1 and 2, i.e. the number of ways that the graph G can be embedded in the lattice with its external vertices on fixed sites 1 and 2, all internal vertices on lattice sites, and each line along a nearest-neighbor

bond. It is important to note at this point that the lattice sums in Rule A(iv) are free, i.e. two or more vertices may fall on the same lattice site. Thus, our "free" embedding constants are not those of Sykes et al.[37] A method of computing the free embedding constants* will be presented in Chapter III and elsewhere.**

The unrenormalized expansion described above is straightforward, but the number of contributing graphs increases very rapidly in high orders. It is more convenient in practice to perform a selective resummation which eliminates all "reducible graphs." A reducible graph in this context is a graph containing one or more parts (not containing either of the fixed points 1 or 2) which can be separated from the rest of the graph by cutting at a single point. Such parts are called reducible parts. Where a graph has been simplified by cutting away all its reducible parts, the remainder is called a skeleton. Skeletons are by construction irreducible. For example, Fig. 1(a) is reducible, having Fig. 1(b) as its irreducible skeleton.

By lumping together all graphs belonging to the same skeleton, one arrives at a renormalized prescription[35,36] for calculating $\mathcal{M}_{\alpha\beta}(12)$:

Rule B: Same as Rule A with the following exceptions:

(a) Replace M_ℓ^{0}'s by M_ℓ's (to be defined below) in A(ii) and (iii).

---

*Actually only irreducible graph embedding constants are needed (see below).

**D. Jasnow, M. Wortis and M. A. Moore (to be published).

(b) To find $\mathcal{M}_{\alpha\beta}$, sum over all topologically distinct irreducible graphs* in A(vi).

An example is provided by Fig. 1(b), which contributes to $\mathcal{M}_{\alpha\beta}(12)$

$$\sum_{\gamma_1\gamma_2\gamma_3} \sum_{3} \left(\prod_{i=1}^{3} \eta_{\gamma_i} \right) v(12)v(13)v(23)$$

$$\times M_3(1;\alpha\gamma_1\gamma_2)M_3(2;\beta\gamma_1\gamma_3)M_2(3;\gamma_2\gamma_3).$$

The renormalized semi-invariants M_ℓ are obtained in terms of self-energy parts,** G_n. $G_n(1;\alpha_1\cdots\alpha_n)$ is computed by considering irreducible graphs with one fixed, external vertex (labeled 1), into which come n lines with fixed, Cartesian labels $\alpha_1\cdots\alpha_n$. All additional lines and vertices are given dummy labels. Each graph contributes according to:

Rule C:

(i) Same as A(i).

(ii) For each internal vertex (e.g. 3) assign a factor $M_{\ell_3}(3;\gamma_1\cdots\gamma_{\ell_3})$.

(iii) To the vertex 1 assign a factor unity.

(iv) Sum freely over all dummy labels.

(v) Divide the result of (iv) by g', the symmetry factor for the graph with one fixed point.

---

*Stanley[34] lists necessary graphs for loose-packed lattices to order v^9 and close-packed lattices to order v^8. He calculates correlation functions for the isotropic Heisenberg model, but his method does not apply to the anisotropic case.

**The G_n's are analogs of the mass operator of many body theory; M^0_ℓ and M_ℓ are analogs of bare and renormalized propagators; Eq. (2.11) is an integral form of the Dyson equation, and the whole procedure of going from Rule A to Rule B is simply a propagator renormalization.

(vi) To find $G_n(1;\alpha_1\cdots\alpha_n)$, sum contributions from all topologically distinct irreducible graphs with <u>one</u> fixed point, 1, into which come n lines labeled $\alpha_1\cdots\alpha_n$.

The relation between M_ℓ and the G_n's is given by

$$M_\ell(1;\alpha_1\cdots\alpha_\ell)=\left[\exp\left(\sum_{n=1}\sum_{\gamma_1\cdots\gamma_n} G_n(1;\gamma_1\cdots\gamma_n)\frac{\delta^n}{\delta b_{\gamma_1}(1)\cdots\delta b_{\gamma_n}(1)}\right)\right]M^o_\ell(1;\alpha_1\cdots\alpha_\ell), \tag{2.11}$$

where the derivatives act only on the M^o_ℓ. An example of a graph contributing $G_2(1;\gamma_1\gamma_2)$ is shown in Fig. 1(b). Its contribution is,

$$\frac{1}{2}\sum_{\gamma_3}\sum_{2,3}\left(\prod_{i=1}^{3}\eta_{\gamma_i}\right)v(12)v(13)v(23)M_2(2;\gamma_1\gamma_3)M_2(3;\gamma_2\gamma_3)\ .$$

A derivation of the vertex renormalization of Rules B and C is given in Appendix B. Now, the G_n's depend on the interaction v(ij) and the M_n's, so that (2.11) has the form of a non-linear equation determining the M_ℓ's in terms of the M^o_n's and the interaction. The observation that G_n is at least order v^n allows (2.11) to be solved iteratively in powers of v at high temperatures.

The graphical simplification of Rule B carries with it the necessity of calculating the G_n graphs (Rule C) and unscrambling (2.11). In practice the limiting factor in our calculation was the rapid proliferation of graphs in higher orders.* M_2 was obtained

---

*Through 8^{th} order on the close-packed lattices one needs 71 graphs for the G_n's and 202 graphs for the spin-spin correlation function.

in analytic form to $O(v^7)$ as a function of the parameters η_α; other M_ℓ's were found to correspondingly lower order. These were fed (along with graphs, symmetry factors and embedding constants*) into a computer program which evaluated M_ℓ's to $O(v^8)$ and carried out the calculation of Rule B and the subsequent summations (2.8). This program ran in single precision on an IBM 7094 and took roughly three minutes per set of anisotropy parameters per lattice type. For a large fraction of the cases considered, the program was run in double precision on the IBM 360/75. We have obtained series for the triangle lattice, the three cubic lattices, and the spinel. Results for the f.c.c. lattice are presented in detail in Chapter V; in Appendix C the series for χ and μ_2 are presented for several combinations of the η_α on the various lattices.** The series for lattices other than the f.c.c. are somewhat less regular (particularly the two-dimensional lattices); therefore, it is more difficult to form reliable estimates of critical exponents. To demonstrate the difficulties the extreme case of the spinel lattice is presented in Chapter VII.

Careless errors tend to creep into this sort of graphical expansion. Our series agree with available series in the Ising[28]

---

*We point out that a relation exactly analogous to (2.10) holds, under conditions (2.2), for irreducible graphs contributing to G_n and $\mathcal{W}_{\alpha\beta}$. Embedding constants for irreducible graphs were input to the program.

**In addition, several specific heat series are given for the f.c.c. lattice only.

and isotropic Heisenberg[22,23] limits. In addition, our methods apply with only trivial modifications* to the Ising model with arbitrary spin. We have checked with available S = 1/2 Ising series.[30] These checks are quite comprehensive for the following reasons:

(a) All components of $\mathcal{M}_{\alpha\beta}(12)$ show up in the susceptibility (2.8a); thus a check of χ_α checks the complete $\mathcal{M}_{\alpha\beta}(12)$.

(b) Once a lattice was chosen, the only input variables were the η_α. Hence, a check of the series for one set of anisotropy parameters provides a check on the whole program.

In addition, there are internal checks. A fairly strong check is to calculate $\langle \underset{\sim}{S}(1)^2 \rangle \equiv 1$ as a power series in v. Terms of first order and higher must vanish identically. This, in addition, gives some indication of computer round-off.

C. Symmetry Properties

In this section various symmetries of the Hamiltonian (2.1), when applied to lattices with a simple sublattice structure, are pointed out. Such lattices support antiferromagnetic ordering under conditions (2.2), and the relations presented here connect the thermodynamic properties of the model under sign changes of some or all of the η_α. Quite general symmetry relations can be shown to hold, but for our purposes it is sufficient to consider $T > T_c$ and the situation (2.2) on loose-packed lattices.

---

*Appropriate changes in the renormalized semi-invariants are all that is required.

Consider the dimensionless free-energy, W, defined in (2.4b). It is quite easy to show that

$$W[\eta_x, \eta_y, \eta_z] = W[\pm\eta_x, \pm\eta_y, \pm\eta_z] \tag{2.12}$$

for any combination of the $\pm$ signs. A change in sign $\eta_\alpha \to -\eta_\alpha$ for any given α can be compensated by the corresponding change of variables, $S_\alpha(1) \to -S_\alpha(1)$, at all sites of one of the two sublattices. For any configuration of the spins on the lattice, these two transformations leave the value* of the Hamiltonian unchanged (under conditions (2.2)); since W is related to a sum (trace) over all configurations, it is left invariant. The generality of this and following results depends on the fact that we are dealing with classical spins. For finite spin there is an analogous relation involving simultaneous sign changes of two anisotropy parameters.** A special case of (2.12) is the change of sign of all three of the anisotropy parameters. However, that transformation is exactly equivalent to $v \to -v$; that is,

$$W[v] = W[-v] \, . \tag{2.13}$$

This relation is the basis for the statement that the ferromagnet and antiferromagnet, described by (2.1) under conditions (2.2) on a loose-packed lattice, behave symmetrically, and have the same

---

*For these classical models, such terminology is permissible.

**For finite spin, the transformation, $S_\alpha(1) \to -S_\alpha(1)$, for any two Cartesian components, α, is unitary.

critical temperature. The result (2.13) also implies that a series expansion of W in powers of v (high-temperature expansion) contains only even powers of v. This leads to the result that the expansion of the specific heat, C_α in (2.8c), in powers of v, contains only even terms.*

Similar results can be derived for the spin-spin correlation function. For $T > T_c$ and conditions (2.2) we need only consider

$$\mathcal{M}_{\alpha\alpha}(12) = \langle S_\alpha(1) S_\alpha(2) \rangle \ . \tag{2.14}$$

By arguments similar to those above for W, it can be shown that

$$\mathcal{M}_{xx}(12;\eta_x,\eta_y,\eta_z) = \mathcal{M}_{xx}+12;\eta_x,\pm\eta_y,\pm\eta_z). \ , \tag{2.15a}$$

and

$$\mathcal{M}_{xx}(12;-\eta_x,\pm\eta_y,\pm\eta_z) = P(12)\mathcal{M}_{xx}(12;\eta_x,\eta_y,\eta_z) \ . \tag{2.15b}$$

These hold for any combination of the $\pm$ signs. (2.15a) is independent of which sublattice the sites 1 and 2 belong to; but in (2.15b)

$$P(12) = \begin{cases} 1, & \text{if 1 and 2 are on same sublattice} \\ -1, & \text{if 1 and 2 on different sublattices} \end{cases} \ . \tag{2.16}$$

Analogous relations hold for $\mathcal{M}_{yy}$ and $\mathcal{M}_{zz}$. (2.15b) implies that when all three of the η_α change sign ($v \to -v$),

$$\mathcal{M}_{\alpha\alpha}(12;-v) = P(12)\mathcal{M}_{\alpha\alpha}(12;v) \ ,$$

so that in an expansion in powers of v, the correlation function

---

*It is for this reason that the loose-packed lattices are relatively useless in determining the specific heat index α.

of spins on the same (different) sublattice contains only even (odd) powers.

It is convenient to define a staggered susceptibility[38] and second moment by

$$\chi_\alpha^S = \sum_2{}' P(12)\pi_{\alpha\alpha}(12)$$

$$(\mu_2^\alpha)^S = \sum_2{}' |\underset{\sim}{R}_1 - \underset{\sim}{R}_2|^2 P(12)\pi_{\alpha\alpha}(12) \ . \qquad (2.17)$$

Imagine that there were a homogeneous magnetic field in the $+\alpha$-direction on sublattice A and an equal-in-magnitude but oppositely directed uniform field on sublattice B. Then χ_α^S has the physical interpretation: χ_α^S measures the linear response (in the limit of zero-field) of the α-component of the sublattice magnetization per site to the homogeneous magnetic field in the α-direction on the sublattice, under the above (staggered) conditions. Then (2.15) gives

$$\psi_x(\eta_x, \eta_y, \eta_z) = \psi(\eta_x, \pm\eta_y, \pm\eta_z)$$

and

$$\psi_x(-\eta_x, \eta_y, \eta_z) = \psi_x^S(\eta_x, \pm\eta_y, \pm\eta_z) \ , \qquad (2.18)$$

where ψ stands for χ and μ_2. (2.18) holds for any combination of the $\pm$ signs, and similar relations hold for ψ_y, ψ_z.

Equations (2.18) will be very important in the discussion of the results of the series analysis. In the first place, (2.18) means that for the loose-packed lattices only the cases of all $\eta_\alpha \geq 0$ need be considered. Second, a reinterpretation of the

indices γ and ν_1, (in the case of antiferromagnetism) in terms of the staggered susceptibility and second moment allows a unification of the results.

III. EMBEDDING CONSTANTS

In this chapter a method is given for calculating the embedding constants, C[1,2;G], for irreducible graphs, G, contributing to $\mathcal{M}_{\alpha\beta}(12)$ in the renormalized expansion. As defined in Chapter II, C[1,2;G] is the number of ways a graph G can be fit on the lattice with the external (fixed) points on lattice sites 1 and 2, all internal vertices on lattice sites, and each line connecting nearest-neighbors. The major problem in calculating C[1,2;G] is to be certain that two vertices connected by a line in G are always nearest-neighbor sites when G is fit on the lattice. Without loss of generality the site 1 may be taken to be the origin, in which case C[2;G] (or $C[\underset{\sim}{R};G]$) is written, indicating that the second external point of G is at site 2 (or at the site located at $\underset{\sim}{R}$).

It is important to point out that the methods used to derive $\mathcal{M}_{\alpha\beta}(12)$ in Chapter II are not restricted to the spin-S Ising model and our model. The spin-S anisotropic Heisenberg model can be formulated in this manner, allowing calculation of time-dependent correlation functions, and virtually any nearest-neighbor lattice model can be set up in this fashion.* A large variety of different lattice problems can be attacked by methods which require knowledge of the C[1,2;G].

*The calculation of the bare semi-invariants may become more difficult. For the Heisenberg model they become time-ordered expectation values of spin-operator products. Other models may require the iteration of an integral equation.

Several observations make the calculation of the embedding constants relatively easy:

(i) Multiple bonds directly connecting two vertices in a graph are irrelevant to the calculation of C[ ], and can be stripped away. This forms a new type of skeleton with, at most, one line connecting two vertices directly. In Fig. 2, (a) and (b) have the same skeleton, (c).

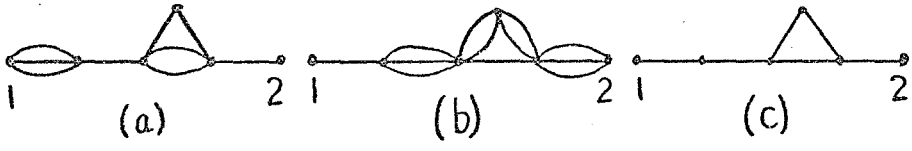

Figure 2. Removal of multiple lines in a graph in calculating C[1,2;G]. Graphs in (a) and (b) have the same skeleton (c).

(ii) Graphs G (ladder graphs), which when cut at external points 1 and 2, fall into two or more parts represented by graph types G_i, have

$$C[1,2;G] = \prod_i C[1,2;G_i] \,. \tag{3.1}$$

This type of reduction is shown in Fig. 3. There is a useful corollary to this observation: if there is a ladder of paths between any two vertices 3 and 4 (which may be the external vertices), one element of which is a single direct bond, the elements other than the direct bond can be stripped away. The C[1,2;G'] for the

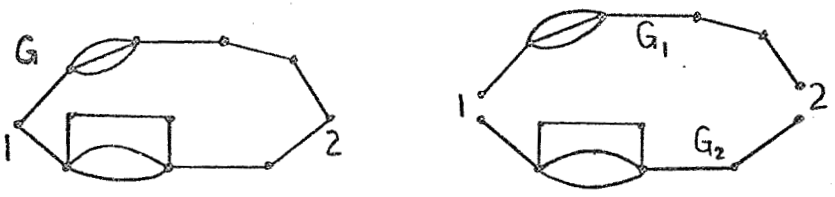

$$C[1,2;G] = C[1,2;G_1]C[1,2;G_2]$$

Figure 3. A ladder graph and its constituent parts G_1 and G_2.

remaining graph G' is multiplied by $\prod_i C[\underset{\sim}{\delta};G_i]$, where G_i make up the ladder elements stripped away, and $\underset{\sim}{\delta}$ is a nearest-neighbor lattice vector. An example is shown in Fig. 4.

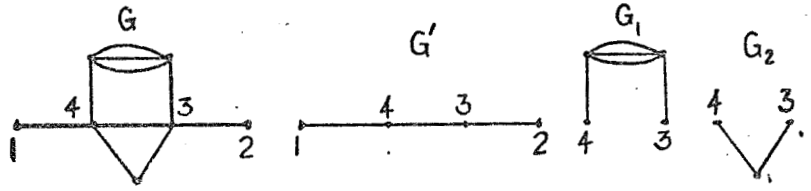

$$C[1,2;G] = C[1,2;G'] \times C[\underset{\sim}{\delta};G_i] \times C[\underset{\sim}{\delta};G_2]$$

Figure 4. A ladder of paths connecting 3 and 4, one path a direct bond.

(iii) If, in a graph G, <u>all</u> paths connecting 1 and 2 pass through a vertex, then that vertex is a <u>node</u> of the graph. If a graph G has a node, which we label 3, and the graph element connecting 1 to 3 is G_1, and the graph element connecting 3 to 2 is G_2,

$$C[1,2;G] = \sum_3 C[1,3;G_1]C[3,2;G_2] , \qquad (3.2)$$

where vertex 3 is summed over all the lattice sites. This relation is particularly useful when, say, G_2 consists of just a single direct bond. Then the sum is over the nearest-neighbors to the site 2. This situation is shown in Fig. 5. Of course the other

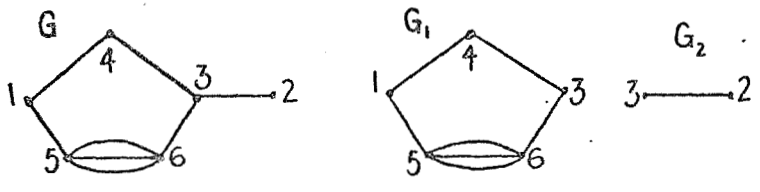

$$C[1,2;G] = \sum_{\underset{\sim}{\delta}} C[1,2+\underset{\sim}{\delta};G_1]C[2+\underset{\sim}{\delta},2;G_2]$$

Figure 5. The embedding constant for a graph with a node.

observations can be used to further simplify the elements making up the node diagram. In Fig. 5, G_1 is clearly a ladder graph connecting 1 to 3, and $C[1,2+\underset{\sim}{\delta};G_1]$ can be simplified by (ii).

(iv) When multiple bonds are stripped away as in (i), the remaining graphs are made up of chains, where a chain graph between two points, 3 and 4, has one path of single bond "links" connecting 3 to 4 (G' in Fig. 4 is a 3-chain, a chain of three bonds). When {C[1,2;n-chain]} is known completely, all the ingredients are available for finding the C[ ] for a large class of graphs (see below). The chain constants are built up from the embedding constant of the 1-chain using (iii) above. The embedding constant for the 1-chain between sites 1 and 2 is unity, if 1 and 2 are nearest-neighbors ($\underset{\sim}{R}_1$-$\underset{\sim}{R}_2$ is of the type $\underset{\sim}{\delta}$), and zero otherwise.

Knowing this fact, use of (iii) yields the 2-chain constants; and in general, knowledge of the n-chain constants is sufficient to determine the n+1-chain constants. Consider an n-chain connecting 1 to 2 (the external vertices), and give the label 3 to the vertex connected directly to 2. Notice that the vertex labeled 3 is a node of the special type shown in Fig. 5; that is, the graph element connecting 3 to 2 is a single bond (1-chain). From (3.2) and the discussion that follows,

$$C[1,2;\text{n-chain}] = \sum_{\underset{\sim}{\delta}} C[1,2+\underset{\sim}{\delta};\text{n-1-chain}] \ , \qquad (3.3)$$

since $C[2+\underset{\sim}{\delta},2;\text{1-chain}] = 1$. To illustrate the procedure we consider a square lattice and give the chain graph embedding constants up to the 3-chain. To calculate, say, $C[\underset{\sim}{R};\text{3-chain}]$ for $\underset{\sim}{R} = (2,1)$, note

Table 2. Square lattice n-chain embedding constants for the n-chain connecting the origin to $\underset{\sim}{R}$.

$\underset{\sim}{R}$	0,0	1,0	1,1	2,0	2,1	3,0
1-chain	0	1	0	0	0	0
2-chain	4	0	2	1	0	0
3-chain	0	9	0	0	3	1

that the nearest-neighbors of $\underset{\sim}{R}$ are (3,1), (1,1), (2,2), (2,0). The 2-chain embedding constant to each of these sites is 0, 2, 0, 1, respectively. The sum in (3.3) is then equal to 3, which is the proper entry in Table 2.

(v) If $\underset{\sim}{R}$ and $\underset{\sim}{R}'$ can be transformed into one another by the point symmetry operations of the lattice, $C[\underset{\sim}{R};G] = C[\underset{\sim}{R}';G]$, for all graphs G. In particular, lattice reflection symmetry implies $C[-\underset{\sim}{R};G] = C[\underset{\sim}{R};G]$. This means that a graph which is asymmetrical under an interchange of labeling of the external vertices, $1 \leftrightarrow 2$, has the same embedding constants for both relative orientations on the lattice.

Because the chain graph embedding constants are so important, two checks are mentioned, the second providing an alternate scheme to the one presented in (iv), for calculating $C[\underset{\sim}{R};n\text{-chain}]$. In the first place,

$$\sum_{\underset{\sim}{R}} C[\underset{\sim}{R};n\text{-chain}] = z^n , \tag{3.4}$$

where z is the coordination number of the lattice. This follows because the sum in (3.4) is the total number of unrestricted random walks of n steps on the lattice (steps only allowed between nearest-neighbor sites). Second, the embedding constant can be written

$$C[1,2;n\text{-chain}] = \sum_{3,4\cdots} \epsilon(13)\epsilon(34)\cdots\epsilon(n+1,2), \tag{3.5}$$

where

$$\epsilon(34) = \begin{cases} 1, & \text{if 3 and 4 are nearest-neighbors} \\ 0, & \text{otherwise} \end{cases} . \tag{3.6}$$

Taking Fourier transforms, assuming a three-dimensional lattice,

$$C[1,2;n\text{-chain}] = V \int \frac{d^3q}{(2\pi)^3} (\epsilon(\underset{\sim}{q}))^n e^{i\underset{\sim}{q}\cdot(\underset{\sim}{R}_1-\underset{\sim}{R}_2)} , \tag{3.7}$$

where the integral is over the first Brillouin zone, V is the volume of the unit cell, and

$$\epsilon(\underset{\sim}{q}) = \sum_{\underset{\sim}{\delta}} e^{-i\underset{\sim}{q}\cdot\underset{\sim}{\delta}} \quad . \tag{3.8}$$

As stated in Chapter II, the irreducible graphs necessary to calculate $\mathcal{M}_{\alpha\beta}(12)$ (using the renormalized expansion), through $\mathcal{O}(v^8)$ on the close-packed and through $\mathcal{O}(v^9)$ on the loose-packed lattices, have been listed by Stanley[34] (who connects the external vertices with a wavy "correlation line"). We adhere to Stanley's notation, in which a graph (for $\mathcal{M}_{\alpha\beta}(12)$) is denoted by (n,t), where n is the number of lines and t is the index specifying the topological type. The graphs are unlabeled, and ones which are asymmetrical under external point interchange are drawn only once.* By convention (n,1) is chosen to be the n-chain.

In the lists of nearly three hundred graphs, the embedding constants for only one basic type cannot be calculated for any lattice using the observations of this chapter. The anomalous graphs are just those which fall outside the convolution approximation[35] (hyper-netted chain), and are based on graphs referred to as <u>elementary</u> in the terminology of De Dominicis.[39] In Fig. 6 these graphs are drawn, and in Table 3 the embedding constants on the various lattices are given. Once the C[1,2;n,t] for these types are known,

---

*They must, however, be considered with both possible external vertex labelings in calculating $\mathcal{M}_{\alpha\beta}(12)$.

Table 3. The embedding constants $C[\underset{\sim}{R};n,t]$ for the anomalous graphs.*

square

n,t \ $\underset{\sim}{R}$	0,0	1,1	2,0	1,0	2,1	3,0
7,34	0	0	0	0	0	0
8,12	36	12	4	0	0	0
8,62	0	0	0	0	0	0
9,16	0	0	0	64	8	1

triangle

0,0	1,0	1,1	2,0
12	0	2	0
90	16	16	6
24	16	6	4
—	—	—	—

s.c.

n,t \ $\underset{\sim}{R}$	0,0,0	1,1,0	2,0,0	1,0,0	1,1,1	2,1,0	3,0,0
7,34	0	0	0	0	0	0	0
8,12	90	16	6	0	0	0	0
8,62	0	0	0	0	0	0	0
9,16	0	0	0	160	24	8	1

f.c.c.

0,0,0	1,1,0	2,0,0	2,1,1	2,2,0
48	4	8	2	0
540	88	96	32	12
192	88	48	22	8
—	—	—	—	—

b.c.c.

n,t \ $\underset{\sim}{R}$	0,0,0	2,0,0	2,2,0	2,2,2	1,1,1	3,1,1	3,3,1	3,3,3
7,34	0	0	0	0	0	0	0	0
8,12	216	72	24	8	0	0	0	0
8,62	0	0	0	0	0	0	0	0
9,16	0	0	0	0	512	64	8	1

spinel

0,0,0	1,0,0	2,0,0	2,-1,0
12	2	0	0
78	16	6	6
24	16	2	2
—	—	—	—

*$\underset{\sim}{R}$ given in terms of the lattice vectors defined in Chapter II. A graph has the same embedding constants for all sites related by the point symmetry operations of the lattice. A dash (—) indicates the particular constant is not needed for the order series which have been calculated.

the embedding constants for graphs which contain them as ladder elements or sections of node graphs can be calculated using observations (ii)-(v). In addition graphs which have the same skeleton in the sense of (i) have the same embedding constants.

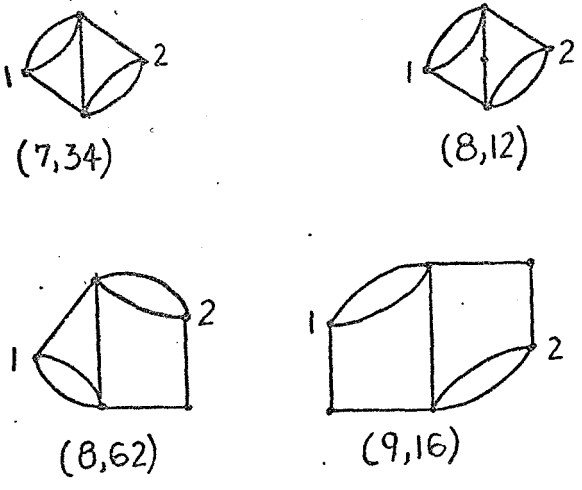

Fig. 6. The anomalous graphs for which the embedding constants cannot be calculated simply, using (i)-(v).

In Table 4, the symmetry factors (Rule A(v), Chapter II) for all graphs (n,t) listed by Stanley[34] are given, and the embedding constants, for all but the anomalous graphs, of Fig. 6, are given by an application of (i)-(v) above. For completeness, all necessary embedding constants are listed, for the f.c.c. lattice, in Table 5.

Table 4. Symmetry factors and embedding constants for correlation graphs, (n,t).

Notation

$\Delta(\underset{\sim}{R},\underset{\sim}{\delta}) = \begin{cases} 1, & \underset{\sim}{R} = \underset{\sim}{\delta}, \text{ any nearest-neighbor lattice vector} \\ 0, & \text{otherwise} \end{cases}$

$C_n \equiv C[\underset{\sim}{\delta};n,1]$ = embedding constant for the n-chain to a nearest-neighbor site.

$\sum \Longrightarrow$ sum over the z nearest-neighbor vectors $\{\underset{\sim}{\delta}\}$.

p = "parity" index = $\left\{ \begin{array}{l} \text{s, graph symmetric} \\ \text{a, graph asymmetric} \end{array} \right\}$ under interchange of external (fixed) vertices 1 $\longleftrightarrow$ 2.

(n',t') entry $\Longrightarrow$ (n,t) and (n',t') have same skeleton and, hence, same embedding constants.

* See Table 3.

---

n,t	g,p	$C[\underset{\sim}{R};n,t]$	n,t	g,p	$C[\underset{\sim}{R};n,t]$
1,1	1,s	$\Delta(\underset{\sim}{R},\underset{\sim}{\delta})$	5,6	2,s	$C_2^2\Delta(\underset{\sim}{R},\underset{\sim}{\delta})$
2,1	1,s	$\sum C[\underset{\sim}{R}+\underset{\sim}{\delta};1,1]$	5,7	2,a	$C_2C[\underset{\sim}{R};2,1]$
3,1	1,s	$\sum C[\underset{\sim}{R}+\underset{\sim}{\delta};2,1]$	5,8	4,s	(4,3)
3,2	6,s	(1,1)	6,1	1,s	$\sum C[\underset{\sim}{R}+\underset{\sim}{\delta};5,1]$
4,1	1,s	$\sum C[\underset{\sim}{R}+\underset{\sim}{\delta};3,1]$	6,2	6,a	(4,1)
4,2	6,a	(2,1)	6,3	6,a,	(4,1)
4,3	2,s	$C_2\Delta(\underset{\sim}{R},\underset{\sim}{\delta})$	6,4	2,a	$C_3C[\underset{\sim}{R};2,1]$
5,1	1,s	$\sum C[\underset{\sim}{R}+\underset{\sim}{\delta};4,1]$	6,5	6,s	$C[\underset{\sim}{R};2,1]^3$
5,2	2,s	$C_3\Delta(\underset{\sim}{R},\underset{\sim}{\delta})$	6,6	4,s	$C[\underset{\sim}{R};2,1]^2$
5,3	6,a	(3,1)	6,7	36,s	(2,1)
5,4	6,s	(3,1)	6,8	120,a	(2,1)
5,5	120,s	(1,1)	6,9	2,s	$C_4\Delta(\underset{\sim}{R},\underset{\sim}{\delta})$
			6,10	1,s	$C_2C_3\Delta(\underset{\sim}{R},\underset{\sim}{\delta})$

Table 4 (continued)

n,t	g,p	$C[\underset{\sim}{R};n,t]$
6,11	2,a	$C_2C[\underset{\sim}{R};3,1]$
6,12	2,s	$C_2C[\underset{\sim}{R};3,1]$
6,13	2,a	$C_2^2C[\underset{\sim}{R};2,1]$
6,14	2,a	$C_2^2\Delta(\underset{\sim}{R},\underset{\sim}{\delta})$
6,15	4,a	(5,7)
6,16	12,a	(4,3)
6,17	24,s	(4,3)
7,1	1,s	$\sum C[\underset{\sim}{R}+\underset{\sim}{\delta};6,1]$
7,2	6,a	$\sum C[\underset{\sim}{R}+\underset{\sim}{\delta};6,5]$
7,3	2,a	$C_3C[\underset{\sim}{R};3,1]$
7,4	2,s	$C_3^2\Delta(\underset{\sim}{R},\underset{\sim}{\delta})$
7,5	2,s	$C_3C[\underset{\sim}{R};3,1]$
7,6	2,s	$C_5\Delta(\underset{\sim}{R},\underset{\sim}{\delta})$
7,7	6,a	(5,1)
7,8	6,a	(5,1)
7,9	6,s	(5,1)
7,10	4,a	$\sum C[\underset{\sim}{R}+\underset{\sim}{\delta};6,6]$
7,11	4,a	$C[\underset{\sim}{R};7,10]\Delta(\underset{\sim}{R},\underset{\sim}{\delta})$
7,12	12,a	(5,2)
7,13	36,a	(3,1)
7,14	24,s	(5,2)
7,15	120,a	(3,1)
7,16	120,s	(3,1)
7,17	12,s	(5,2)
7,18	36,s	(3,1)
7,19	8,s	(5,2)
7,20	5040,s	(1,1)
7,21	2,s	$C[\underset{\sim}{R};2,1]^2C[\underset{\sim}{R};3,1]$
7,22	1,a	$C_2C_3C[\underset{\sim}{R};2,1]$
7,23	2,a	$C_2^2C[\underset{\sim}{R};3,1]$
7,24	2,s	$C_2^2C[\underset{\sim}{R};3,1]$
7,25	1,s	$C_2^3\Delta(\underset{\sim}{R},\underset{\sim}{\delta})$
7,26	2,a	$C_2^2C[\underset{\sim}{R};2,1]$
7,27	2,a	$C_2C[\underset{\sim}{R};2,1]^2$
7,28	2,a	$C_2^2C[\underset{\sim}{R};2,1]$
7,29	1,s	$C_4C_2\Delta(\underset{\sim}{R},\underset{\sim}{\delta})$
7,30	2,a	$C_2C[\underset{\sim}{R};4,1]$
7,31	2,a	$C_4C[\underset{\sim}{R};2,1]$
7,32	2,a	$C_2C[\underset{\sim}{R};4,1]$
7,33	4,s	$C[\underset{\sim}{\delta};7,34]\Delta(\underset{\sim}{R},\underset{\sim}{\delta})$
7,34	4,s	*
7,35	2,a	$C_3C_2\Delta(\underset{\sim}{R},\underset{\sim}{\delta})$
7,36	4,s	$C[\underset{\sim}{R};3,1]C[\underset{\sim}{R};2,1]$
7,37	4,a	(6,11)
7,38	4,s	(6,12)
7,39	12,s	(5,6)
7,40	24,a	(5,7)
7,41	4,a	(6,14)
7,42	6,a	(5,6)
7,43	12,a	(5,7)
7,44	12,a	(5,7)
7,45	12,a	(5,7)
7,46	24,s	(4,3)
7,47	48,a	(4,3)
8,1	1,s	$\sum C[\underset{\sim}{R}+\underset{\sim}{\delta};7,1]$
8,2	6,a	$\sum C[\underset{\sim}{R}+\underset{\sim}{\delta};7,2]$
8,3	6,s	$\sum C[\underset{\sim}{R}+\underset{\sim}{\delta};7,2]$
8,4	2,a	$C_3^2C[\underset{\sim}{R};2,1]$
8,5	2,s	$C[\underset{\sim}{R};2,1]^2C[\underset{\sim}{R};4,1]$
8,6	4,a	$C[\underset{\sim}{\delta};7,11]C[\underset{\sim}{R};2,1]$
8,7	4,a	$C[\underset{\sim}{\delta};7,11]C[\underset{\sim}{R};2,1]$
8,8	2,a	$C_3C[\underset{\sim}{R};4,1]$

Table 4 (continued)

n,t	g,p	$C[\underset{\sim}{R};n,t]$	n,t	g,p	$C[\underset{\sim}{R};n,t]$
8,9	2,a	$c_3C[\underset{\sim}{R};4,1]$	8,41	2,a	$c_2^2C[\underset{\sim}{R};4,1]$
8,10	2,a	$c_5C[\underset{\sim}{R};2,1]$	8,42	2,a	$c_2^2C[\underset{\sim}{R};4,1]$
8,11	2,a	$c_3C[\underset{\sim}{R};2,1]^2$	8,43	2,a	$c_2C[\underset{\sim}{\delta};7,11]\Delta(\underset{\sim}{R},\underset{\sim}{\delta})$
8,12	4,s	*	8,44	4,a	$C[\underset{\sim}{R};2,1]C[\underset{\sim}{R};7,10]$
8,13	12,a	(6,5)	8,45	2,a	$c_2C[\underset{\sim}{R};7,10]$
8,14	4,a	$\sum C[\underset{\sim}{R}+\underset{\sim}{\delta};7,10]$	8,46	2,a	$c_2C[\underset{\sim}{R};7,10]$
8,15	4,s	$\sum C[\underset{\sim}{R}+\underset{\sim}{\delta};7,10]$	8,47	1,s	$c_3c_4\Delta(\underset{\sim}{R},\underset{\sim}{\delta})$
8,16	4,s	$C[\underset{\sim}{R};4,1]C[\underset{\sim}{R};2,1]$	8,48	2,a	$c_4C[\underset{\sim}{R};3,1]$
8,17	6,a	(6,1)	8,49	2,s	$c_4C[\underset{\sim}{R};3,1]$
8,18	6,a	(6,1)	8,50	1,s	$c_5c_2\Delta(\underset{\sim}{R},\underset{\sim}{\delta})$
8,19	6,a	(6,1)	8,51	2,a	$c_2C[\underset{\sim}{R};5,1]$
8,20	24,a	(6,4)	8,52	2,a	$c_2C[\underset{\sim}{R};5,1]$
8,21	8,a	(6,4)	8,53	2,s	$c_2^2C[\underset{\sim}{R};5,1]$
8,22	12,a	(6,4)	8,54	1,a	$c_2^2c_3\Delta(\underset{\sim}{R},\underset{\sim}{\delta})$
8,23	12,a	(6,4)	8,55	2,a	$c_2c_3C[\underset{\sim}{R};2,1]$
8,24	12,a	(6,4)	8,56	2,a	$c_2c_3C[\underset{\sim}{R};2,1]$
8,25	12,a	(6,4)	8,57	2,a	$c_2C[\underset{\sim}{R};3,1]C[\underset{\sim}{R};2,1]$
8,26	48,a	(6,6)	8,58	2,a	$c_2^2C[\underset{\sim}{R};3,1]$
8,27	24,a	(6,6)	8,59	2,a	$c_2^2C[\underset{\sim}{R};3,1]$
8,28	120,a	(4,1)	8,60	2,a	$c_2^2C[\underset{\sim}{R};3,1]$
8,29	120,a	(4,1)	8,61	2,a	$C[\underset{\sim}{\delta};8,62]\Delta(\underset{\sim}{R},\underset{\sim}{\delta})$
8,30	36,s	(4,1)	8,62	4,a	*
8,31	36,a	(4,1)	8,63	4,a	$\sum C[\underset{\sim}{R}+\underset{\sim}{\delta};7,34]$
8,32	36,a	(4,1)	8,64	4,a	$c_2^3\Delta(\underset{\sim}{R},\underset{\sim}{\delta})$
8,33	36,a	(4,1)	8,65	12,a	(6,13)
8,34	5040,a	(2,1)	8,66	6,a	(6,13)
8,35	720,a	(2,1)	8,67	6,a	(6,13)
8,36	2,a	$\sum C[\underset{\sim}{R}+\underset{\sim}{\delta};7,21]$	8,68	2,a	$C[\underset{\sim}{\delta};8,69]\Delta(\underset{\sim}{R},\underset{\sim}{\delta})$
8,37	1,a	$c_2c_3C[\underset{\sim}{R};3,1]$	8,69	4,a	$\sum C[\underset{\sim}{R}+\underset{\sim}{\delta};7,36]$
8,38	1,s	$c_2c_3C[\underset{\sim}{R};3,1]$	8,70	2,a	$c_2c_4\Delta(\underset{\sim}{R},\underset{\sim}{\delta})$
8,39	2,s	$C[\underset{\sim}{R};3,1]^2C[\underset{\sim}{R};2,1]$	8,71	4,a	$c_2C[\underset{\sim}{R};4,1]$
8,40	1,a	$c_2c_4C[\underset{\sim}{R};2,1]$	8,72	4,a	$c_2C[\underset{\sim}{R};4,1]$

Table 4 (continued)

n,t	g,p	$C[\underset{\sim}{R};n,t]$
8,73	2,s	$C_6\Delta(\underset{\sim}{R},\underset{\sim}{\delta})$
8,74	6,s	(6,10)
8,75	24,a	(6,11)
8,76	24,s	(6,12)
8,77	4,s	$C_2C_3\Delta(\underset{\sim}{R},\underset{\sim}{\delta})$
8,78	4,a	$C_2C_3\Delta(\underset{\sim}{R},\underset{\sim}{\delta})$
8,79	8,s	(7,36)
8,80	4,a	$C_2C_3\Delta(\underset{\sim}{R},\underset{\sim}{\delta})$
8,81	6,a	(6,10)
8,82	12,a	(6,11)
8,83	12,a	(6,11)
8,84	12,a	(6,12)
8,85	4,a	(8,78)
8,86	12,a	(6,11)
8,87	12,a	(6,12)
8,88	6,a	(6,10)
8,89	4,s	(8,77)
8,90	12,a	(6,11)
8,91	6,s	(6,10)
8,92	12,a	(6,14)
8,93	24,a	(6,14)
8,94	48,a	(5,7)
8,95	48,a	(5,7)
8,96	8,a	(6,14)
8,97	12,a	(6,14)
8,98	12,a	(6,14)
8,99	24,a	(5,7)
8,100	24,s	(6,9)
8,101	12,a	(6,9)
8,102	12,a	(6,9)
8,103	720,s	(4,3)
8,104	144,a	(4,3)
8,105	240,a	(4,3)
8,106	1,a	$C_2{}^3C[\underset{\sim}{R};2,1]$
8,107	1,s	$C_2{}^2C[\underset{\sim}{R};2,1]^2$
8,108	2,s	$C_2C[\underset{\sim}{\delta};7,33]\Delta(\underset{\sim}{R},\underset{\sim}{\delta})$
8,109	4,a	$C[\underset{\sim}{\delta};7,33]C[\underset{\sim}{R};2,1]$
8,110	2,a	$C_2C[\underset{\sim}{R};7,34]$
8,111	4,s	$C[\underset{\sim}{R};2,1]C[\underset{\sim}{R};7,34]$
8,112	12,s	$C_2{}^3\Delta(\underset{\sim}{R},\underset{\sim}{\delta})$
8,113	12,a	(6,13)
8,114	2,a	$C_2{}^3\Delta(\underset{\sim}{R},\underset{\sim}{\delta})$
8,115	4,s	$C_{2_2}{}^2C[\underset{\sim}{R};2,1]$
8,116	4,a	$C_{2_2}{}^2C[\underset{\sim}{R};2,1]$
8,117	4,a	$C_2{}^2C[\underset{\sim}{R};2,1]$
8,118	8,a	(7,33)
8,119	8,s	(7,34)
8,120	8,s	(5,6)
8,121	12,a	(6,14)
8,122	24,a	(5,7)
8,123	72,s	(4,3)
9,1	1,s	$\sum C[\underset{\sim}{R}+\underset{\sim}{\delta};8,1]$
9,2	6,s	$C[\underset{\sim}{R};3,1]^3$
9,3	2,a	$C_3{}^2C[\underset{\sim}{R};3,1]$
9,4	2,s	$C_3{}^2C[\underset{\sim}{R};3,1]$
9,5	2,a	$\sum C[\underset{\sim}{R}+\underset{\sim}{\delta};8,5]$
9,6	6,a	$\sum C[\underset{\sim}{R}+\underset{\sim}{\delta};8,2]$
9,7	6,a	$\sum C[\underset{\sim}{R}+\underset{\sim}{\delta};8,2]$
9,8	1,s	$C_3C_5\Delta(\underset{\sim}{R},\underset{\sim}{\delta})$
9,9	2,a	$C_3C[\underset{\sim}{R};5,1]$
9,10	2,a	$C_3C[\underset{\sim}{R};5,1]$
9,11	2,s	$C_3C[\underset{\sim}{R};5,1]$
9,12	2,a	$C_5C[\underset{\sim}{R};3,1]$
9,13	2,s	$C_5C[\underset{\sim}{R};3,1]$

Table 4 (continued)

n,t	g,p	C[$\underset{\sim}{R}$;n,t]	n,t	g,p	C[$\underset{\sim}{R}$;n,t]
9,14	2,s	$C[\underset{\sim}{\delta};9,16]\Delta(\underset{\sim}{R},\underset{\sim}{\delta})$	9,46	12,a	(7,3)
9,15	4,a	$\sum C[\underset{\sim}{R}+\underset{\sim}{\delta};8,12]$	9,47	12,s	(7,4)
9,16	4,s	*	9,48	24,a	(7,3)
9,17	12,a	$C[\underset{\sim}{\delta};7,2]\Delta(\underset{\sim}{R},\underset{\sim}{\delta})$	9,49	24,s	(7,5)
9,18	12,a	(7,2)	9,50	8,a	(7,11)
9,19	12,a	(7,2)	9,51	12,a	(7,11)
9,20	36,a	(7,2)	9,52	12,a	(7,11)
9,21	2,a	$C[\underset{\sim}{\delta};9,22]\Delta(\underset{\sim}{R},\underset{\sim}{\delta})$	9,53	24,a	(7,10)
9,22	4,a	$\sum C[\underset{\sim}{R}+\underset{\sim}{\delta};8,16]$	9,54	24,a	(7,10)
9,23	4,a	$\sum C[\underset{\sim}{R}+\underset{\sim}{\delta};8,14]$	9,55	24,a	(7,10)
9,24	4,a	$\sum C[\underset{\sim}{R}+\underset{\sim}{\delta};8,14]$	9,56	24,a	(7,11)
9,25	2,s	$C_7\Delta(\underset{\sim}{R},\underset{\sim}{\delta})$	9,57	48,a	(7,11)
9,26	6,a	(7,1)	9,58	48,a	(7,10)
9,27	6,a	(7,1)	9,59	48,a	(7,10)
9,28	6,a	(7,1)	9,60	24,s	$C_5\Delta(\underset{\sim}{R},\underset{\sim}{\delta})$
9,29	6,s	(7,1)	9,61	120,a	(5,1)
9,30	4,a	$C_3{}^2\Delta(\underset{\sim}{R},\underset{\sim}{\delta})$	9,62	120,a	(5,1)
9,31	4,s	$C_3{}^2\Delta(\underset{\sim}{R},\underset{\sim}{\delta})$	9,63	120,s	(5,1)
9,32	8,s	$C[\underset{\sim}{R};3,1]^2$	9,64	12,a	$C_5\Delta(\underset{\sim}{R},\underset{\sim}{\delta})$
9,33	8,a	(7,3)	9,65	36,a	(5,1)
9,34	8,s	(7,5)	9,66	36,a	(5,1)
9,35	4,s	$C_3{}^2\Delta(\underset{\sim}{R},\underset{\sim}{\delta})$	9,67	12,a	$C_5\Delta(\underset{\sim}{R},\underset{\sim}{\delta})$
9,36	6,s	(7,4)	9,68	36,s	(5,1)
9,37	12,s	(7,5)	9,69	36,a	(5,1)
9,38	12,a	(7,3)	9,70	36,s	(5,1)
9,39	12,a	(7,3)	9,71	12,s	$C_5\Delta(\underset{\sim}{R},\underset{\sim}{\delta})$
9,40	4,a	$C_3{}^2\Delta(\underset{\sim}{R},\underset{\sim}{\delta})$	9,72	36,a	(5,1)
9,41	6,a	(7,4)	9,73	2,a	$C_3C[\underset{\sim}{\delta};7,11]\Delta(\underset{\sim}{R},\underset{\sim}{\delta})$
9,42	12,a	(7,5)	9,74	2,a	$C_3C[\underset{\sim}{R};7,10]$
9,43	12,a	(7,3)	9,75	2,a	$C_3C[\underset{\sim}{R};7,10]$
9,44	12,a	(7,3)	9,76	4,a	$C[\underset{\sim}{R};3,1]C[\underset{\sim}{R};7,10]$
9,45	12,a	(7,5)	9,77	4,a	$C[\underset{\sim}{\delta};7,11]C[\underset{\sim}{R};3,1]$

Table 4 (continued)

n,t	g,p	C[$\underset{\sim}{R}$;n,t]	n,t	g,p	C[$\underset{\sim}{R}$;n,t]
9,78	4,a	C[$\underset{\sim}{\delta}$;7,11]C[$\underset{\sim}{R}$;3,1]			
9,79	4,a	C[$\underset{\sim}{\delta}$;7,11]C[$\underset{\sim}{R}$;3,1]			
9,80	720,a	(5,2)			
9,81	5040,a	(3,1)			
9,82	5040,s	(3,1)			
9,83	144,a	(5,2)			
9,84	240,a	(5,2)			
9,85	720,a	(3,1)			
9,86	720,a	(3,1)			
9,87	144,s	(5,2)			
9,88	240,s	(5,2)			
9,89	720,a	(3,1)			
9,90	72,s	(5,2)			
9,91	72,a	(5,2)			
9,92	216,s	(3,1)			
9,93	48,s	(5,2)			
9,94	96,a	(5,2)			
9,95	96,s	(5,2)			
9,96	9!,s	(1,1)			

Table 5. Complete non-vanishing embedding constants C[R;n,t] for the f.c.c. lattice. 6-,7-, and 8-chain constants given separately.*

SITES

n,t \ R	000	110	200	211	220	310	222	321	400	411	330	420	332
1,1	0	1	0	0	0								
2,1	12	4	4	2	1								
3,1	48	45	24	18	12	9	6	3	0	0	1	0	0
3,2	0	1	0	0	0								
4,1	540	360	288	204	148	96	72	52	36	24	24	16	12
4,2	12	4	4	2	1								
4,3	0	4	0	0									
5,1	4320	3520	2640	2080	1600	1240	960	710	480	370	405	280	220
5,2	0	45	0	0	0								
5,3	48	45	24	18	12	9	6	3	0	0	1	0	0
5,4	48	45	24	18	12	9	6	3	0	0	1	0	0
5,5	0	1	0	0	0								
5,6	0	16	0	0	0								
5,7	48	16	16	8	4								
5,8	0	4	0	0	0								
6,2	Each entry same as for (4,1)												
6,3	Each entry same as for (4,1)												
6,4	540	180	180	90	45								
6,5	1728	64	64	8	1								
6,6	144	16	16	4	1								
6,7	12	4	4	2	1								
6,8	12	4	4	2	1								
6,9	0	360	0	0	0								
6,10	0	180	0	0	0								
6,11	192	180	96	72	48	36	24	12	0	0	4	0	0
6,12	192	180	96	72	48	36	24	12	0	0	4	0	0
6,13	192	64	64	32	16								
6,14	0	16	0	0	0								
6,15	48	16	16	8	4								
6,16	0	4	0	0	0								
6,17	0	4	0	0	0								

* $\underset{\sim}{R}$ given in terms of the cubic unit cell lattice vectors. The triplet ijk is written without commas for lack of space.

Table 5 (continued)

	SITES										
n,t \ R	422	510	431	521	440	530	433	442	532	541	550
4,1	6	0	4	0	1	0	0	0	0	0	0
5,1	160	100	115	50	40	25	30	20	10	5	1

Table 5 (continued)

SITES

n,t \ R	000	110	200	211	220	310	222	321	400	411	330	420	332
7,2	768	2145	288	210	96	81	24	9	0	0	1	0	0
7,3	2160	2025	1080	810	540	405	270	135	0	0	45	0	0
7,4	0	2025	0	0	0								
7,5	2160	2025	1080	810	540	405	270	135	0	0	45	0	0
7,6	0	3520	0	0	0								
7,7	Each entry same as for (5,1)												
7,8	Each entry same as for (5,1)												
7,9	Each entry same as for (5,1)												
7,10	192	257	80	58	32	25	12	5	0	0	1	0	0
7,11	0	257	0	0	0								
7,12	0	45	0	0	0								
7,13	48	45	24	18	12	9	6	3	0	0	1	0	0
7,14	0	45	0	0									
7,15	48	45	24	18	12	9	6	3	0	0	1	0	0
7,16	48	45	24	18	12	9	6	3	0	0	1	0	0
7,17	0	45	0	0	0								
7,18	48	45	24	18	12	9	6	3	0	0	1	0	0
7,19	0	45	0	0	0								
7,20	0	1	0	0	0								
7,21	6912	720	384	72	12								
7,22	2160	720	720	360	180								
7,23	768	720	384	288	192	144	96	48	0	0	16	0	0
7,24	768	720	384	288	192	144	96	48	0	0	16	0	0
7,25	0	64	0	0	0								
7,26	192	64	64	32	16								
7,27	576	64	64	16	4								
7,28	192	64	64	32	16								
7,29	0	1440	0	0	0								
7,30	Each entry 4 times entry for (4,1)												
7,31	4320	1440	1440	720	360								
7,32	Each entry 4 times entry for (4,1)												
7,33	0	4	0	0	0								
7,34	48	4	8	2	0								
7,35	0	180	0	0	0								
7,36	576	180	96	36	12								
7,37	192	180	96	72	48	36	24	12	0	0	4		
7,38	192	180	96	72	48	36	24	12	0	0	4		
7,39	0	16	0	0	0								
7,40	48	16	16	8	4								

Table 5 (continued)

SITES

n,t \ R	000	110	200	211	220	310	222	321	400	411	330	420	332
7,41	0	16	0	0	0								
7,42	0	16	0	0	0								
7,43	48	16	16	8	4								
7,44	48	16	16	8	4								
7,45	48	16	16	8	4								
7,46	0	4	0	0	0								
7,47	0	4	0	0	0								
8,2	25740	10860	9744	5394	3184	984	684	430	324	180	132	100	42
8,3	25740	10860	9744	5394	3184	984	684	430	324	180	132	100	42
8,4	24300	8100	8100	4050	2025	0	0						
8,5	77760	5760	4608	816	148								
8,6	3084	1028	1028	514	257								
8,7	3084	1028	1028	514	257								
8,8	24300	16200	12960	9180	6660	4320	3240	2340	1620	1080	1080	720	540
8,9	24300	16200	12960	9180	6660	4320	3240	2340	1620	1080	1080	720	540
8,10	42240	14080	14080	7040	3520								
8,11	6480	720	720	180	45								
8,12	540	88	96	32	12								
8,13	1728	64	64	8	1								
8,14	3084	1644	1360	846	560	288	204	138	100	60	52	36	22
8,15	3084	1644	1360	846	560	288	204	138	100	60	52	36	22
8,16	6480	1440	1152	408	148								
8,17	Each entry same as for (6,1)												
8,18	Each entry same as for (6,1)												
8,19	Each entry same as for (6,1)												
8,20	540	180	180	90	45								
8,21	540	180	180	90	45								
8,22	540	180	180	90	45								
8,23	540	180	180	90	45								
8,24	540	180	180	90	45								
8,25	540	180	180	90	45								
8,26	144	16	16	4	1								
8,27	144	16	16	4	1								
8,28	Each entry same as for (4,1)												
8,29	Each entry same as for (4,1)												
8,30	Each entry same as for (4,1)												
8,31	Each entry same as for (4,1)												

Table 5 (continued)

n,t	R	SITES											
		422	510	431	521	440	530	433	600	442	611	532	620	541
8,2	18	0	10	0	1	0	0							
8,3	18	0	10	0	1	0	0							
8,8	270	0	180	0	45	0	0							
8,9	270	0	180	0	45	0	0							
8,14	10	0	6	0	1	0	0							
8,15	10	0	6	0	1	0	0							

Table 5 (continued)

SITES

n,t \ R	000	110	200	211	220	310	222	321	400	411	330	420	332
8,32	Each entry same as for (4,1)												
8,33	Each entry same as for (4,1)												
8,34	12	4	4	2	1								
8,35	12	4	4	2	1								
8,36	8640	10860	3168	1992	1008	540	216	84	0	0	12	0	0
8,37	8640	8100	4320	3240	2160	1620	1080	540	0	0	180	0	0
8,38	8640	8100	4320	3240	2160	1620	1080	540	0	0	180	0	0
8,39	27648	8100	2304	648	144								
8,40	17280	5760	5760	2880	1440								
8,41	Each entry 16 times entry for (4,1)												
8,42	Each entry 16 times entry for (4,1)												
8,43	0	1028											
8,44	2304	1028	320	116	32								
8,45	768	1028	320	232	128	100	48	20	0	0	4	0	0
8,46	768	1028	320	232	128	100	48	20	0	0	4	0	0
8,47	0	16200	0	0	0								
8,48	17280	16200	8640	6480	4320	3240	2160	1080	0	0	360	0	0
8,49	17280	16200	8640	6480	4320	3240	2160	1080	0	0	360	0	0
8,50	0	14080	0	0	0								
8,51	Each entry 4 times entry for (5,1)												
8,52	Each entry 4 times entry for (5,1)												
8,53	Each entry 4 times entry for (5,1)												
8,54	0	720	0	0	0								
8,55	2160	720	720	360	180								
8,56	2160	720	720	360	180								
8,57	2304	720	384	144	48								
8,58	768	720	384	288	192	144	96	48	0	0	16	0	0
8,59	768	720	384	288	192	144	96	48	0	0	16	0	0
8,60	768	720	384	288	192	144	96	48	0	0	16	0	0
8,61	0	88	0	0	0								
8,62	192	88	48	22	8								
8,63	48	88	24	20	12	12	6	2	0	0			
8,64	0	64	0	0	0								
8,65	192	64	64	32	16								
8,66	192	64	64	32	16								
8,67	192	64	64	32	16								
8,68	0	1644	0	0	0								
8,69	2160	1644	864	552	324	180	108	48	0	0	12	0	0

Table 5 (continued)

	SITES												
n,t \ R	000	110	200	211	220	310	222	321	400	411	330	420	332
8,70	0	1440	0	0	0								
8,71	Each entry 4 times entry for (4,1)												
8,72	Each entry 4 times entry for (4,1)												
8,73	0	33600	0	0	0								
8,74	0	180	0	0	0								
8,75	192	180	96	72	48	36	24	12	0	0	4		
8,76	192	180	96	72	48	36	24	12	0	0	4		
8,77	0	180	0	0	0								
8,78	0	180	0	0	0								
8,79	576	180	96	36	12								
8,80	0	180	0	0	0								
8,81	0	180	0	0	0								
8,82	192	180	96	72	48	36	24	12	0	0	4		
8,83	192	180	96	72	48	36	24	12	0	0	4		
8,84	192	180	96	72	48	36	24	12	0	0	4		
8,85	0	180	0	0	0								
8,86	192	180	96	72	48	36	24	12	0	0	4		
8,87	192	180	96	72	48	36	24	12	0	0	4		
8,88	0	180	0	0	0								
8,89	0	180	0	0	0								
8,90	192	180	96	72	48	36	24	12	0	0	4		
8,91	0	180	0	0	0								
8,92	0	16	0	0	0								
8,93	0	16	0	0	0								
8,94	48	16	16	8	4								
8,95	48	16	16	8	4								
8,96	0	16	0	0	0								
8,97	0	16	0	0	0								
8,98	0	16	0	0	0								
8,99	48	16	16	8	4								
8,100	0	360	0	0	0								
8,101	0	360	0	0	0								
8,102	0	360	0	0	0								
8,103	0	4	0	0	0								
8,104	0	4	0	0	0								
8,105	0	4	0	0	0								
8,106	768	256	256	128	64								
8,107	2304	256	256	64	16								
8,108	0	16	0	0	0								

Table 5 (continued)

SITES

n,t \ R	000	110	200	211	220	310	222	321	400	411	330	134	332
8,109	48	16	16	8	4								
8,110	192	16	32	8	0								
8,111	576	16	32	4	0								
8,112	0	64	0	0	0								
8,113	192	64	64	32	16								
8,114	0	64	0	0	0								
8,115	192	64	64	32	16								
8,116	192	64	64	32	16								
8,117	192	64	64	32	16								
8,118	0	4	0	0	0								
8,119	48	4	8	2	0								
8,120	0	16	0	0	0								
8,121	0	16	0	0	0								
8,122	48	16	16	8	4								
8,123	0	4	0	0	0								

Table 5 (continued)

SITES

n,t	0,0,0	1,1,0	2,0,0	2,1,1	2,2,0	3,1,0	2,2,2
6,1	42240	33600	27360	21900	17565	13800	11160
7,1	403200	336525	277200	229950	189700	155925	129150
8,1	4038300	3413200	2889600	2441320	2060296	1728160	1463280
	3,2,1	4,0,0	4,1,1	3,3,0	4,2,0	3,3,2	4,2,2
6,1	8850	6840	5400	5500	4260	3450	2610
7,1	105385	84000	69090	70581	56560	47040	37800
8,1	1227128	1015840	853440	862512	715904	607096	501956
	5,1,0	4,3,1	5,2,1	4,4,0	5,3,0	4,3,3	6,0,0
6,1	1800	2040	1110	936	660	720	400
7,1	28945	30562	19005	15904	12369	13020	8400
8,1	402080	418488	280784	239540	193984	200816	147840
	4,4,2	6,1,1	5,3,2	6,2,0	5,4,1	6,2,2	6,3,1
6,1	540	300	300	225	216	120	90
7,1	10332	6790	7931	5460	5019	3500	2772
8,1	165068	122640	133728	101584	90440	69216	57008
	4,4,4	7,1,0	5,5,0	5,4,3	6,4,0	7,2,1	6,3,3
6,1	90	0	60	60	36	0	20
7,1	2520	1225	1897	1925	1344	735	1050
8,1	51240	31360	40208	41104	31360	21168	25536

Table 5 (continued)

SITES

n,t	5,5,2	6,4,2	7,3,0	7,3,2	6,5,1	8,0,0	8,1,1
6,1	30	15	0	0	6	0	0
7,1	1134	812	441	245	364	0	0
8,1	26824	20748	14112	9296	10920	4900	3920

	7,4,1	5,5,4	8,2,0	6,4,4	6,5,3	8,2,2	6,6,0
6,1	0	0	0	0	0	0	1
7,1	147	210	0	140	105	0	84
8,1	6048	7280	3136	5600	4424	1960	3480

	7,5,0	7,4,3	8,3,1	6,6,2	7,5,2	8,4,0	8,3,3
7,1	49	35	0	42	21	0	0
8,1	2464	2408	1568	2128	1512	784	560

	8,4,2	7,6,1	6,5,5	6,6,4	7,5,4	8,5,1	7,6,3
7,1	0	7	0	0	0	0	0
8,1	448	568	560	420	280	224	168

	8,4,4	7,7,0	8,5,3	8,6,0	7,7,2	8,6,2	8,7,1
7,1	0	1	0	0	0	0	0
8,1	70	112	56	64	56	28	8

	8,8,0
8,1	1

The graphs for the G_n's can be found from the lists of $\mathcal{M}_{\alpha\beta}(12)$ (correlation) graphs by a simple (but somewhat redundant*) prescription. To determine the graphs contributing to G_ℓ, just put together the external vertices of all $\mathcal{M}_{\alpha\beta}(12)$ graphs which have 1 line terminating at one of the external vertices and ℓ-1 lines terminating at the other. In Fig. 7(a) and (b) this process is demonstrated. In Fig. 7(c) the redundancy is indicated, since two different correlation graphs, (a) and (c), yield the same G_4 graph, (b).

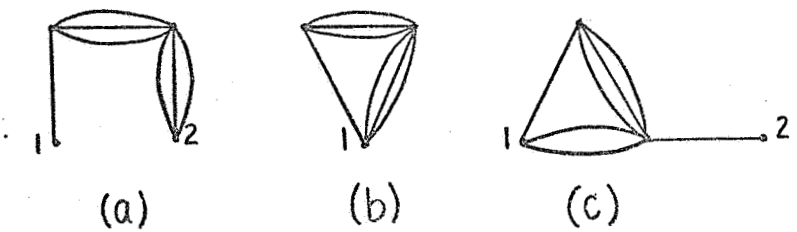

Figure 7. Forming a G_4 graph from a correlation graph. (a) Graph contributing to $\mathcal{M}_{\alpha\beta}(12)$. (b) G_4 graph from (a) by putting external vertices together. (c) Second correlation graph yielding G_4 graph, (b).

*Use of the completely renormalized formulation of the expansion of $\mathcal{M}_{\alpha\beta}(12)$, based on the work of De Dominicis,[39] yields the G_n contributions without redundancy. M. Wortis, M. A. Moore, D. Jasnow (to be published).

By Rule C of Chapter II, each distinct topological type is considered, and duplicate graphs must be eliminated before evaluating a G_n. The graphs used to get the G_n's can be asymmetrical under interchange $1 \leftrightarrow 2$, but both labelings yield the same G_n graph. This means that for the purposes of finding G_n graphs, the lists of unlabeled correlation graphs are sufficient.

In Table 6 we present a set of correlation graphs which, using the above prescription, yields the necessary G_n graphs to calculate $\mathcal{M}_{\alpha\beta}(12)$ (in zero-field) through $\mathcal{O}(v^8)$ on close-packed and $\mathcal{O}(v^9)$ on loose-packed lattices.* For each graph we give the symmetry factor, g', (calculated by Rule C (v) of Chapter II) for the corresponding G_n graph with 1 external vertex. In calculating G_n, the embedding constants of the corresponding correlation graphs (Tables 3,4), for $\underset{\sim}{R} = \underset{\sim}{0}$, can be used.

To calculate χ, μ_2 or any moment of the correlation function, a rearrangement of the graphical expansion can prove useful. As shown in Chapter II, in zero-field with $T > T_c$, $\mathcal{M}_{\alpha\alpha}(12)$ can be written (see Eq. (2.10))

$$\mathcal{M}_{\alpha\alpha}(12) = \sum_{G} W[G]C[1,2;G] + M_2(1;\alpha\alpha)\delta(12), \tag{3.9}$$

where W[G] is the "weight" of a graph, G, contributing to $\mathcal{M}_{\alpha\alpha}(12)$, and depends only on the topology of the graph (it is independent of the fixed lattice points 1 and 2). W[G] is given symbolically by

---

*For $T > T_c$ and zero magnetic field, the G_n's for odd n vanish to all orders.

Table 6. Set of correlation graphs (n,t) which yield the G_ℓ graphs. g' is the symmetry factor of the corresponding G_ℓ graph.

	n,t	g'	n,t	g'	n,t	g'	n,t	g'
G_2	2,1	2	7,1	2	8,1	2	8,38	2
	3,1	2	7,5	4	8,3	12	8,42	2
	4,1	2	7,8	6	8,8	2	8,49	4
	5,1	2	7,9	12	8,15	8	8,52	2
	5,4	12	7,16	240	8,18	6	8,53	4
	6,1	2	7,24	4	8,19	6	8,59	2
	6,3	6	7,32	2	8,29	120	8,72	4
	6,12	4	7,38	8	8,30	72	8,76	48
							8,84	12
G_4	4,2	24	7,7	6	8,10	6	8,45	2
	5,3	6	7,10	4	8,14	8	8,46	4
	6,2	6	7,13	36	8,21	32	8,55	8
	6,11	4	7,26	8	8,24	36	8,56	4
	6,15	16	8,2	24	8,25	36	8,63	8
	7,2	6	8,4	4	8,36	2	8,67	12
	7,3	2	8,6	16	8,40	2	8,95	192
							8,116	12
G_6	6,8	720	7,45	72	8,23	72	8,75	48
	7,15	120	8,20	120	8,66	12	8,94	96
G_8	8,34	8!						

$$\frac{1}{g} v^n \sum_{\{\gamma\}} \Big(\prod_{\substack{\text{vertices} \\ \text{in } G}} M \Big) \Big(\prod_{\substack{\text{lines} \\ \text{in } G}} \eta_\gamma \Big)$$

if G has n lines. The m^{th} moment of correlations is defined by

$$\mu_m^\alpha = \sum_2 |\underset{\sim}{R}_1 - \underset{\sim}{R}_2|^m \, \pi_{\alpha\alpha}(12). \tag{3.10}$$

Using (3.9), this can be written (for non-negative m)

$$\mu_m^\alpha = \sum_G W[G] \sum_2 |\underset{\sim}{R}_1 - \underset{\sim}{R}_2|^m \, C[1,2;G] + M_2(1;\alpha\alpha)\delta(m,0) \, . \tag{3.11}$$

m = 0 corresponds to χ and m = 2 corresponds to μ_2, defined in (2.8). The quantities,

$$T_m[G] = \sum_2 |\underset{\sim}{R}_1 - \underset{\sim}{R}_2|^m \, C[1,2;G] \tag{3.12}$$

have been tabulated for the various lattices, for m = 0,2.* $T_0[G]$ has the interpretation of the "total embedding constant" for a graph G, i.e. the total number of ways it can be fit on a lattice with all possible relative positions of the external points. It is pointed out once again that these constants can be used in a large variety of lattice problems.

---

*They are available on request from the author.

IV. ANALYSIS OF SERIES

The methods by which the critical point and the critical exponents are extracted from the high-temperature series are described in this chapter. The extrapolations are by no means rigorous, but, as mentioned in Chapter I, they provide, systematically, a set of successive approximations to the quantities of interest. The results must be judged on the apparent consistency of the various methods of extrapolation and on the regularity and "rapidity of convergence" of the successive estimates. The excellent general performance of these methods, in the few cases in which exact results are known, has increased the confidence with which they are used.

The chapter is divided into several subsections describing, in general, the location of the critical point and the evaluation of the critical indices. The methods employed rely heavily on the use of the Neville Table (section A) and apply, in the form stated, to the close-packed lattices. The series for the loose-packed lattices require slight modification (section G) of the methods presented. The basic principles are the same, however. Unless otherwise stated, all examples in this chapter are for the f.c.c. lattice.

Suppose $F(v)$ is one of the functions to be studied (χ, μ_2, $C_{H=0}$); it is known through a finite number of terms in its expansion,

$$F(v) = \sum_{l=0}^{L} f_l v^l + R(v) , \qquad (4.1)$$

where $R(v) = \sum_{l=L+1}^{\infty} f_l v^l$ is the unknown remainder. The circle of

convergence of the series for F(v) passes through the singularity (or singularities) of the function which lie nearest the origin. In addition, the nearest singularity in the physical region* of the v-plane will generally be identified with the critical point. In the series analyzed, the known coefficients are all positive, indicating (if the trend continues) that a singularity at $v = v_c$ on the positive real axis is on the circle of convergence.[40] It is assumed[15] that the coefficients f_n have the asymptotic form

$$f_n \sim A\left(\frac{1}{v_c}\right)^n n^g, \text{ as } n \to \infty , \tag{4.2}$$

since, by Appell's comparison theorem,[41] (4.2) implies

$$F \sim \frac{B}{(v_c - v)^{1+g}} , \quad v \to v_c^- \text{ (along real axis)}, \tag{4.3}$$

for $g > -1$.** If all the coefficients f_n are non-negative, the converse is true by the theorem of Hardy and Littlewood,[42] namely, (4.3), in turn, implies (4.2). All available evidence[3-5] indicates that (4.3) is the form taken by the quantities represented by F.

Analysis of the series essentially reduces to fitting the asymptotic behavior of the coefficients to the form (4.2), which is the starting point of the ratio test analysis.[15] Forming the ratios

---

*The physical region corresponds to positive temperature. Hence, if the exchange interaction $J > 0$, the positive real axis of the v-plane is the physical domain.

**For g a negative integer, F has logarithmic behavior. For $g < -1$, the singular part of F behaves as in (4.3). See the review by M. E. Fisher,[3] for example.

$$\rho_n \equiv f_n/f_{n-1} \ , \tag{4.4}$$

we take Eq. (4.2) literally; this suggests that for large n, the asymptotic behavior of ρ_n is

$$\rho_n \sim \frac{1}{v_c}\left(1 + \frac{g}{n} + O(\frac{1}{n^2})\right), \ n \to \infty \ . \tag{4.5}$$

The leading dependence on 1/n yields the familiar result that if one plots the numbers ρ_n vs. 1/n, the limiting straight line through the points intersects the 1/n = 0 axis at the critical point $1/v_c = kT_c/J \equiv t_c$, and the limiting slope is g/v_c. The rapidity with which the ρ_n settle down to linear behavior is indicative of the approach to the asymptotic form (4.3). There are numerous examples of this type of extrapolation in the literature.[3,15]

A. The Neville Table

To aid in the extrapolation procedure we form the Neville Table[21,43] (N.T.). The construction of the table for an arbitrary sequence $\{z_n\}$ is demonstrated. The sequence of linear extrapolants $\{\ell_n^{(1)}\}$, quadratic extrapolants $\{\ell_n^{(2)}\}$, etc., are formed by:

$$\ell_n^{(0)} \equiv z_n$$

$$\ell_n^{(p)} = \frac{1}{p}[n\ell_n^{(p-1)} - (n-p)\ell_{n-1}^{(p-1)}] \ , \ p=1,2,\ldots \ . \tag{4.6}$$

The number $\ell_n^{(p)}$ is just the intercept at the 1/n = 0 axis of the curve of the p^{th} degree drawn through the p+1 successive points $z_n, z_n-1,\ldots,z_{n-p}$, with $\{z_n\}$ considered a function of 1/n. The

sequences $\{\ell_n^{(p)}\}$ are displayed in a tabular form called the Neville Table. The various sequences give estimates for the extrapolation of $1/n = 0$ of the sequence $\{z_n\}$ allowing for curvature of successively higher degree. For example, if

$$z_n = z'(1 + \frac{a}{n} + \frac{b}{n^2}) \text{ , for all n,}$$

the sequences $\{\ell_n^{(2)}\}, \{\ell_n^{(3)}\}, \cdots$ would all be constant and equal to z'. If a and b were both positive, the sequence $\{\ell_n^{(1)}\}$ would monotonically increase toward the value z'.

B. Finding the Critical Point

There are two basic methods used to extrapolate to the value of $t_c = 1/v_c$ for a given series F(v). The first is to form the N.T. for the sequence $\{\rho_n\}$. Then, as described in the example above, each sequence of extrapolants should tend to the value $1/v_c = t_c$, as defined in Eq. (4.5). If higher order terms in 1/n are not important in (4.5), then the early sequences should provide a good estimate of $1/v_c$. An example of this type of N.T. for the series $\chi_z(0,0,1)$ is shown in Table 7.

If one has an estimate, g', for the value g appearing in Eq. (4.2), then one can form the sequence of estimates $\{t_n\}$ for t_c, where

$$t_n = \frac{n\rho_n}{n+g'} \quad . \tag{4.7}$$

The second method for extrapolating the value $t_c = 1/v_c$ is then to form the N.T. for the sequence $\{t_n\}$. The sequence of extrapolants

Table 7. Neville Table for $\{\rho_n\}$ from $\chi_z(0,0,1)$. Entries are estimates of t_c.

n	ρ_n	$\ell_n^{(1)}$	$\ell_n^{(2)}$	$\ell_n^{(3)}$
2	3.8000			
3	3.7263	3.5789		
4	3.6804	3.5428	3.5066	
5	3.6503	3.5299	3.5105	3.5132
6	3.6292	3.5234	3.5106	3.5106
7	3.6135	3.5194	3.5093	3.5076
8	3.6014	3.5168	3.5091	3.5087

should again approach t_c. An example of this type N.T. for $\chi_z(0,0,1)$ is shown in Table 8.

C. Evaluating the Critical Index

Two basic methods are used to determine the critical index g defined in Eq. (4.2). Given an estimate $t'_c = 1/v'_c$ to t_c, the sequence of estimates $\{g_n\}$ to g can be formed, where[15,44]

$$g_n = n\left[\frac{\rho_n}{t'_c} - 1\right]. \tag{4.8}$$

From Eq. (4.5) $\{g_n\} \to g$ as 1/n if the estimate t'_c is good.* Then one can form the N.T. for the sequence $\{g_n\}$. An example of this type of N.T. is shown in Table 9 for the same case $\chi_z(0,0,1)$.

It is felt that a method for finding g which does not rely on a choice of t_c should be used as a check. The procedure due to Stanley[23] is to form the sequence $\{g_n\}$, where

$$g_n = n\left[\frac{\rho_n}{\ell_n^{(1)}} - 1\right]. \tag{4.9}$$

The number $\ell_n^{(1)}$ is given by Eq. (4.6) with $\{\rho_n\}$ in place of the general sequence $\{z_n\}$. Then Eq. (4.5) implies that $\{g_n\} \to g$ as 1/n. The extrapolation is performed by forming the N.T. for the sequence $\{g_n\}$. The method is good if the early variations in the series are not too large; that is, if $\{\ell_n^{(1)}\}$ converges smoothly and quickly to t_c. This procedure is not successful, therefore, if

*This means that $\frac{|t_c - t'_c|}{t_c} \ll \frac{1}{L}$, where L is the number of terms available in the series for F(v). This is usually satisfied in practice.

Table 8. The Neville Table for the sequence $\{t_n\}$ defined in (4.7) for $\chi_z(0,0,1)$ using $g' = 0.25$.

n	t_n	$\ell_n^{(1)}$	$\ell_n^{(2)}$	$\ell_n^{(3)}$	$\ell_n^{(4)}$
2	3.3778				
3	3.4397	3.5635			
4	3.4639	3.5367	3.5100		
5	3.4765	3.5267	3.5118	3.5130	
6	3.4840	3.5216	3.5112	3.5106	3.5094
7	3.4889	3.5182	3.5097	3.5077	3.5055
8	3.4923	3.5160	3.5093	3.5088	3.5098

Table 9. Neville Table for $\{g_n = (\gamma-1)_n\}$ from $\chi_z(0,0,1)$ using Eq. (4.8) with $t'_c = 3.509$.

n	g_n	$\ell_n^{(1)}$	$\ell_n^{(2)}$	$\ell_n^{(3)}$
2				
3	.1858			
4	.1954			
5	.2014	.2252		
6	.2055	.2261	.2278	
7	.2085	.2262	.2266	.2250
8	.2107	.2263	.2264	.2260

$\{\rho_n\}$ shows a high degree of curvature.* In general, the method is useful in determining trends in the series.

D. Specific Methods for the Second-Moment Series

Two other techniques were used to reduce the second moment series data. Recalling that $\mu_2 \sim (T-T_c)^{-(2\nu_1+\gamma)}$, it is advantageous to form a series involving only ν_1.[30] To do this one need only divide the series, $R(v) = \mu_2(v)/\chi(v)$. Then $R(v)$ has the asymptotic behavior

$$R(v) \sim (v_c - v)^{-2\nu_1} ,$$

and is studied by the methods described above. Alternatively,[30] one may form the sequence $\{\overline{(r^2)}_n\}$, where

$$\overline{(r^2)} = b_n/a_n$$

with b_n the coefficient of v^n in the second moment series and a_n the coefficient of v^n in χ. Recalling the asymptotic behavior assumed for the $\{a_n\}$ and $\{b_n\}$, the generating function

$$Q(v) \equiv \sum_n \overline{(r^2)}_n v^n \sim \frac{1}{(1-v)^{2\nu_1+1}} , \quad v \to 1^- .$$

The important feature here is that $Q(v)$ has radius of convergence equal to unity. This allows an estimate of $(2\nu_1)$ without knowledge of v_c. The series $Q(v)$ may be studied by the methods described above,

---

*That appears to be the case for the second moment series.

as if the critical point were known exactly. As a final consistency check, the series for[45]

$$\frac{d}{dv} \ln Q(v)$$

has been formed for several cases. Each coefficient is then an estimate of the quantity $2\nu_1+1$.

E. The "n-shift" Method

An alternative means of taking account of $1/n^2$ terms in (4.5) is the "n-shift" method.[3,9,30] Instead of forming the linear extrapolants $\{\ell_n^{(1)}\}$ from the ρ_n as shown in (4.6), the sequence $\{\ell_n^{(1)}(\epsilon)\}$ is formed, where

$$\ell_n^{(1)}(\epsilon) = (n+\epsilon)\rho_n - (n+\epsilon-1)\rho_{n-1} . \tag{4.10}$$

In practice, several values of ϵ of order unity are tried, and the results taken together give an indication of the trends in the series. There is usually a choice of ϵ which yields the smoothest $\{\ell_n^{(1)}(\epsilon)\}$, and this sequence can be extrapolated as in (4.6), or n-shift extrapolated. Table 10 shows the results of an n-shift analysis for t_c on $\chi_z(0,0,1)$. The N.T. for the same case, Table 7 should be compared with these results for consistency.

To find a sequence of estimates for the particular critical index, (4.8) is modified to read

$$g_n(\epsilon) = (n+\epsilon)\left[\frac{\rho_n}{t_c'} - 1\right] . \tag{4.11}$$

Again, several values of ϵ can be tried to obtain a smooth sequence

Table 10. n-shift estimates for t_c using (4.10) on $\chi_z(0,0,1)$.

n	$\ell_n^{(1)}(0)$	$\ell_n^{(1)}(\frac{1}{2})$	$\ell_n^{(1)}(1)$	$\frac{1}{2}[\ell_n^{(1)}(\frac{1}{2})+\ell_n^{(1)}(1)]$
3	3.5789	3.5421	3.5053	
4	3.5428	3.5198	3.4969	
5	3.5299	3.5148	3.4998	3.5073
6	3.5234	3.5129	3.5023	3.5076
7	3.5194	3.5116	3.5037	3.5076
8	3.5168	3.5108	3.5047	3.5078

which can itself be extrapolated by n-shifts or other techniques. The sequences $\{g_n(\epsilon)\}$, which should approach γ-1, for several values of ϵ in the sample case $\chi_z(0,0,1)$, are shown in Table 11. These should be compared, for consistency, with the N.T., Table 9, for the same case.

F. Method of Padé Approximants

The method of Padé Approximants[20,46] has been used to support results from the ratio tests. Best results came from using the value v_c from the ratio tests as input in the Padé analysis. The Padé results were fairly consistent with results of other methods.

We adhere to the notation of Fisher[3] in which the approximant is the ratio of two polynomials, the numerator of order L and the denominator of order M. As an example, a few of the results from approximants to $\frac{d}{dv}$ ln $\chi_z(0,0,1)$ are listed in Table 12. These results should be compared to those by the N.T. and n-shift methods, for the same sample case, given in tables above.

G. Modification for Loose-Packed Lattices

The sequences $\{\rho_n\}$ for the loose-packed lattices customarily have alternating behavior* superimposed on what appears to be a smooth trend.[3,15] This is presumably a reflection of the enhancement of antiferromagnetic behavior due to the sublattice

---

*This is shown clearly in several figures in the paper by H. E. Stanley,[23] for example.

Table 11. n-shift estimates for $(\gamma-1)$ using (4.11) on $\chi_z(0,0,1)$ with $t'_c = 3.509$.

n	$g_n(0)$	$g_n(\frac{1}{2})$	$g_n(1)$
3	.1858	.2168	.2477
4	.1954	.2198	.2443
5	.2014	.2215	.2416
6	.2055	.2226	.2397
7	.2085	.2233	.2382
8	.2107	.2238	.2370

Table 12. Estimates of t_c and γ from Padé Approximants to $\frac{d}{dv} \log \chi_z(0,0,1)$.

[L,M]	t_c	γ
[1,1]	3.5778	1.125
[2,2]	3.5200	1.191
[2,3]	2.5157	1.200
[3,2]	3.5147	1.202
[3,3]	3.5076	1.225
[3,4]	3.5107	1.213
[4,3]	3.5122	1.210

structure. As shown in Chapter II, for loose-packed lattices under conditions (2.2), the free-energy is invariant under the replacement $v \to -v$. Under the same replacement the ferromagnetic physical (staggered) susceptibility goes into the antiferromagnetic staggered (physical) susceptibility. The very plausible additional assumption of a unique critical point leads one to suppose (for example, in the case of the ferromagnetic physical susceptibility) that there is, at $v = -v_c$ on the circle of convergence, a singularity due to the (weak) anomaly in the antiferromagnetic physical susceptibility. While this additional singularity is always asymptotically dominated by the stronger singularity at $v = v_c$, it nevertheless slows the approach to the limiting behavior.

To smooth out the alternations it is possible to form the sequence $\{\tilde{\rho}_n\}$, where

$$\tilde{\rho}_n = [f_n/f_{n-2}]^{\frac{1}{2}}, \tag{4.12}$$

in addition to the sequence defined in (4.4). The asymptotic form for $\tilde{\rho}_n$ is also given by (4.5), so the n-shift analysis can be performed on the sequence $\{\tilde{\rho}_n\}$ as well as on $\{\rho_n\}$.* The only change that should be made is that alternate (rather than successive) points should be extrapolated. For loose-packed lattices, (4.10) should be rewritten

$$\mathcal{L}_n^{(1)}(\epsilon) = \frac{1}{2}[(n+\epsilon)\rho_n - (n+\epsilon-2)\rho_{n-2}], \tag{4.13}$$

*The oscillations are not smoothed out completely by forming $\{\tilde{\rho}_n\}$, so N.T. extrapolations as described above, will be very erratic. Of course the N.T. extrapolations for $\{\rho_n\}$ will be even more irregular. To use the N.T. method, the alternate terms must be considered to form two separate sequences. This is impractical with the number of terms available.

but to obtain smoother sequences of estimates for t_c,

$$\tilde{\chi}_n^{(1)}(\epsilon) = \frac{1}{2}[(n+\epsilon)\tilde{\rho}_n - (n+\epsilon-2)\tilde{\rho}_{n-2}] \tag{4.14}$$

should be used. Similarly (4.11) should be modified to read

$$g_n(\epsilon) = (n+\epsilon)\left[\frac{\tilde{\rho}_n}{t'_c} - 1\right], \tag{4.15}$$

for generally better results.

Even with these modifications of the basic ratio method, accurate extrapolation for loose-packed lattices is difficult. It is frequently helpful to draw 1/n plots of the various sequences to help estimate the limit points.

To show the extent of the alternations, in Table 13 we give $\{g_n(\epsilon)\}$ calculated from (4.11) and (4.15) for $\chi_z(0,0,1)$ on the b.c.c. lattice.

H. Comments

We have dealt at length with the methods used to extract information from the series. The series analyzed in this work converge more slowly to their asymptotic behavior than one is used to in Ising model studies, and the presence of curvature is the norm rather than the exception. The N.T. is a good way to perform the extrapolation under these conditions. Systematizing the extrapolation procedure by means of the N.T. is therefore felt warranted.

The use of N.T.'s is definitely not a cure-all. When series are regular but, for example, the ρ_n sequence is curved (as indicated by linear extrapolants), the N.T. helps one estimate the

Table 13. Estimates of γ-1, calculated from (4.11) and (4.15) for $\chi_z(0,0,1)$ on the b.c.c. lattice. $t'_c = 2.299$.

	From (4.11)			From (4.15)		
n	$g_n(-\frac{1}{2})$	$g_n(0)$	$g_n(\frac{1}{2})$	$g_n(-\frac{1}{2})$	$g_n(0)$	$g_n(\frac{1}{2})$
4	.1577	.1803	.2028	.2021	.2310	.2599
5	.1988	.2209	.2430	.2008	.2231	.2454
6	.1784	.1946	.2108	.2106	.2298	.2489
7	.2079	.2239	.2399	.2094	.2255	.2416
8	.1899	.2026	.2152	.2149	.2292	.2435
9	.2127	.2252	.2377	.2139	.2265	.2391

limit point of the sequence. When there is a change in trend, for example, in the ρ_n or in one of the sequences derived from it, the N.T. must be used with care in conjunction with the usual 1/n plot. Also, the $\{\mathcal{L}_n^{(p)}\}$ for the larger values of p are not reliable, as they depend on the early terms in the sequence. The early terms reflect the behavior of the system far from the critical region.

The method of n-shifts provides a good cross check on N.T. results. It too must be used with care, as a too-large n-shift can change the whole complexion of the series (reflected in the available terms). Taken together with the N.T. method, the n-shifts can provide an important consistency check. In addition, they are very valuable in analysis of series for the loose-packed lattices.

V. RESULTS

This chapter presents in detail the results of series analysis for the f.c.c. lattice. A careful analysis was also done on the b.c.c. series and gave the same critical indices as the f.c.c. except where specifically mentioned below. The b.c.c. series are somewhat more difficult to extrapolate reliably, because the loose-packed structure allows antiferromagnetic ordering as discussed in Chapters II and IV. Consequently the corresponding confidence limits for b.c.c. results are larger than f.c.c. in a ratio of roughly 3 to 2. Series for the triangle, simple cubic, and spinel lattices are quite irregular and do not allow precise estimation of critical exponents from the number of terms which we have derived. There is no indication that these lattices would not support our general f.c.c. and b.c.c. conclusions, if sufficient terms were available to estimate their asymptotic behavior.

For a given set of anisotropy parameters (η_x,η_y,η_z), there is a choice of which component χ_α, μ_2^α, C_α to study. In practice we will concentrate on the component which yields the most regular and strongly singular series. For example, for $\eta_x=\eta_y=0$, $\eta_z=1$ ($S = \infty$ Ising model), the quantity χ_z is analogous to the usual Ising model static susceptibility, which for $S = \frac{1}{2}$ in three-dimensions behaves as $(T-T_c)^{-5/4}$. On the other hand $\chi_x=\chi_y$ is similar to the $S = \frac{1}{2}$ Ising model static perpendicular susceptibility, which is a much more weakly singular quantity, thought to behave like the energy

density.[47] "Prolate" and "oblate" anisotropy were defined in (2.3d and e). Other cases which do not fall directly into these classes will be defined in terms of the anisotropy parameters (η_x, η_y, η_z).

A. Critical Point

Figure 8 shows a plot of kT_c/J as a function of λ for both prolate and oblate cases, as obtained from susceptibility and second moment series. The curve for the prolate case is qualitatively similar to the one presented by Dalton and Wood[31] for the $S = \frac{1}{2}$ anisotropic Heisenberg model in the random phase approximation. For the three limiting cases, $\lambda = 0,1$. (See Eq. (2.3d and e)), T_c decreases as the symmetry of the Hamiltonian increases from up-down (Ising) through planar rotation (x-y model) to complete rotational invariance (isotropic Heisenberg). For both prolate and oblate cases, as λ increases from zero to one, the increase of the "disordering" component of the Hamiltonian causes T_c to decrease.

For λ in the range $0 \leq \lambda \lesssim 0.6$ and for $\lambda = 1$, the series are smooth and kT_c/J is given to within confidence limits* of 0.10 - 0.15%. For $0.6 \lesssim \lambda < 1$ the series become more difficult to

*Of course, no statements can be made about the uncertainty in the true T_c or the true critical indices on the basis of series of finite length. The numbers given reflect the apparent smoothness of the series and the apparent consistency of various different extrapolation procedures, as based on the number of terms which we have available. Even where the series are smooth, there is always the hidden hypothesis that the series are long enough for the true asymptotic behavior to have set in. We refer to such uncertainties as "confidence limits." The criterion is in the last analysis subjective: we would be "surprised" if the number in question fell outside the quoted limits.

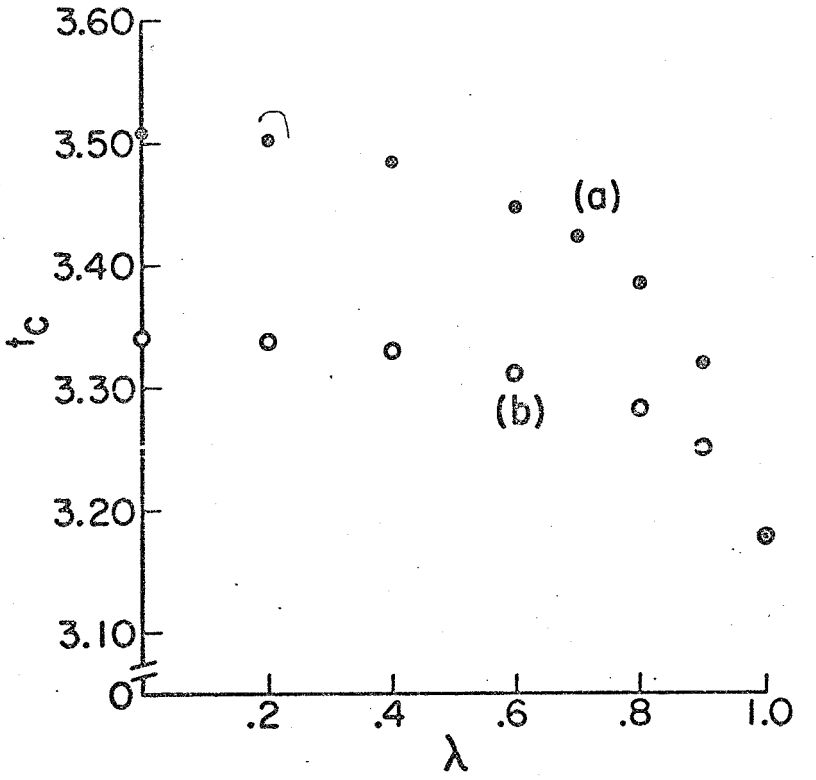

Figure 8. The critical temperature $t_c = kT_c/J$ vs. anisotropy λ for the f.c.c. lattice in the case of (a) prolate anisotropy and (b) oblate anisotropy. See Eq. (2.3d,e).

analyze. The sequences $\{\rho_n\}$ (defined in (4.4)) for the susceptibility series seem to develop a point of inflection, making it very difficult to extrapolate the latest trends. We take this as evidence that in this region the series have not yet fully settled down to their symptotic behavior. One might say that, as $\lambda \to 1^-$, it takes the system more and more interaction bonds (i.e. more and more powers of λ) to "realize" that it is not isotropic. All things considered, we set confidence limits of $\pm$ .2 - .3% for $0.6 \lesssim \lambda < 1$.

B. Indices γ and ν_1

In this section the values of the indices γ and ν_1 are presented as a function of anisotropy. For the cases of prolate and oblate anisotropy γ and $2\nu_1$ are shown for various values of λ in Table 14. In the former case the indices refer to χ_z and μ_2^z and in the latter, to χ_x and μ_2^x. The values of the indices for several typical cases in which all three parameters (η_x, η_y, η_z) differ in magnitude and/or sign are shown in Table 15. In each instance the indices apply to χ_α and μ_2^α, where the Cartesian component α is listed. Except in cases explicitly noted to the contrary, the confidence limits are $\pm$ 1%.*

The results in Table 14 suggest that, as far as the critical indices are concerned, the isotropic Heisenberg limit, $\lambda = 1$, is singular. For both prolate and oblate anisotropy γ and

*This is a conservative estimate based on the difference in the result of extrapolations using t_c's which differ by 0.10 - 0.15%.

Table 14. Indices γ and $2\nu_1$ for prolate and oblate anisotropy.*

PROLATE CASE $\lambda = \eta_x = \eta_y \leq \eta_z = 1$			OBLATE CASE $1 = \eta_x = \eta_y \geq \eta_z = \lambda$	
λ	γ	$2\nu_1$	γ	$2\nu_1$
0	1.23	1.25	1.32	1.34
0.2	1.23	1.25	1.32	1.34
0.4	1.23	1.25	1.32	1.34
0.6	1.24	1.25	1.32	1.34
0.7†	1.21	1.23	1.30	1.32
0.8†	1.19	1.20	1.28	1.31
0.9†	1.19	1.20	1.28	1.30
1.0	1.38	1.40	1.38	1.40

*Unless otherwise noted, confidence limits are $\pm$ 1%.

†No confidence limits given; series not showing asymptotic behavior.

Table 15. Indices γ and $2\nu_1$ for various typical combinations of the anisotropy parameters.*

	η_x	η_y	η_z	Comp.	γ	$2\nu_1$
1	0.1	0.5	1.0	z	1.23	1.25
2	0.2	0.5	1.0	z	1.23	1.25
3	0.4	0.5	1.0	z	1.23	1.25
4	0.5	-0.5	1.0	z	1.225	1.245
5	-0.5	-0.5	1.0	z	1.225	1.25
6	0.4	-0.5	1.0	z	1.225	1.245
7	1.0	1.0	-0.5	x	1.31	1.33
8†	1.0	0.75	0.0	x	1.21	1.23
9	1.0	0.2	0.0	x	1.23	1.25
10‡	1.0	-1.0	0.0	x	1.23 (1.32)	1.24 (1.34)
11‡	1.0	1.0	-1.0	x	1.32 (1.38)	1.33 (1.40)
12‡	1.0	-1.0	-1.0	x	1.23 (1.38)	1.24 (1.40)

*Unless otherwise noted, confidence limits are $\pm$ 1%.

†No confidence limits given; series not showing asymptotic behavior.

‡b.c.c. indices in parenthesis, confidence limits $\pm$ 1.5%; f.c.c. confidence limits $\pm$ 1.5 - 2.0%.

$2\nu_1$ remain nearly constant for $0 \leq \lambda \lesssim 0.6$, dip slightly in the region $0.6 \lesssim \lambda < 1$, and shoot up to the isotropic Heisenberg value very close to $\lambda = 1$. There is evidence, as already suggested in section A, that the series are not fully asymptotic in the region of the dip, $0.6 \lesssim \lambda < 1$. In Fig. 9, for the case of prolate anisotropy, the values of $g_n = (\gamma-1)_n$, calculated from Eq. (4.9) applied to χ_z, are plotted vs. 1/n for various values of λ. For $\lambda = 0.2$, the points are quite linear and extrapolate to $g \cong 0.23$. For $\lambda = 0.6$, there is a break with an indication of a rapid increase in the g_n. For $\lambda = 0.7$ and 0.8, there is indication that the curves will turn upward, but at $\lambda = 0.9$ there is no indication. However, at $\lambda = 1$ (Heisenberg limit, not shown) the curve is again quite linear (comparable to $\lambda = 0.2$), extrapolating to $g \cong 0.38$.[22,23] The oblate case behaves similarly. Fig. 9 is taken as evidence that for $0.6 \lesssim \lambda < 1$ the true asymptotic behavior is not being reflected in the terms available. On the basis of this discussion, we surmise that the critical indices γ and $2\nu_1$ are constant for all prolate (oblate) anisotropies at their Ising (x-y) values and change discontinuously at the discrete point $\lambda = 1$ to the isotropic Heisenberg values.* It is interesting to note that this step-function

---

*In this light, the characteristic overshoot of the region $0.6 \lesssim \lambda < 1$ seems like a kind of Gibbs phenomenon and would most likely disappear from the left as more terms in the series become available. Each coefficient in the series is a finite polynomial in λ. The ρ_n's and, therefore, the critical indices must vary smoothly with λ except in the limit $n \to \infty$.

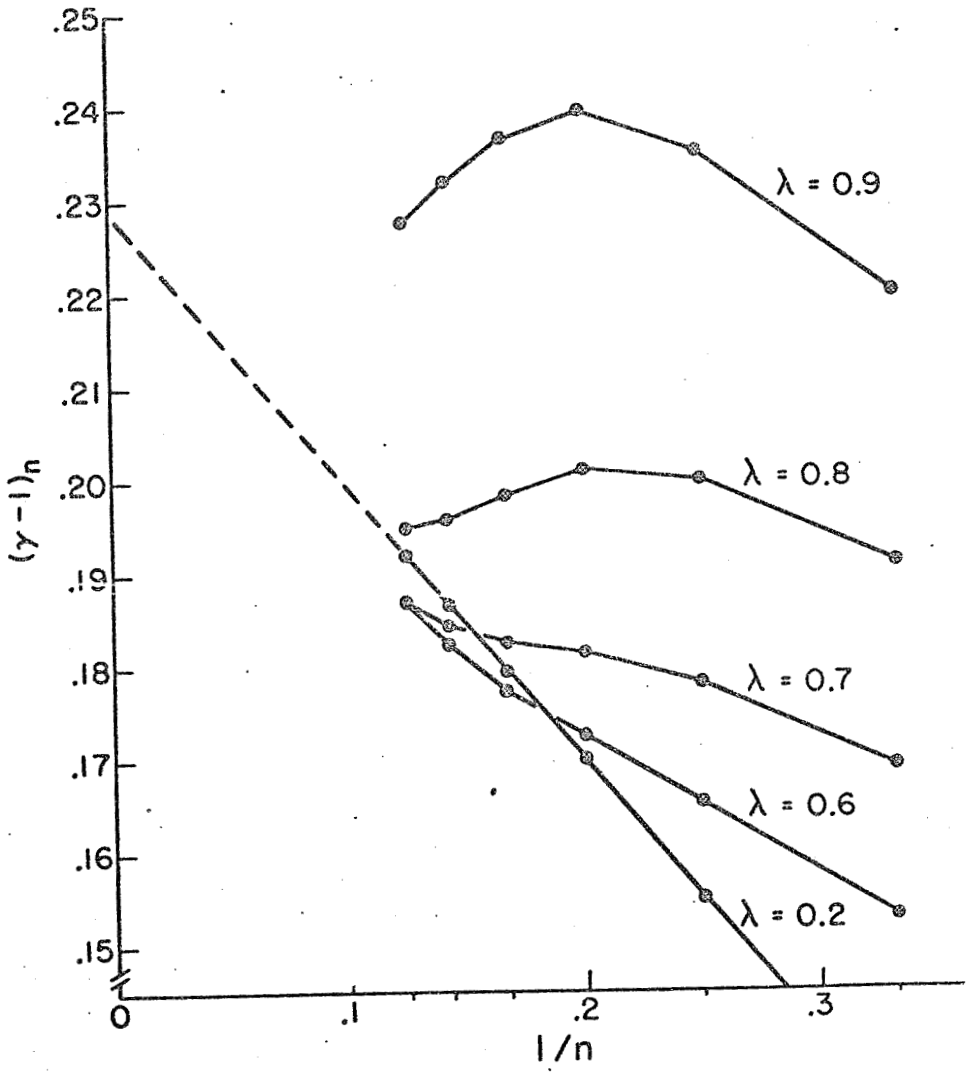

Figure 9. The sequences $\{g_n\}$, defined by Eq. (3.9) applied to χ_z, vs. 1/n for various values of λ in the case of prolate anisotropy. From (3.5), $\{g_n\} \to (\gamma-1)$.

behavior for γ was found by Dalton and Wood[31] for the spin-$\frac{1}{2}$ prolate Heisenberg model in the random phase approximation.

With this understanding of Table 14, we proceed to examine the more complex combinations of anisotropy parameters represented in Table 15. We propose that three sets of critical indices are sufficient to characterize the dominant singularities for all cases we have been able to analyze.* We will refer to these as

$$\text{Ising-like:} \quad \gamma = 1.23, \; 2\nu_1 = 1.25 \tag{5.1a}$$

$$\text{x-y like:} \quad \gamma = 1.32, \; 2\nu_1 = 1.34 \tag{5.1b}$$

$$\text{Heisenberg-like:} \quad \gamma = 1.38, \; 2\nu_1 = 1.40 \tag{5.1c}$$

with confidence limits of $\pm$ 1%. Which of these sets of indices is to be associated with a given set of anisotropy parameters appears to be determined by the lattice type and the relative magnitudes and signs of the η_α's as shown in Table 16. Note how the entries of Table 15 fit into the scheme of Table 16. For example, the first six entries of Table 15 have a dominant z-coupling which is ferromagnetic and give Ising-like indices in accordance with Table 16, A(i). The confidence limits shown in (5.1) refer to the well-behaved cases. When, as in Table 15, 8, one nears the discontinuity of the step-function, one observes the characteristic overshoot phenomenon

*In the specific (f.c.c.) case when all dominant couplings are antiferromagnetic, the series are not sufficiently regular to analyze reliably. See below, Table 16, and Appendix D. All other cases are covered by the indices (5.1).

Table 16. Critical indices and ground state behavior as functions of the anisotropy parameters.

Anisotropy Parameters			Indices and Ground State		Component Studied
magnitudes		signs	fcc	bcc	
A. $\|\eta_z\|>\|\eta_x\|,\|\eta_y\|$	(i)	$\eta_z>0$	I	I	z
	(ii)	$\eta_z<0$	?	I	? (z^s)
B. $\|\eta_x\|=\|\eta_y\|>\|\eta_z\|$	(i)	$\eta_x,\eta_y>0$	xy	xy	x,y
	(ii)	$\eta_x>0;\eta_y<0$	I	xy	x (y^s)
	(iii)	$\eta_x,\eta_y<0$	?	xy	? (x^s,y^s)
C. $\|\eta_x\|=\|\eta_y\|=\|\eta_z\|$	(i)	$\eta_x,\eta_y,\eta_z>0$	H	H	x,y,z
	(ii)	$\eta_x,\eta_y>0;\eta_z<0$	xy	H	x,y (z^s)
	(iii)	$\eta_z>0;\eta_x,\eta_y<0$	I	H	z (x^s,y^s)
	(iv)	$\eta_x,\eta_y,\eta_z<0$	?	H	? (x^s,y^s,z^s)

I = "Ising-like"; xy = "x-y-like"; H = "Heisenberg-like" (isotropic). See Eq. (5.1).

The notation α^s refers to the staggered version of the α component.

Parenthesized quantities were studied on the b.c.c. lattice only.

mentioned above. Correspondingly, the series indicate internally that they are not yet fully asymptotic, and our critical exponent estimates are expected to be unreliable, as discussed in connection with the simple prolate and oblate anisotropies of Table 14. In addition, the cases (e.g. Table 15, 10-12) where the dominant anisotropy parameters have mixed signs are quite difficult to extrapolate. Confidence limits in these cases are correspondingly wider; however, it does seem possible to assign these cases unambiguously to one of the three categories (5.1 a-c).

When the dominant anisotropy parameters are all positive (Table 16, A(i), B(i), C(i)), there are no lattice effects. In other cases, there are marked differences between f.c.c. and b.c.c. behavior. The fact that the indices for the b.c.c. lattice do not depend upon the sign of the anisotropy parameters is a consequence of the general symmetry for loose-packed lattices discussed in Chapter II. For example, (2.18) gives

$$\chi_x(\eta_x,\eta_y,\eta_z) = \chi_x(\eta_x,\pm\eta_y,\pm\eta_z)$$

and

$$\chi_x(-\eta_x,\eta_y,\eta_z) = \chi_x^s(\eta_x,\pm\eta_y,\pm\eta_z), \tag{5.2}$$

which holds for any combination of the $\pm$ signs. χ_α^s refers to the staggered susceptibility, defined in (2.17). Consider, for example, the case B(ii) of Table 16 for the b.c.c. lattice:

$$\chi_x(\eta_x,\eta_y,\eta_z) = \chi_x(\eta_x,|\eta_y|,\eta_z)$$

$$= \chi_y(\eta_x,|\eta_y|,\eta_z) = \chi_y^s(\eta_x,\eta_y,\eta_z)\ , \tag{5.3}$$

where the first and third equality signs depend on (5.2), while the second expresses rotational symmetry in the x-y plane. Thus, for this case, the series for χ_x and χ_y^s are identical not only with each other (as indicated in the "component" column of Table 16) but also with the susceptibility $\chi_x(\eta_x, |\eta_y|, \eta_z)$, which falls into category B(i). The dominant singularities in the b.c.c. antiferromagnetic cases A(ii), B(iii), C(iv) are entirely in the staggered susceptibilities, and it is the index of these singularities which we identify with γ. The much weaker physical susceptibilities (which are, of course, the staggered susceptibilities of the corresponding ferromagnets) are entirely masked.*

It is a remarkable empirical fact that the classification of the critical indices in their dependence on the anisotropy parameters (as given in Table 16) exactly parallels the classification of ground state symmetry (degeneracy) as a function of anisotropy parameters. For most** combinations of anisotropy parameters the ground state of the Hamiltonian (2.1) subject to (2.2) can be obtained from entirely elementary arguments, as outlined in Appendix D. When these arguments go through — and they do go through for

---

*We have attempted to remove the strong singularity in a manner similar to that used by M. E. Fisher and M. F. Sykes,[48] for the $S = \frac{1}{2}$ Ising model. The resulting series were not analyzable.

**The exception is for the close-packed lattices when the dominant anisotropy parameters are all negative. See above and Table 16.

just those cases in which our series are analyzable — they predict three different types of ground-state structure: (a) Ising-like, in which the ground state is doubly degenerate with respect to a coherent flipping of every spin in the lattice, (b) x-y-like, in which the ground state is degenerate with respect to a coherent planar rotation of every spin, and (c) isotropic Heisenberg-like, in which the ground state is degenerate with respect to a coherent three-dimensional rotation of every spin. The cases (a)-(c) above are in exact correspondence with the occurrence of the indices (5.1a-c). (For the close-packed lattices with dominant antiferromagnetic coupling the ground state has a more complex structure.*) This, then, is the content of the hypothesis stated in Chapter I.

C. The Specific Heat

The specific heat series are very difficult to analyze. The loose-packed lattices cannot be used here because the odd terms in the series vanish,** leaving too few to extrapolate reliably. For the f.c.c. lattice the specific heat index behaves roughly the way γ and ν_1 do, and for the important limits,

$$\begin{aligned} \alpha &\cong +0.1 \quad (S = \infty \text{ Ising})^{(28)} \\ \alpha &\cong 0 \quad (\text{classical x-y}) \\ \alpha_s &\cong -0.1 \quad (\text{classical Heisenberg}), \end{aligned} \tag{5.4}$$

---

* Examples in the context of the $S = \frac{1}{2}$ Ising model may be found in the paper by G. Wannier[19] and in the paper of D. D. Betts and C. J. Elliott.[49]

** See Chapter II.

where α_s is the index for the singular part of the specific heat. In (5.4) reasonable confidence limits for the extrapolations might be as large as $\pm$ .1. In each case quoted in (5.4) the specific heat, $C_{H=M=0}$, is either equal to or proportional to the non-vanishing component, $C_{\alpha'}$, defined in (2.8c). In other cases both the total specific heat and the components were considered. Generally the component which yields the most singular (and most regular) χ and μ_2 series also yields the smoothest specific heat component. The other components are, in comparison, numerically small and slightly retard convergence of the total specific heat series.

The results indicate that the specific heat of the classical Heisenberg model may be finite,[22] in agreement with the latest results[21] for the $S = \frac{1}{2}$ case. There is an indication of the possibility that the x-y model has a logarithmic specific heat.

D. Comment on the $S = \infty$ Ising Model

For this model our series are the longest that have been derived to date. We find quite convincing differences between the indices of this model and the $S = \frac{1}{2}$ Ising model. These differences are summarized in (5.5) for the three-dimensional lattices.*

$$\gamma_{\frac{1}{2}} = 1.250 \pm .002, \quad \gamma_\infty \cong 1.23 \pm 1\%$$
$$2\nu_{\frac{1}{2}} = 1.286 \pm .005, \quad 2\nu_\infty \cong 1.25 \pm 1\% \,. \qquad (5.5)$$

*See the paper by M. E. Fisher and R. J. Burford.[30] We have added two terms to their μ_2(f.c.c.), and have corrected a small error in the eighth and added the ninth term in μ_2(b.c.c.). M. A. Moore, D. Jasnow, M. Wortis (to be published). Using the most recent estimates for T_c(f.c.c.) in the paper by M. F. Sykes, J. L. Martin and D. L. Hunter,[50] might cause the lowering of the estimate for $2\nu_{\frac{1}{2}}$ in (5.5) by a few tenths of a percent.

Recalling the tables of results (see also Table 9), we consistently find, for cases with Ising-like ordering, values of γ and $2\nu_1$ lower than the $S = \frac{1}{2}$ results. Results for general spin Ising model have now been extended to ten terms.*

E. Summary and Comments on the Scaling Laws

In the context of the anisotropic classical Heisenberg model, the results provide some information in relation to the questions (a) and (b) posed in the Introduction. We find three sets of critical indices. The anisotropy parameters can be varied, altering the dynamical situation, without changing the critical indices, as long as the ground state manifold does not change. That is to say, the cases which could be treated** indicated that the interactions matter only insofar as they determine the symmetry of the order parameter in the ground state. If, as is plausible, the order parameter has the same symmetry for $T < T_c$ as it does at $T = 0$, the results correlate the high-temperature critical indices with the symmetry of the ordered phase.

Several comments can be made on the relation of our numerical results to the scaling laws.[7,8] Dropping the distinction between ν and ν_1, we can comment on

$$\gamma = (2-\eta)\nu \tag{5.6}$$

---

*M. A. Moore, D. Jasnow, M. Wortis (to be published). For $S = \frac{1}{2}$ and ∞ the results on the basis of ten terms agree with those in (5.5). It is not certain at this time whether all finite spins have the $S = \frac{1}{2}$ indices.

**The exception is for the close-packed lattices when the dominant anisotropy parameters are all negative. See above.

and

$$d\nu = 2 - \alpha \,, \tag{5.7}$$

where d is the dimensionality of the lattice. In the first place, the results (5.1a-c) all indicate that $2\nu > \gamma$, implying a small positive value of η. However, γ and 2ν differ by roughly 2%, and, as stated previously, we have confidence in our values for each of these quantities to about $\pm$ 1%. Hence the possibility that $\eta = 0$ is not out of the question, although numerically we find a consistent slight difference between γ and 2ν, suggesting $\eta \cong .02\text{-}.03$.

Our estimates of α are admittedly imprecise (possibly $\pm$ .1), but, taken at face value, (5.7) is remarkably well satisfied for our three sets of indices (5.1a-c) and (5.4) (using α_s in (5.7) for the Heisenberg limit). Recall that the $S = \frac{1}{2}$ three-dimensional Ising model presents a difficulty with respect to (5.6) and (5.7), since[50] $\alpha = 1/8$ and $\gamma = 5/4$ implies $\eta = 0$ and $2\nu = \gamma$. The last equality does not appear to be the case.* The results of this work, on the other hand, indicate that the $S = \infty$ Ising model (and, indeed, all cases considered) are consistent with the relations (5.6) and (5.7). As stated above in section D, the series for the $S \neq \frac{1}{2}$ Ising models (and μ_2 for $S = \frac{1}{2}$) are being extended. In view of present problems with scaling theory, more precise estimates of α and ν will be most useful.

---

*See the paper by M. E. Fisher and R. J. Burford[30] and note the additions reported in section D above. A direct check on the value of η for the Ising model is in progress. M. Wortis, M. A. Moore and D. Jasnow (to be published).

F. A Recent Experiment

Very recently* a series of experiments have been performed on the critical behavior of the S = 5/2 "isotropic Heisenberg antiferromagnet" $RbMnF_3$ (see Chapter I). Neutron scattering techniques have been used to determine the scattering function,[3,30] $\chi(\underset{\sim}{k})$, at different temperatures. The results of these experiments indicate that $\eta \neq 0$ and that

$$\gamma = 1.397 \pm .034$$

$$\nu = 0.724 \pm .008 ,$$

where γ refers to the index for the staggered susceptibility. These results are in excellent agreement with our S = ∞ isotropic Heisenberg results ($\gamma \cong 1.38$, $\nu \cong 0.70$). The fact that both of the experimental indices are slightly greater than those of the model is consistent with the observed decrease in the indices as the spin of the Heisenberg model is increased from $\frac{1}{2}$ to ∞.** It is important to note that γ is bounded away from 4/3 and ν is bounded away from 2/3, since experimental values frequently fall near those values.[4,5] There is need for more precise estimates of ν for the spin-S (particularly spin-$\frac{1}{2}$) Heisenberg model.

---

*The author is indebted to Dr. L. Corliss for a discussion of these results prior to their publication.

**As noted in the Chapter I, for the isotropic Heisenberg model, $\gamma(S = \frac{1}{2}) \cong 1.43$[21] and $\gamma(S = \infty) \cong 1.38$.[22,23]

VI. THE PLANAR HEISENBERG MODEL

Consider the Hamiltonian (2.1), with $\alpha = x,y$ only and $\underset{\sim}{S}(l) = (S_x(l), S_y(l))$, under conditions (2.2). The isotropic limit of this model of interacting two-dimensional classical unit vectors has been proposed, by Vaks and Larkin,[51] as a lattice model of the λ transition of liquid He^4.

They reason as follows. The grand partition function for the Bose gas is

$$\Xi = \mathrm{Tr}\, e^{-\beta(H-\mu N)}$$

$$= \mathrm{Tr} \exp\left\{-\beta \int d^3\underset{\sim}{r}\left[\frac{\hbar^2}{2m} \nabla\psi^\dagger\cdot\nabla\psi - \mu\psi^\dagger\psi + \frac{g}{2}(\psi^\dagger\psi)^2\right]\right\}, \qquad (6.1)$$

where ψ is the field operator and g is the strength of a δ-function interaction. The authors argue that close to the transition, long wavelength correlations dominate, and the details of the interaction are unimportant. They further reason that in the small $\underset{\sim}{k}$ limit the space can be made discrete, and, near the critical point, the field operator $\psi(\underset{\sim}{R}_l)$ can be replaced by a classical field $\psi_{\underset{\sim}{R}_l}$ defined at the site $\underset{\sim}{R}_l$. In first approximation there are no amplitude fluctuations of the field ψ, and the Hamiltonian (2.1), with the modifications given above, describes the system. The correspondence between quantities relating to the planar spin model and liquid helium is*:

---

*More precisely, ψ is a complex field with $S_x(l) \leftrightarrow \mathrm{Re}\psi$ and $S_y(l) \leftrightarrow \mathrm{Im}\psi$, for example.

	He^4		planar Heisenberg
order parameter	$\langle\psi\rangle$	$\leftrightarrow$	$\langle \underset{\sim}{S}(1)\rangle$
correlation function	$\langle\psi^\dagger(1)\psi(1')\rangle$	$\leftrightarrow$	$\langle \underset{\sim}{S}(1)\cdot\underset{\sim}{S}(1')\rangle$.

(6.2)

The indices γ and ν_1 are, as usual, determined by spatial moments of the correlation function $\langle \underset{\sim}{S}\cdot\underset{\sim}{S}\rangle$ for the planar model. However, γ is not subject to experimental verification with liquid He^4 since the analog of the magnetic susceptibility is an unphysical quantity for the Bose fluid. By an argument due originally to Josephson,[52] the index ν (dropping the distinction between ν and ν_1), which measures the range of the decaying part of the correlation function, does have an experimental interpretation. It specifies the decrease of the superfluid density, ρ_s, to zero just below T_λ,

$$\rho_s \sim (T_\lambda - T)^\nu \ , \quad T \to T_\lambda^- \ . \tag{6.3}$$

The relation (6.3) follows from hydrodynamics and scaling. The spirit of Josephson's argument is sketched here. In the hydrodynamic regime the decaying part of the correlation function (integrated over ω) has the form

$$\langle\psi^\dagger\psi\rangle_{\underset{\sim}{k}} \sim \frac{|\langle\psi\rangle|^2}{\rho_s k^2} \ . \tag{6.4}$$

Making a scaling hypothesis for the form of the left hand side of (6.4),

$$\frac{|\langle\psi\rangle|^2}{\rho_s k^2} \sim \frac{f(k\xi)}{k^{2-\eta}} \tag{6.5}$$

where ξ is the coherence length. Inserting factors of ξ,

$$\frac{|\langle\psi\rangle|^2}{\rho_s \xi^{-\eta}} \sim 1 \tag{6.6}$$

or

$$\rho_s \sim |\langle\psi\rangle|^2 \xi^{\eta} \sim (T_\lambda - T)^{2\beta - \eta\nu} \ , \ T \to T_\lambda^- \ . \tag{6.7}$$

In (6.7) the fact that the order parameter goes to zero as $(T_\lambda - T)^\beta$ has been used. Now using[3,4]

$$\begin{aligned} 2\beta &= 2-\gamma-\alpha \\ (2-\eta)\nu &= \gamma \\ 3\nu &= 2-\alpha \end{aligned} \tag{6.8}$$

(6.3) is verified.*

The specific heat of liquid He^4 has a logarithmic singularity ($\alpha=\alpha'=0$) at $T = T_\lambda$, as has been demonstrated experimentally** by Buckingham and Fairbank[53] and Kellers.[54] In addition, Clow and Reppy, and Tyson and Douglass[55] have measured the temperature dependence of ρ_s near T_λ and found

$$\rho_s \sim (T_\lambda - T)^{2/3} \ . \tag{6.9}$$

If the scaling arguments sketched above hold, one would expect $\nu \cong 2/3$ for liquid He^4 and its analog, the planar Heisenberg model.

---

*To be precise, the indices γ, α, ν should have been written with primes to signify $T < T_\lambda$. In the scaling point of view the indices are equal above and below the critical point.

**For good discussion of the experimental situation in general see the reviews by L. P. Kadanoff, et al.[4] and P. Heller.[5]

By suitably changing the unrenormalized semi-invariants, we have been able to derive series for the anisotropic planar Heisenberg model using the methods of Chapter II. To date, only the f.c.c. lattice has been studied.

In the light of the measurements quoted above and the arguments of Vaks and Larkin,[51] it is very interesting to compare the planar isotropic Heisenberg model with the x-y-like models. The difference between them is one of phase space; the ground state manifolds are identical. For comparison, the values of the indices* and confidence limits are:

	γ	$2\nu_1$	α
x-y-like	$1.32 \pm 1\%$	$1.34 \pm 1\%$	$0 \pm .1$
isotropic planar	$1.315 \pm 1\%$	$1.34 \pm 1\%$	$0 \pm .05$.

(6.10)

In both cases the specific heat index is most difficult to determine, and the approximate confidence limits reflect this situation. Within confidence limits, both the x-y-like and the isotropic planar models have indices in good agreement with the experimental values for the λ transition.

Qualitatively the anisotropic planar model behaves (at least on the f.c.c. lattice) exactly as the anisotropic Heisenberg does. The isotropic limit appears to be singular, and an abrupt

*Bowers and Joyce[56] find for the isotropic planar model on three-dimensional lattices $0 \leq \alpha \leq 1/32$ and $\gamma = 1.312 \pm .006$. The confidence limits quoted here are somewhat wider, but agreement in general is good. See also the paper by H. E. Stanley.[57]

change in the indices accompanies the change in the symmetry of the ground state manifold. On the f.c.c. lattice there are two sets of indices; we will refer to these as

Ising-like	$\gamma = 1.24$	$2\nu_1 = 1.265$	$\alpha = .1 \pm .1$ (6.11a)
x-y-like	$\gamma = 1.315$	$2\nu_1 = 1.34$	$\alpha = 0 \pm .05$, (6.11b)

where all estimates of γ and $2\nu_1$ have confidence limits of about $\pm$ 1%. The situation is summarized in Table 17. As for the three-dimensional spin model, the classification of the critical indices exactly parallels the classification of the ground state symmetry* (degeneracy) as a function of anisotropy. It is found that Ising-like and x-y-like ground states correspond respectively to the occurrence of indices (6.11a) and (6.11b). This limited study of the planar model indicates that the hypothesis stated in Chapter I is probably not limited to the three-dimensional spin model.

The coefficients for χ, μ_2 and C for the two limiting cases ($\eta_x=\eta_y=1$ and $\eta_x=1, \eta_y=0$) on the f.c.c. lattice are given in Table 18.

---

*"Ising-like" and "x-y-like" ground states in this context mean the same thing as in the context of the three-dimensional spin problem. In cases where elementary arguments suffice to determine the ground state, the method sketched in Appendix D has been used. See Chapter V.

Table 17. Critical indices and ground state behavior for the anisotropic planar Heisenberg model on the f.c.c. lattice as a function of anisotropy parameters.

Anisotropy Parameters			Indices and Ground State	Component Studied
magnitudes		signs	(f.c.c.)	
A. $\lvert\eta_x\rvert>\lvert\eta_y\rvert$	(i)	$\eta_x>0$	I	x
	(ii)	$\eta_x<0$	?	?
B. $\lvert\eta_x\rvert=\lvert\eta_y\rvert$	(i)	$\eta_x,\eta_y>0$	xy	x,y
	(ii)	$\eta_x>0,\eta_y<0$	I	x
	(iii)	$\eta_x,\eta_y<0$	?	?

I = "Ising-like"; xy = "x-y-like." See Eq. (6.11).

Table 18. Selected zero-field susceptibility, second moment and specific heat coefficients for the planar Heisenberg model on the f.c.c. lattice.

	$\eta_x = \eta_y = 1$			$\eta_x = 1, \eta_y = 0$		
n	a_n^x	b_n^x	c_n^x	a_n^x	b_n^x	c_n^x
1	3.0	3.0	.25	3.0	3.0	.25
2	16.5	36.0	1.0	16.875	36.0	1.0
3	87.375	306.375	4.03125	92.53125	310.78125	5.1328125
4	453.0	2243.25	16.25	499.828125	2330.4375	23.4375
5	2317.09375	15068.96875	65.8854	2673.7421875	16134.765625	106.9303
6	11742.6797	95688.15625	272.78125	14206.5254	106074.5664	491.6406
7	59110.8564	583946.8564	1153.4830	75111.7916	672437.5214	2278.6285
8	296031.6117	3459600.2923	4955.5360	395626.7191	4149043.9626	10650.1952

$$\chi_\alpha(\eta_x, \eta_y) = 1/2 + \sum_{n=1} a_n^\alpha v^n$$

$$\mu_2^\alpha(\eta_x, \eta_y) = \frac{zv}{2} \sum_{n=1} b_n^\alpha v^n$$

$$C_\alpha(\eta_x, \eta_y) = \sum_{n=1} c_n^\alpha v^n$$

VII. THE SPINEL

In this chapter some results for the anisotropic Heisenberg model on the B-site spinel lattice are presented.* In Chapters IV and V the characteristics which make series analyzable were mentioned. In essence there had to be signs of "convergence" in the extrapolation procedures. Series for the spinel are not analyzable (with the number of terms available). They provide a good example of the possible errors that can be made by considering too-short series.

One prediction of the scaling hypothesis for lattice models is the independence of the critical indices on the lattice type. But if the scaling laws are really only correct to within a few percent, then one might expect to see a slight departure from this prediction. Some recent measurements are not inconsistent with this view,[58] but there is a large amount of evidence[3,15] from exact series expansions to support the hypothesis of the independence of critical exponents of lattice type, at least for lattices with cubic symmetry. Very little work has been done on lattices without cubic symmetry. However, Stanley and Kaplan,[59] and Baltzer et al.[60] have found the first six terms in the susceptibility series for the Heisenberg ferromagnet on the spinel structure, using a formula of Rushbrooke and Wood,[61] on the basis of which

---

*D. Jasnow and M. A. Moore (to be published).

Stanley and Kaplan surmised* that $\gamma \cong 1.0$. This is completely at variance with the predictions, from the same number of terms, of $\gamma \cong 1.33\text{-}1.4$ for the lattices with cubic symmetry.(63)

Interest in the spinel structure was spurred by the discovery of the insulating ferromagnets,(64) $CdCr_2S_4$, and $CdCr_2Se_4$, and $HgCr_2Se_4$. One very approximate model for these systems is that of an array of spins located on the B-sites of a spinel lattice and interacting via equal nearest-neighbor exchange forces J, and this was the model used by Stanley and Kaplan.** In the case of the $S = \infty$ Heisenberg model we have extended their series from six to eight terms and also obtained for the first time the first eight terms in the second moment series. We have also studied the classical x-y and $S = \infty$ Ising models on the same structure and found the same qualitative behavior.*** Namely, that with only six terms in the series a value $\gamma \cong 1.0$ seems reasonable, but that on extending the series to eight terms, larger values of γ appear more likely.

In Table 19 the coefficients for χ and μ_2 are given for the three limiting cases. Fig. 10 shows a plot of the sequence $\{\rho_n\}$ vs. 1/n for $\chi_z(1,1,1)$ on the spinel. Notice that the slope of the curve, which asymptotically is a measure of γ-1, is nearly

---

*Using a Padé approximant analysis, Freeman and Wojtowicz(62) concluded that $\gamma \cong 1.2\text{-}1.3$. Where ratio methods can be used (as here) they are usually more reliable, and their use is more easily justified.

**Stanley and Kaplan considered $S = 3/2$ corresponding to the spin-only moment of the chromium ion.

***The $S = \frac{1}{2}$ Ising model on the spinel has also been studied and behaves similarly.

Table 19. Zero-field susceptibility and second moment coefficients for the three limiting cases on the B-site spinel lattice.

	$\eta_x=\eta_y=0, \eta_z=1$		$\eta_x=\eta_y=\eta_z=1$		$\eta_x=\eta_y=1, \eta_z=0$	
n	a_n^z	b_n^z	a_n^z	b_n^z	a_n^x	b_n^x
1	.6667	.6667	.6667	.6667	.6667	.6667
2	1.2	2.6667	1.1111	2.6667	1.1556	2.6667
3	2.0622	7.4844	1.6593	7.1407	1.8607	7.3126
4	3.4637	17.9556	2.3556	15.7037	2.8958	16.8296
5	5.7458	39.3773	3.3050	30.6992	4.4414	34.9756
6	9.4654	81.4844	4.6456	55.6692	6.7673	68.0573
7	15.5249	161.9436	6.5224	96.0403	10.2684	126.5696
8	25.3776	312.4684	9.0848	160.0297	15.5162	227.8101

$$\chi_\alpha(\eta_x,\eta_y,\eta_z) = 1/3 + \sum_{n=1} a_n^\alpha v^n$$

$$\mu_2^\alpha(\eta_x,\eta_y,\eta_z) = \sum_{n=1} b_n^\alpha v^n$$

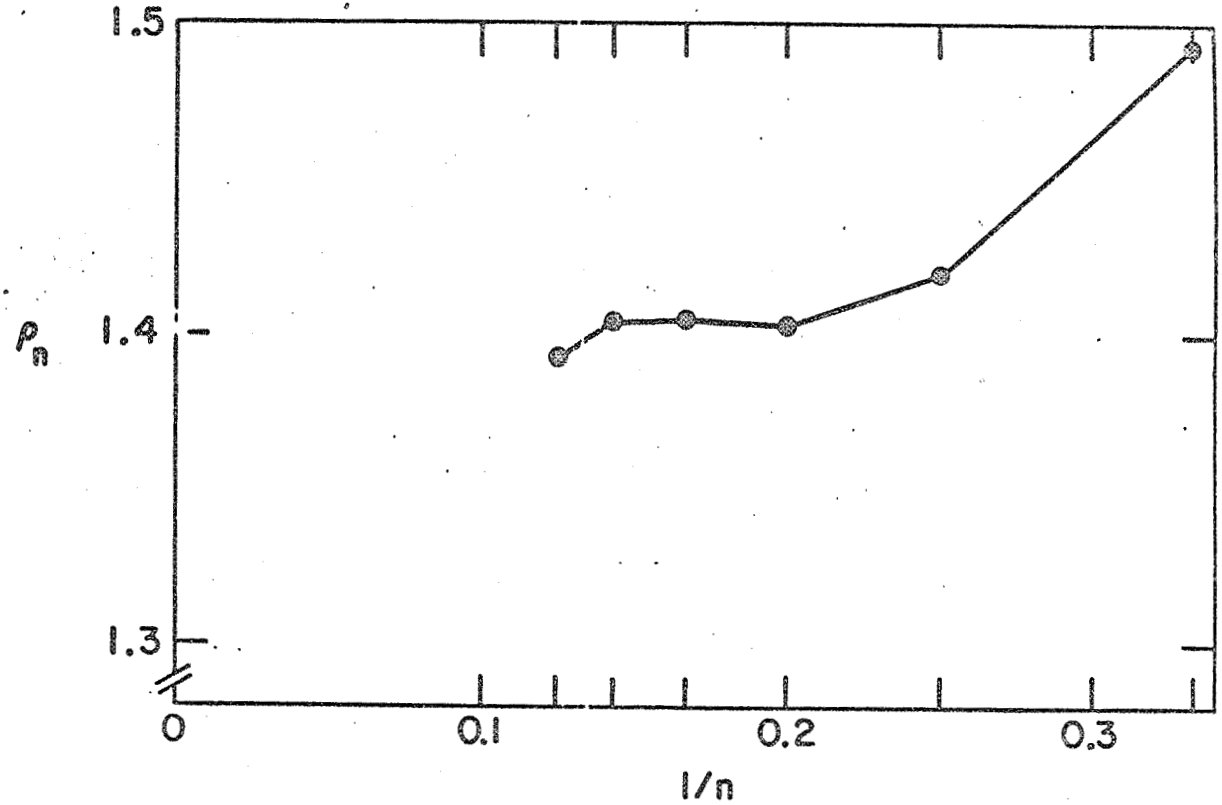

Figure 10. The sequence $\{\rho_n\}$ vs. 1/n for $\chi_z(1,1,1)$ on the B-site spinel.

zero at n = 6, implying $\gamma \tilde{=} 1.0$, but that the later terms indicate that estimates of γ will probably return to their customary values.* Very similar behavior is seen in the other models. We hesitate to make definite statements about γ, ν_1, or ν_c, even with eight terms.

The low value of γ obtained with only six terms on the spinel is probably connected with its four sublattice structure, little of which is "sampled" in the first six terms of the expansions. Series expansion methods cannot be expected to be reliable until enough terms are enumerated to sample the lattice complexity. Too-short series are of course an ever present danger in the exact series expansion method of obtaining critical exponents, and may well be the cause of other discrepancies between the results of series analysis and scaling law predictions.**

---

*See Chapter V.

**In particular, the work of Fisher and Burford,[30] on the effective correlation range index ν_1, for the S = ½ Ising model, revealed a discrepancy of 2-3% between their value of ν_1, and the value predicted by the scaling relation, $3\nu_1 = 2-\alpha$, with $\alpha = 1/8$.[50]

APPENDIX A. SKETCH OF THE DERIVATION OF THE UNRENORMALIZED EXPANSION

A sketch of the origin of the rules for calculating $\mathcal{M}_{\alpha\beta}(12)$ in the unrenormalized (bare) expansion is presented in this appendix. The first few terms of the linked cluster expansion for the dimensionless free energy, W, defined in (2.4), are derived below.

The Hamiltonian (2.1) is rewritten with the site sum being replaced by a sum over interacting pairs $\langle 12\rangle$, and the combination $\eta_\alpha v(12)$ is replaced by $v_\alpha(12)$:

$$-\beta H = \sum_{\substack{\langle 12\rangle \\ \alpha}} v_\alpha(12) S_\alpha(1) S_\alpha(2) + \sum_{\substack{1 \\ \alpha}} b_\alpha(1) S_\alpha(1). \tag{A.1}$$

W is a functional* of $v_\alpha(12)$ and $b_\alpha(1)$ and is expressed formally as a functional power series,

$$W[\{v\},\{b\}] = W_0 + W_1 + \cdots , \tag{A.2}$$

with

$$W_0[\{b\}] = \ln \mathrm{Tr}\, e^{\sum_1 \underset{\sim}{b}(1)\cdot\underset{\sim}{S}(1)} = \sum_1 \ln(4\pi)\, \frac{\sinh|\underset{\sim}{b}(1)|}{|\underset{\sim}{b}(1)|}, \tag{A.3a}$$

and

$$W_n = \frac{1}{n!}\frac{1}{2^n} \sum_{\substack{\bar 1\,\bar 2\ldots\bar n \\ \bar 1'\bar 2'\ldots\bar n'}} \left.\frac{\delta^n W[\{v\},\{b\}]}{\delta v(\bar 1\bar 1')\ldots\delta v(\bar n\bar n')}\right|_0 v(\bar 1\bar 1')\ldots v(\bar n\bar n'). \tag{A.3b}$$

*Actually, in this discrete case, W is a function of the $3\frac{N(N-1)}{2}$ variables $v_\alpha(12)$ and the 3N variables $b_\alpha(1)$.

In writing (A.3b) we have introduced the notation in which a barred integer stands for a site and a Cartesian index, e.g. $\bar{1} \leftrightarrow 1,\alpha_1$. Two barred variables connected by being arguments of a v must have the same Cartesian index;

$$v(\bar{1}\bar{2}) = v(1\alpha_1, 2\alpha_2) = v_\alpha(12)\delta(\alpha\alpha_1\alpha_2) \tag{A.4}$$

where

$$\delta(\alpha_1\cdots\alpha_n) = \begin{cases} 1, & \text{all arguments equal} \\ 0, & \text{otherwise .} \end{cases} \tag{A.5}$$

The factor 2^{-n} in (A.3b) arises from a sum over pairs going to a sum in which each site index runs freely over the sites of the lattice, subject only to

$$\underset{\sim}{v}(11) \equiv 0 \ , \ \text{all sites } 1, \alpha{=}x,y,z. \tag{A.6}$$

In (A.3b), $\Big|_0$ means the functional derivative is evaluated for $\{v\} = 0$, that is, in the absence of all interactions. The key to the derivation is to express the v-derivatives in terms of b-derivatives, which will eventually operate on W_o, and are easily evaluated.

The correlation functions $\mathcal{M}_n$ are defined by

$$\mathcal{M}_n(12\cdots n) \equiv \mathcal{M}_n(1\gamma_1, 2\gamma_2, \cdots n\gamma_n)$$

$$\equiv \frac{\delta^n W[\{v\},\{b\}]}{\delta b(\bar{1})\cdots\delta b(\bar{n})} \ . \tag{A.7}$$

Notice that $\mathcal{M}_2(1\gamma_1, 2\gamma_2) = \mathcal{M}_{\gamma_1\gamma_2}(12)$ as defined in (2.7). From (2.4),

$$\frac{\delta W[\{v\},\{b\}]}{\delta v(\bar{1}\bar{2})} = \langle S(\bar{1})S(\bar{2})\rangle = m_2(\bar{1}\bar{2}) + m_1(\bar{1})m_1(\bar{2}) \ , \qquad (A.8)$$

subject, of course, to $\gamma_1 = \gamma_2$ with $\bar{1} = 1,\gamma_1$ and $\bar{2} = 2,\gamma_2$. (A.8) is the important step in the derivation, since by (A.7) the right hand side contains only b-derivatives. Then to proceed

$$\frac{\delta}{\delta v(\bar{1}'\bar{2}')} m_n(\bar{1}\bar{2}\cdots\bar{n}) = \frac{\delta^n}{\delta b(\bar{1})\cdots\delta b(\bar{n})} \langle S(\bar{1}')S(\bar{2}')\rangle$$

$$= \frac{\delta^n}{\delta b(\bar{1})\cdots\delta b(\bar{n})} \left(m_2(\bar{1}'\bar{2}') + m_1(\bar{1}')m_1(\bar{2}')\right)$$

$$= m_{n+2}(\bar{1}'\bar{2}'\bar{1}\cdots\bar{n}) + \sum_{k=0}^{n} \sum_{k\text{-splits}} m_{1+k}(\bar{1}'\cdots)m_{1+n-k}(\bar{2}'\cdots), \qquad (A.9)$$

where $\sum_{k\text{-splits}}$ is intended to mean a sum over all different ways of putting k of the variables $\bar{1},\bar{2}\cdots\bar{n}$ into the $\bar{1}'$ bracket and the remaining n-k into the $\bar{2}'$ bracket. Then

$$\frac{\delta^2 W}{\delta v(\bar{1}\bar{2})\delta v(\bar{3}\bar{4})} = m_4(\bar{1}\bar{2}\bar{3}\bar{4}) + m_1(\bar{1})m_3(\bar{2}\bar{3}\bar{4}) + m_2(\bar{1}\bar{3})m_2(\bar{2}\bar{4})$$

$$+ m_2(\bar{1}\bar{4})m_2(\bar{2}\bar{3}) + m_1(\bar{2})m_3(\bar{1}\bar{3}\bar{4})$$

$$+ m_1(\bar{3})[m_3(\bar{4}\bar{1}\bar{2}) + m_1(\bar{1})m_2(\bar{2}\bar{4}) + m_1(\bar{2})m_2(\bar{1}\bar{4})]$$

$$+ m_1(\bar{4})[m_3(\bar{3}\bar{1}\bar{2}) + m_1(\bar{1})m_2(\bar{2}\bar{3}) + m_1(\bar{2})m_2(\bar{1}\bar{3})]. \qquad (A.10)$$

It is important to notice that when the derivative is evaluated in the non-interacting limit $\big|_0$,

$$\mathcal{M}_n(\bar{1}\ldots\bar{n})\Big|_0 = M_n^o(1;\gamma_1\ldots\gamma_n)\delta(12\ldots n) \qquad (A.11)$$

where the δ-function is the same as the one in (A.5) with the site (instead of Cartesian) arguments. The unrenormalized (bare) semi-invariants, M_n^o, are given in (2.9). In the limit $\Big|_0$, because of (A.6), the only terms in (A.10) which will contribute to W_2 are $\mathcal{M}_1\mathcal{M}_1\mathcal{M}_2$ and $\mathcal{M}_2\mathcal{M}_2$. Then W_2 is

$$W_2 = \frac{1}{2!}\frac{1}{2^2}\sum_{\bar{1}\bar{2}\bar{3}\bar{4}} \{[M_2^o(1;\gamma_1\gamma_3)M_2^o(2;\gamma_2\gamma_4)\delta(13)\delta(24) + 3 \leftrightarrow 4]$$

$$+ [M_1^o(3;\gamma_3)M_1^o(1;\gamma_1)M_2^o(2;\gamma_2\gamma_4)\delta(24) + 3 \text{ similar terms}]\}$$

$$\times v(\bar{1}\bar{2})v(\bar{3}\bar{4}) \ . \qquad (A.12)$$

Simplifying (A.12) and putting in the complete index complexity

$$W_2 = \frac{1}{4}\sum_{\substack{1,2\\ \gamma_1\gamma_2}} M_2^o(1;\gamma_1\gamma_2)M_2^o(2;\gamma_1\gamma_2)v_{\gamma_1}(12)v_{\gamma_2}(12) \qquad (a)$$

$$+\frac{1}{2}\sum_{\substack{1,2,3\\ \gamma_1\gamma_2}} M_1^o(1;\gamma_1)M_2^o(2;\gamma_1\gamma_2)M_1^o(3;\gamma_2)v_{\gamma_1}(12)v_{\gamma_2}(23). \qquad (b)$$

(A.13)

For completeness, it is noted that relation (A.8) immediately gives W_1 which is

$$W_1 = \frac{1}{2}\sum_{\substack{1,2\\ \gamma}} M_1^o(1;\gamma)M_1^o(2;\gamma)v_\gamma(12) \ , \qquad (A.14)$$

and carrying out the differentiation of (A.10) with respect to

$v(\bar{5}\bar{6})$, using (A.9) term by term, we get W_3,

$$W_3 = \frac{1}{12} \sum_{\substack{1,2 \\ \gamma_1\gamma_2\gamma_3}} M_3^o(1;\gamma_1\gamma_2\gamma_3)M_3^o(2;\gamma_1\gamma_2\gamma_3)v_{\gamma_1}(12)v_{\gamma_2}(12)v_{\gamma_3}(12) \quad \text{(a)}$$

$$+\frac{1}{2} \sum_{\substack{1,2,3 \\ \gamma_1\gamma_2\gamma_3}} M_1^o(1;\gamma_1)M_3^o(2;\gamma_1\gamma_2\gamma_3)M_2^o(3;\gamma_2\gamma_3)v_{\gamma_1}(12)v_{\gamma_2}(23)v_{\gamma_3}(23) \quad \text{(b)}$$

$$+\frac{1}{2} \sum_{\substack{1,2,3,4 \\ \gamma_1\gamma_2\gamma_3}} M_1^o(1;\gamma_1)M_2^o(2;\gamma_1\gamma_2)M_2^o(3;\gamma_2\gamma_3)M_1^o(4;\gamma_3)v_{\gamma_1}(12)v_{\gamma_2}(23)v_{\gamma_3}(34) \quad \text{(c)}$$

$$+\frac{1}{6} \sum_{\substack{1,2,3,4 \\ \gamma_1\gamma_2\gamma_3}} M_1^o(1;\gamma_1)M_3^o(2;\gamma_1\gamma_2\gamma_3)M_1^o(3;\gamma_2)M_1^o(4;\gamma_3)v_{\gamma_1}(12)v_{\gamma_2}(23)v_{\gamma_3}(24) \quad \text{(d)}$$

$$+\frac{1}{6} \sum_{\substack{1,2,3 \\ \gamma_1\gamma_2\gamma_3}} M_2^o(1;\gamma_2\gamma_3)M_2^o(2;\gamma_1\gamma_3)M_2^o(3;\gamma_1\gamma_2)v_{\gamma_3}(12)v_{\gamma_1}(23)v_{\gamma_2}(31) \quad \text{(e)} \qquad \text{(A.15)}$$

The general term contributing to W_n has a graphical interpretation. To find W_n, consider a connected graph G with n lines and p vertices. Label the p vertices arbitrarily 1,2,...p. Label each line in G by a Cartesian index γ. Let ℓ_i denote the number of lines terminating in the vertex i. To calculate the contribution of G to W_n:

Rule D:

(i) Same as A(i) of Chapter II.

(ii) For each vertex (e.g. 3) assign a factor $M_{\ell_3}^o(3,\gamma_1\cdots\gamma_{\ell_3})$, where γ_i, i=1,2...,ℓ_3 are the Cartesian labels of the lines

terminating in 3.

(iii) Sum freely the Cartesian label of each line over all directions and the lattice label of each vertex over all lattice sites.

(iv) Divide the result of (iii) by the symmetry factor g of the graph on question. g is the order of the symmetry group of the graph under permutation of lines and points.

(v) To find W_n, sum according to the above rules the contribution of all topologically distinct (connected) graphs of n lines.

As an example, terms (a) - (e) contributing to W_3 in (A.15) have the graphical interpretation shown in Fig. 11. One

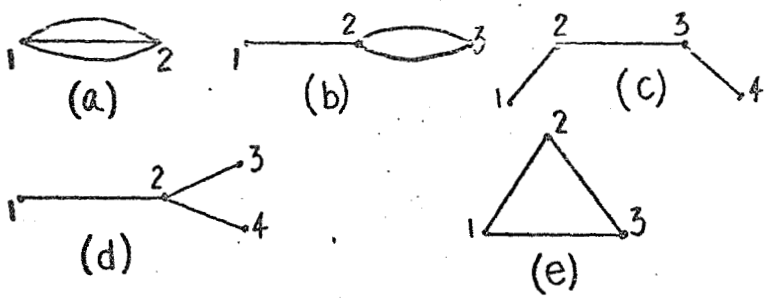

Figure 11. Graphical representation of the terms contributing to W_3.

way to see why only connected graphs enter* the expression for W_n is to consider a particular n^{th} (functional) derivative of W in (A.3b).

*The fact that only connected graphs enter expresses the extensivity of the free energy, W.

Consider the v's to be "bonds," so that they can be labeled in some manner, and the two sites which form the arguments of a v to be the endpoints of the bond. Suppose the endpoints of the bonds in one of the derivatives in (A.3b) form two disjoint subsets, F and F'. Further suppose that the sites of F (and F') are connected; that is, each element of F is connected to each other element by at least one path of bonds. Let B(B') be the set of bonds connecting the points of F(F'). Then a particular derivative in (A.3b) can be written

$$\left(\prod_{\substack{\text{bonds} \\ \in B}} \frac{\delta}{\delta v} \prod_{\substack{\text{bonds} \\ \in B'}} \frac{\delta}{\delta v} \right) W \Big|_0 \qquad \text{(A.16)}$$

Since the derivative is evaluated with $\{v\} = 0$, all bonds in W not in B or B' can be set to zero before differentiation. Then the trace in W factors, and the logarithm yields a sum of two functions, one containing bonds in B, the other containing bonds in B'. The cross terms in (A.16) will always give zero for such a derivative. This means that in a graphical representation of contributions to W, disconnected graphs do not enter.

Rule D(iv) concerning the symmetry factor can be understood by a topological argument. In a graph contributing to W_n there are n lines in some topological arrangement. Given n labeled bonds with labeled endpoints, there are $n!2^n/g$ ways of forming the topological arrangement, the n! coming from the choosing of the bonds and the 2^n from the orientation of each bond. The factor g is just the number of ways that a graph with the labeled bonds and

vertices can be superimposed onto itself under interchange of points and lines.* The number $n!2^n/g$ is just the total number of terms in the expansion of W_n which yield the same graph. Notice that the factors $n!2^n$ cancel with the prefactor in (A.3b). Hence, 1/g is the coefficient of each graph; this gives Rule D(iv). By way of example, the coefficients of the terms (a)-(e) in (A.15) are the 1/g factors corresponding to the graphs in Fig. 11 (a)-(e).

To get Rule A of Chapter II for calculating $\eta'_{\alpha\beta}(12)$ in the unrenormalized expansion, one need only differentiate the expansion for W,

$$\eta'_{\alpha\beta}(12) = \frac{\delta^2 W[\{v\},\{b\}]}{\delta b_\alpha(1)\delta b_\beta(2)} \quad . \tag{A.17}$$

In a term contributing to W, the $M^o_{\underset{\sim}{\alpha}}$'s provide the dependence on the magnetic field via (2.9). The effect of the differentiation in (A.17) is to distinguish two (external) vertices, 1 and 2. All sums, symmetry factors, etc. for Rule A are calculated with these two vertices distinguished. Rule A(iii) results (from (2.9)) because

$$\frac{\delta}{\delta b_\alpha(1)} M^o_n(3;\alpha_1\cdots\alpha_n) = M^o_{n+1}(1;\alpha\alpha_1\cdots\alpha_n)\delta(13) \quad , \tag{A.18}$$

which causes the external points to be treated asymmetrically.

---

*g is the order of the symmetry group of the graph. For an alternate discussion of the symmetry factors, the reader is referred to Appendix A of the paper by F. Englert.[35] For discussion of graph theory in general see the article by G. E. Uhlenbeck and G. W. Ford.[65]

APPENDIX B. THE RENORMALIZATION

The derivation of the renormalized expansion for $\mathcal{M}_{\alpha\beta}(12)$ (Rules B and C of Chapter II) is sketched here and follows the method of Englert.[35] In Fig. 1, (a) shows a reducible graph contributing to $\mathcal{M}_{\alpha\beta}(12)$ and (b) shows its (irreducible) skeleton. To find an expansion involving only irreducible graphs, it is clear that we must sum all the reducible parts which can be attached to a given vertex. This process results in the replacement of the unrenormalized semi-invariants by the M_n's defined by (2.11) and the elimination of all reducible graphs.*

A vertex i of a graph is an articulation point (point of reducibility) if the graph can be split into two or more pieces by cutting it at vertex i. To perform the selective summation indicated above, the self-energy parts $G_n^o(1;\alpha_1\cdots\alpha_n)$ must be evaluated. $G_n^o(1;\alpha_1\cdots\alpha_n)$ is computed by considering connected graphs with one fixed, external vertex (labeled 1) which is not an articulation point. Into this vertex come n lines with fixed Cartesian labels $\alpha_1\cdots\alpha_n$. All additional lines are given dummy Cartesian labels γ, and internal vertices are labeled arbitrarily 2,3,$\cdots$, in the manner described in Chapter II and Appendix A. Each such graph contributes according to the following rule.

---

*To see that all that remains of the symmetry factors is the symmetry factor of the irreducible graph (Rule B of Chapter II), one can work to a given order in v and simultaneously attach reducible parts to all vertices of a skeleton. The inclusion of the symmetry factor of the skeleton compensates for graphical redundancy and allows term by term agreement with the unrenormalized expansion.

Rule E:

(i) Same as A(i).

(ii) Same as A(ii).

(iii) Assign a factor unity to the external vertex 1.

(iv) Sum freely over all directions the dummy Cartesian labels of the internal lines, and sum over all lattice sites the lattice label of each internal vertex, with the external vertex 1 fixed on the lattice.

(v) Same as A(v).

(vi) To find $G_n^o(1;\alpha_1 \ldots \alpha_n)$ sum the contributions according to the above rules of all topologically distinct graphs with one fixed vertex 1.

By construction G_n^o is a functional of the M_ℓ^o's and v, the interaction. Fig. 12 indicates symbolically how a self-energy part G_3^o, when attached to a vertex M_2^o, gives a contribution to M_2

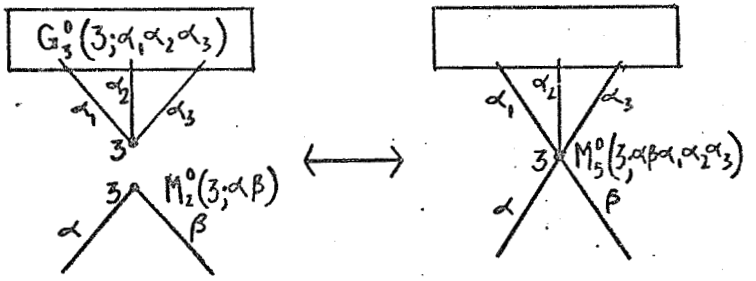

Figure 12. A contribution to M_2. A self-energy part G_3^o attached to a vertex M_2^o gives a M_5^o contribution to M_2.

proportional to M_5^o. In general, a self-energy part of order n, when attached to a vertex 3 (which is not an articulation point) with ℓ lines $(\gamma_1 \cdots \gamma_\ell)$ terminating in it, contributes

$$\sum_{\alpha_1 \cdots \alpha_n} G_n^o(3;\alpha_1 \cdots \alpha_n) M_{n+\ell}^o(3;\gamma_1 \cdots \gamma_\ell \alpha_1 \cdots \alpha_n) \tag{B.1}$$

to M_ℓ. This is because in cutting away all reducible parts from 3 and writing $M_\ell(3;\gamma_1 \cdots \gamma_\ell)$, we must take into account the sum of all graphs coming into 3 with n lines, each of which would cause the assignment of $M_{n+\ell}^o$ to vertex 3 in the unrenormalized expansion. Using (2.9), (B.1) can be written

$$\sum_{\alpha_1 \cdots \alpha_n} G_n^o(3;\alpha_1 \cdots \alpha_n) \frac{\delta^n}{\delta b_{\alpha_1}(3) \cdots \delta b_{\alpha_n}(3)} M_\ell^o(3;\gamma_1 \cdots \gamma_\ell). \tag{B.2}$$

Suppose there were m_n self-energy parts of the type G_n^o attached to the vertex 3. The total contribution would be

$$\frac{1}{m_n!}\left[\sum_{\alpha_1 \cdots \alpha_n} G_n^o(3;\alpha_1 \cdots \alpha_n) \frac{\delta^n}{\delta b_{\alpha_1}(3) \cdots \delta b_{\alpha_n}(3)} \right]^{m_n} M_\ell^o(3;\gamma_1 \cdots \gamma_\ell), \tag{B.3}$$

where it is understood that the derivatives act only on M_ℓ^o. The $m_n!$ is the extra symmetry factor of the graph represented by m_n identical G_n^o self-energy parts. Then summing all reducible parts attached to 3 in all possible combinations,

$$M_\ell(3;\gamma_1 \cdots \gamma_\ell) = \sum_{m_1,\cdots,m_n,\cdots=0}^{\infty} \frac{1}{m_1! \cdots m_n! \cdots} \left[\sum_{\alpha_1} G_1^o(3;\alpha_1) \frac{\delta}{\delta b_{\alpha_1}(3)} \right]^{m_1} \cdots$$

$$\times \left[\sum_{\alpha_1 \cdots \alpha_n} G_n^o(3;\alpha_1 \cdots \alpha_n) \frac{\delta^n}{\delta b_{\alpha_1}(3) \cdots \delta b_{\alpha_n}(3)} \right]^{m_n} \cdots M_\ell^o(3;\gamma_1 \cdots \gamma_\ell). \tag{B.4}$$

This yields (derivatives acting only on M_ℓ^o)

$$M_\ell(3;\gamma_1\cdots\gamma_\ell)=\exp\Big\{\sum_{n=1}^{\infty}\sum_{\alpha_1\cdots\alpha_n} G_n^o(3;\alpha_1\cdots\alpha_n)\,\frac{\delta^n}{\delta b_{\alpha_1}(3)\cdots\delta b_{\alpha_n}(3)}\Big\}M_\ell^o(3;\gamma_1\cdots\gamma_\ell). \tag{B.5}$$

(B.5) is a self-contained equation that can be used to find M_ℓ. The observation that G_n^o is at least of order v^n allows M_ℓ to be found at high temperature by iteration in powers of v. However, the graphs for the self-energy parts G_n^o can themselves be reduced by stripping away all reducible parts and replacing M_ℓ^o's with the renormalized M_ℓ's at all internal vertices. Then G_n^o is expressed as a functional of the M_ℓ's and v. To indicate this we drop the superscript and write $G_n(1;\alpha_1\cdots\alpha_n)$ which is calculated according to Rule C of Chapter II. In addition, (2.11) is the resultant equation for the renormalized semi-invariants. (2.11) is just (B.5) with the G_n's considered functionals of the M_ℓ's themselves — this gives (2.11) the interpretation of a non-linear equation as discussed in Chapter II.

Evaluation of (B.5) directly is certainly possible, but as in the unrenormalized expansion for $\mathcal{M}_{\alpha\beta}$, the graphs proliferate rapidly. To reduce the number of graphs (by considering only irreducible self-energy graphs) one pays the price of having to iterate (self-consistently) (2.11). In practice that has been the preferable procedure.

APPENDIX C. SELECTED ZERO-FIELD SUSCEPTIBILITY, SECOND MOMENT AND SPECIFIC HEAT COEFFICIENTS

$$\chi_\alpha(\eta_x,\eta_y,\eta_z) = 1/3 + \sum_{n=1} a_n^\alpha v^n$$

$$\mu_2^\alpha(\eta_x,\eta_y,\eta_z) = \sum_{n=1} b_n^\alpha v^n$$

(f.c.c. lattice)

	$\eta_x = \eta_y = 0,\ \eta_z = 1$		$\eta_x = \eta_y = 0.5,\ \eta_z = 1$	
n	a_n^z	b_n^z	a_n^z	b_n^z
1	1.3333	1.3333	1.3333	1.3333
2	5.0667	10.6667	5.0222	10.6667
3	18.8800	61.9022	18.5007	61.5526
4	69.4866	313.6000	67.2977	309.2069
5	253.6484	1471.3803	242.8131	1436.7542
6	920.5347	6569.0511	871.0947	6348.4609
7	3326.3463	28321.6706	3111.8314	27079.6495
8	11979.5328	118979.2153	11079.9968	112529.7574

	$\eta_x = \eta_y = 1,\ \eta_z = 1$		$\eta_x = \eta_y = 1,\ \eta_z = 0$	
n	a_n^z	b_n^z	a_n^x	b_n^x
1	1.3333	1.3333	1.3333	1.3333
2	4.8889	10.6667	4.9778	10.6667
3	17.2444	60.5037	18.0622	61.2030
4	59.4864	295.1111	64.4301	304.3556
5	202.2485	1319.7991	227.2428	1395.0621
6	680.7001	5576.1756	795.1252	6063.7043
7	2273.9843	22628.6321	2765.7862	25385.7514
8	7553.1203	89102.6500	9576.8911	103345.8207

(b.c.c. lattice)

	$\eta_x = \eta_y = 0,\ \eta_z = 1$		$\eta_x = \eta_y = 0.5,\ \eta_z = 1$	
n	a_n^z	b_n^z	a_n^z	b_n^z
1	.8889	.6667	.8889	.6667
2	2.1926	3.5556	2.1630	3.5556
3	5.3965	13.5289	5.2425	13.4133
4	12.9657	45.0686	12.4089	44.1521
5	31.1253	138.7230	29.3329	134.1340
6	73.8778	406.5133	68.5982	387.6546
7	175.2775	1149.4870	160.3216	1080.7612
8	413.1654	3167.5920	372.3818	2935.6899
9	973.6307	8552.4153	864.5835	7812.4167

	$\eta_x = \eta_y = \eta_z = 1$		$\eta_x = \eta_y = 1,\ \eta_z = 0$	
n	a_n^z	b_n^z	a_n^x	b_n^x
1	.8889	.6667	.8889	.6667
2	2.0741	3.5556	2.1333	3.5556
3	4.7802	13.0667	5.0884	13.2978
4	10.6206	41.4025	11.7683	43.2356
5	23.4372	119.9779	27.1284	129.2359
6	50.9372	328.5065	61.6871	366.4521
7	110.2478	863.3071	139.9846	1000.0311
8	236.6645	2201.3132	315.2704	2653.8913
9	506.6023	5481.3726	709.0308	6889.3092

(s.c. lattice)

	$\eta_x = \eta_y = 0,\ \eta_z = 1$		$\eta_x = \eta_y = 0.5,\ \eta_z = 1$	
n	a_n^z	b_n^z	a_n^z	b_n^z
1	.6667	.6667	.6667	.6667
2	12.0	2.6667	1.1778	2.6667
3	2.1511	7.4844	2.0652	7.3985
4	3.7541	18.2756	3.5325	17.7659
5	6.5429	41.1029	6.0311	39.2400
6	11.2634	87.8273	10.1780	82.2726
7	19.3761	180.8452	17.1598	166.1778
8	33.1005	362.5272	28.7414	326.6961
9	56.5197	711.5228	48.1100	628.7740

	$\eta_x = \eta_y = \eta_z = 1$		$\eta_x = \eta_y = 1,\ \eta_z = 0$	
n	a_n^z	b_n^z	a_n^x	b_n^x
1	.6667	.6667	.6667	.6667
2	1.1111	2.6667	1.1556	2.6667
3	1.8074	7.1407	1.9793	7.3126
4	2.8395	16.2370	3.2830	17.2563
5	4.4223	33.5779	5.4198	37.2775
6	6.7787	65.3762	8.8192	76.1686
7	10.3330	121.9017	14.3098	149.5166
8	15.6224	220.1664	23.0379	285.0166
9	23.5356	387.8528	37.0177	530.9441

(triangle lattice)

	$\eta_x = \eta_y = 0,\ \eta_z = 1$		$\eta_x = \eta_y = 0.5,\ \eta_z = 1$	
n	a_n^z	b_n^z	a_n^z	b_n^z
1	.6667	.6667	.6667	.6667
2	1.2	2.6667	1.1778	2.6667
3	2.0622	7.4844	1.9689	7.3985
4	3.4341	17.9556	3.1868	17.4202
5	5.5898	39.2706	5.0448	37.2619
6	8.9468	80.7109	7.8563	74.7649
7	14.1327	158.5597	12.0791	143.2527
8	22.0923	300.9375	18.3822	265.0244

	$\eta_x = \eta_y = \eta_z = 1$		$\eta_x = \eta_y = 1,\ \eta_z = 0$	
n	a_n^z	b_n^z	a_n^x	b_n^x
1	.6667	.6667	.6667	.6667
2	1.1111	2.6667	1.1556	2.6667
3	1.6593	7.1407	1.8607	7.3126
4	2.3062	15.7037	2.8563	16.8296
5	3.0449	30.5214	4.2334	34.8334
6	3.8638	54.3773	6.1088	67.0248
7	4.7449	90.7139	8.6293	122.1831
8	5.6662	143.6469	11.9800	213.5681

Selected zero-field specific heat coefficients for the f.c.c. lattice

	$\eta_x=\eta_y=0, \eta_z=1$	$\eta_x=\eta_y=\eta_z=1$	$\eta_x=\eta_y=1, \eta_z=0$
n	c_n^z	c_n^z	c_n^x
1	.111111	.111111	.111111
2	.296296	.296296	.296296
3	1.14222	.792593	.967407
4	3.63457	2.10700	2.87078
5	11.7018	5.60627	8.43416
6	37.6089	15.1818	24.9999
7	121.2898	41.9215	74.7465
8	393.1859	117.5633	225.5134

$$C_\alpha = \frac{zv}{2} \sum_{n=1} c_n^\alpha v^n$$

APPENDIX D. DETERMINATION OF THE GROUND STATE

The ground state structure can be simply determined if and only if the pair ground state of two coupled spins can be coherently imposed over the entire lattice for every nearest neighbor pair. The basic problem, then, is to maximize $\sum_{\alpha} \eta_\alpha S_\alpha S_\alpha'$ subject to the subsidiary conditions $\sum_{\alpha} S_\alpha^2 = \sum_{\alpha} S_\alpha'^2 = 1$. By the method of Lagrange multipliers, we are lead to extremize the quadratic form

$$\sum_{\alpha} \left[\eta_\alpha S_\alpha S_\alpha' - \frac{\lambda_1}{2} S_\alpha^2 - \frac{\lambda_2}{2} S_\alpha'^2 \right] . \tag{D.1}$$

This gives

$$\eta_\alpha S_\alpha' = \lambda_1 S_\alpha \quad \text{and} \quad \eta_\alpha S_\alpha = \lambda_2 S_\alpha' . \tag{D.2}$$

It follows from (D.2) that

$$\sum_{\alpha} \eta_\alpha S_\alpha S_\alpha' = \lambda_1 = \lambda_2 = \lambda \tag{D.3}$$

and that, if

$$\eta_\alpha^2 \neq \lambda^2, \text{ then } S_\alpha = S_\alpha' = 0 . \tag{D.4}$$

If the subsidiary conditions are to be satisfied, there must be at least one α for which $\eta_\alpha^2 = \lambda^2$. It, therefore, follows from (B.3) that the very best we can hope for is $\sum_{\alpha} \eta_\alpha S_\alpha S_\alpha' = |\eta_{max}|$, where η_{max} is the largest in absolute magnitude of the η_α's. A short computation shows that this maximum can always be achieved by choosing

$$S_\alpha = \begin{cases} \mathrm{sgn}(\eta_\alpha) S_\alpha', \text{ for all } \alpha \text{ such that } |\eta_\alpha| = |\eta_{max}| \\ 0, \text{ otherwise}, \end{cases} \tag{D.5}$$

where $\mathrm{sgn}(x) = \pm 1$ for $x \gtrless 0$. (D.5) constitutes the solution of the two-spin problem, and we note that, even after application of the normalization condition, there still remains an up-down (Ising-like), planar rotation (x-y-like), and three-dimensional rotation (isotropic Heisenberg-like) degeneracy according as the maximal anisotropy parameter in absolute value is unique, doubly degenerate, or triply degenerate respectively.

For the b.c.c. lattice (or any loose-packed lattice) the sublattice structure guarantees that (D.5) can be applied coherently, thus giving the ground state for the entire lattice as indicated in Table 16.

For the f.c.c. lattice, on the other hand, nearest-neighbors of a given site, can, themselves, be nearest-neighbors. Thus, (d.5) cannot be imposed coherently without the additional requirement that

$$S_\alpha = S_\alpha' = 0 \text{ whenever } \eta_\alpha < 0. \tag{D.6}$$

This further condition reduces the degeneracy for the entire lattice as shown in Table 16 for the f.c.c. Note that, when all the maximal anisotropy parameters are negative (antiferromagnetic), (D.5) and (D.6) together require $\underset{\sim}{S} = \underset{\sim}{S}' = 0$, which is incompatible with normalization. In this case, our simple argument fails, and the ground state has a more complex structure.

LIST OF REFERENCES

1. M. E. Fisher, in Critical Phenomena, edited by M. S. Green and J. V. Sengers (National Bureau of Standards, Washington, D. C., 1966).

2. L. D. Landau and E. M. Lifshitz, Statistical Physics (Pergamon Press, London, 1958), Chapter 14.

3. M. E. Fisher, in Reports on Progress in Physics 30, 615 (1967).

4. L. P. Kadanoff, Wolfgang Götze, David Hamblen, Robert Hecht, E.A.S. Lewis, V. V. Palciauskas, Martin Rayl, J. Swift, David Aspnes, and Joseph Kane, Rev. Mod. Phys. 39, 395 (1967).

5. P. Heller, in Reports on Progress in Physics 30, 731 (1967).

6. G. S. Rushbrooke, J. Chem. Phys. 39, 842 (1963); R. B. Griffiths, Phys. Rev. Letters 14, 623 (1965).

7. L. P. Kadanoff, Physics 2, 263 (1966).

8. B. Widom, J. Chem. Phys. 43, 3898 (1965).

9. M. E. Fisher, in Lectures in Theoretical Physics (Univ. of Colorado Press, Boulder, Colorado, 1965), Vol. VIIC.

10. L. S. Ornstein and F. Zernike, Proc. Acad. Sci. Amsterdam 17, 793 (1914); Z. Physik 19, 134 (1918); 27, 761 (1926).

11. L. Onsager, Phys. Rev. 65, 117 (1944).

12. G. F. Newell and E. W. Montroll, Rev. Mod. Phys. 25, 253 (1953).

13. C. Domb, Advan. in Physics 9, 151 (1960).

14. R. B. Griffiths, J. Math. Phys. 8, 478 (1967).

15. C. Domb and M. F. Sykes, Proc. Roy. Soc. (London) A240, 214 (1957).

16. L. P. Kadanoff, Nuovo Cim. 44, 276 (1966); T. T. Wu, Phys. Rev. 149, 380 (1966).

17. C. Domb, Proc. Roy. Soc. (London) A199, 199 (1949).

18. C. N. Yang, Phys. Rev. 85, 808 (1952).

19. G. Wannier, Phys. Rev. 79, 357 (1950).

20. G. A. Baker, Jr., Phys. Rev. 124, 768 (1961).

21. G. A. Baker, Jr., H. E. Gilbert, J. Eve and G. S. Rushbrooke, Phys. Rev. 164, 800 (1967).

22. G. S. Joyce and R. G. Bowers, Proc. Phys. Soc. (London) 89, 776 (1966).

23. H. E. Stanley, Phys. Rev. 158, 546 (1967); P. J. Wood and G. S. Rushbrooke, Phys. Rev. Letters 17, 307 (1966).

24. M. E. Fisher, Physics 3, 255 (1967); F. H. Stillinger, Jr., J. Chem. Phys. 47, 2513 (1967).

25. E. Lieb, T. Schultz and D. Mattis, Ann. Phys. (N.Y.) 16, 407 (1961).

26. H. E. Stanley and T. A. Kaplan, Phys. Rev. Letters 16, 981 (1966).

27. G. S. Joyce and R. G. Bowers, Proc. Phys. Soc. (London) 88, 1053 (1966); G. S. Joyce, Phys. Rev. 155, 478 (1967).

28. C. Domb and M. F. Sykes, Phys. Rev. 128, 168 (1962).

29. R. J. Burford, Ph.D. thesis, University of London, 1966 (unpublished).

30. M. E. Fisher and R. J. Burford, Phys. Rev. 156, 583 (1967).

31. N. W. Dalton and D. W. Wood, Proc. Phys. Soc. (London) 90, 459 (1967).

32. M. E. Fisher, Phys. Rev. Letters 16, 11 (1966).

33. T. Obokata, I. Ono, and T. Oguchi, J. Phys. Soc. Japan 23, 516 (1967).

34. H. E. Stanley, Phys. Rev. 158, 537 (1967).

35. F. Englert, Phys. Rev. 129, 567 (1963).

36. C. Bloch and J. S. Langer, J. Math. Phys. 6, 554 (1965).

37. M. F. Sykes, J. W. Essam, B. R. Heap, and B. J. Hiley, J. Math. Phys. 7, 1557 (1966).

38. G. S. Rushbrooke and P. J. Wood, Mol. Phys. 6, 409 (1963).

39. C. De Dominicis, J. Math. Phys. 3, 983 (1962).

40. E. C. Titchmarsh, The Theory of Functions (Oxford University Press, London, 1939), Chapter 7.

41. P. Dienes, The Taylor Series (Dover Publications, New York, 1957).

42. E. W. Hobson, The Theory of Functions of a Real Variable and the Theory of Fourier's Series (Cambridge University Press, Cambridge, 1926), Second Edition, Volume II, Chapter III.

43. D. R. Hartree, Numerical Analysis (Oxford University Press, London, 1952).

44. C. Domb and M. F. Sykes, J. Math. Phys. 2, 63 (1961).

45. D. S. Gaunt, Proc. Phys. Soc. (London) 92, 150 (1967).

46. G. A. Baker, Jr., in Advances in Theoretical Physics, edited by K. A. Brueckner (Academic Press, Inc., New York, 1965), Volume I.

47. M. E. Fisher, J. Math. Phys. 4, 124 (1963).

48. M. E. Fisher and M. F. Sykes, Physica 28, 939 (1962).

49. D. D. Betts and C. J. Elliott, Phys. Letters 18, 18 (1965).

50. M. F. Sykes, J. L. Martin and D. L. Hunter, Proc. Phys. Soc. (London) 91, 671 (1967).

51. V. G. Vaks and A. I. Larkin, Zh. Eksperim. i Teor. Fiz. 49, 975 (1965). [Translation: Sov. Phys. JETP 22, 678 (1966).]

52. B. D. Josephson, Physics Letters 21, 608 (1966).

53. M. J. Buckingham and W. M. Fairbank, in Progress in Low Temperature Physics (North-Holland Publishing Co., Amsterdam, 1961), Vol. III.

54. C. F. Kellers, Ph.D. thesis, Duke University, 1960 (unpublished).

55. J. R. Clow and J. D. Reppy, Phys. Rev. Letters 16, 887 (1966); J. A. Tyson and D. H. Douglass, Phys. Rev. Letters 17, 472 (1966).

56. R. G. Bowers and G. S. Joyce, Phys. Rev. Letters 19, 630 (1967).

57. H. E. Stanley, Phys. Rev. Letters 20, 150 (1968).

58. G. K. Wertheim, H. J. Guggenheim and D.N.E. Buchanan, Phys. Rev. 169, 465 (1968).

59. H. E. Stanley and T. A. Kaplan, J. Appl. Phys. 38, 977 (1967).

60. P. K. Baltzer, P. J. Wojtowicz, M. Robbins and E. Lopatin, Phys. Rev. 151, 367 (1966).

61. G. S. Rushbrooke and P. J. Wood, Mol. Phys. 1, 257 (1958).

62. S. Freeman and P. J. Wojtowicz, Phys. Letters 26A, 231 (1968).

63. W. Marshall, J. Gammel and L. Morgan, Proc. Roy. Soc. (London) A275, 257 (1963).

64. P. K. Baltzer, H. W. Lehmann and M. Robbins, Phys. Rev. Letters 15, 493 (1965); N. Menyuk, K. Dwight, R. J. Arnott and A. Wold, J. Appl. Phys. 37, 1387 (1966).

65. G. E. Uhlenbeck and G. W. Ford, in Studies in Statistical Mechanics, edited by J. DeBoer and G. E. Uhlenbeck (North-Holland Publishing Company, Amsterdam, 1962), Volume I.

VITA.

David Michael Jasnow was born in [redacted] on [redacted] He received an A.B. in Physics from Cornell University in June, 1964, and an M.S. in Physics from the University of Illinois in June, 1965.